Optimization and Evaluation of CMC-BB Membranes with and without Electrolytic salt for Supercapacitors

Thesis submitted in

Partial Fulfilment of the

Degree of Master of Philosophy (M.Phil)

By

M.ROOPASRI

18MPPHF004

DEPARTMENT OF PHYSICS

AVINASHILINGAM INSTITUTE FOR HOME SCIENCE AND HIGHER EDUCATION FOR WOMEN

COIMBATORE – 641 043

JULY 2019

Optimization and Evaluation of CMC-BB Membranes with and without Electrolytic salt for Supercapacitors

Thesis submitted in

Partial Fulfilment of the

Degree of Master of Philosophy (M.Phil)

By

M.ROOPASRI

18MPPHF004

DEPARTMENT OF PHYSICS

AVINASHILINGAM INSTITUTE FOR HOME SCIENCE AND HIGHER EDUCATION FOR WOMEN

COIMBATORE – 641 043

JULY 2019

CERTIFIED AS A BONAFIDE RESEARCH WORK

31/7/2019
Signature of Head of the Department

31/07/19
Signature of the Supervisor

DECLARATION

I declare that the dissertation entitled **Optimization and Evaluation of CMC-BB Membranes withand without Electrolytic salt for Supercapacitors** submitted by me for the degree of Master of Philosophy (M.Phil) is the record of work carried out by me during the period from **August 2018 to July 2019** under the guidance of **Dr.(Tmt.) B. Nalini,** M.Sc., Ph.D., M.S (Edu.Mgt.), STA fellow, AIST Fellow (Japan), Assistant Professor (SS), Department of Physics, Avinashilingam Institute for Home Science and Higher Education for Women, Coimbatore and has not formed the basis for the award of any Degree, Diploma, Associateship, Fellowship, Titles in this University or any other University or other similar institution of Higher Learning.

M. Rajeswari

Signature of the Candidate

CERTIFICATE

I certify that the dissertation entitled **Optimization and Evaluation Of CMC-BB Membranes with and without Electrolytic salt for Supercapacitors** submitted for the degree of Master of Philosophy (M.Phil.) by **M. Roopasri** is the record of research work carried out by her during the period from **August 2018 to July 2019** under my guidance and supervision, and that this work has not formed the basis for the award of any Degree, Diploma, Associateship, Fellowship, Titles in this University or any other University or other similar institution of Higher Learning.

31/7/2019

Signature of the
Head of the Department

31/07/19

Signature of the
Supervisor with designation
ASSISTANT PROFESSOR.

ACKNOWLEDGEMENT

I owe my sincere thanks to **Lord Almighty** and **My Loveable Parents** for showering their generous blessings upon me in all endeavours.

I wish to express my gratitude to **Dr. P.R. Krishnakumar,** Chancellor, Avinashilingam Institute for Home Science and Higher Education for Women, Coimbatore, for providing the facilities to conduct this study.

I extend my thanks to **Dr. (Tmt.) Premavathy Vijayan,** M.Sc., M.Ed., Dip. Spl. Edn., M.Phil., Ph.D., Vice Chancellor, Avinashilingam Institute for Home Science and Higher Education for Women, Coimbatore, for providing flamboyant help towards the completion of the study.

I record my deep sense of gratitude and indebtedness to **Dr. (Tmt.) S. Kowsalya,** M.Sc., M.Phil., Ph.D., Registrar, Avinashilingam Institute for Home Science and Higher Education for Women, Coimbatore, for providing adequate help for the study.

I gratefully record my sincere thanks to **Dr. (Mrs.) K. UdhayaChandrika**, M.Sc., M.Phil., Ph.D., Dean, School of Physical Sciences and Computational Sciences, Avinashilingam Institute for Home Science and Higher Education for Women, Coimbatore, for timely help rendered throughout the course of this work.

I whole heartily thank **Dr. (Mrs.) Rajeswari,** M.Sc., M.Phil., M.C.A., SLET, Ph.D.,Assistant Professor-SG and Head (i/c) of the Department of Physics, Avinashilingam Institute for Home Science and Higher Education for Women, Coimbatore, for her encouragement and generous help which was of great value.

I am very much obliged to record my deep sense of gratitude and indebtedness to my respectful guide **Dr.(Tmt.) B. Nalini,** M.Sc., Ph.D., M.S (Edu.Mgt.), STA fellow, AIST Fellow (Japan), Assistant Professor, Avinashilingam Institute for Home Science and Higher Educationfor Women, Coimbatore, for her valuable guidance learned counsel, cordial treatment, keen interest, constant encouragement and care rendered throughout the course of my investigation. I express my sincere gratitude to all the staff members of the Department

of Physics, Avinashilingam Institute for Home Science and Higher Education for Women, Coimbatore, for their help and support.

I would like to express my special thanks to **my parents, my friends** and all **my well-wishers** for their constant encouragement, support and help in carrying out this work successfully.

ROOPASRI. M

CONTENT

CHAPTER-I

1.1 INTRODUCTION

In recent years, energy is becoming a critical societal issue, which greatly impacts world economy, environment and human life. There has been demand for energy storage materials due to the decrease of fossil fuel resources and the environmental impact of fuel combustion. Energy issues become one of the greatest challenges in the 21st century. The global energy consumption will keep growing in the following decades. Although traditional combustion-based energy technologies, including coal, oil and natural gas, dominates in energy needs, alternative energy sources and technologies are imperative due to the disadvantages of traditional counterparts, such as emission of greenhouse gases and long-term environmental consequences [1-2].

Energy production from solar energy, wind power, tidal power and biomass are considered as promising alternatives with their few drawbacks like accuracy, less efficiency and high cost. However, the solar energy supports large scale conversion. To improve all the properties which can help to produce/store the charge, mass production, efficient and stable under ambient conditions are essential. Electricity generated from renewable sources, such as solar and wind power, offers enormous potential for meeting future energy demands [3]. Over the past few years, major interest has been focused on developing energy devices that are environmentally friendly, sustainable, renewable, cheap and efficient. The fast growing market of portable electronics and electric vehicles stimulates the development of

environmental energy storage devices with high energy and power density, such as batteries, fuel cells and super capacitors. [4]

1.2 ENERGY STORAGE DEVICES

The most practical application of electrochemical energy storages are capacitors, batteries and supercapacitor**.**

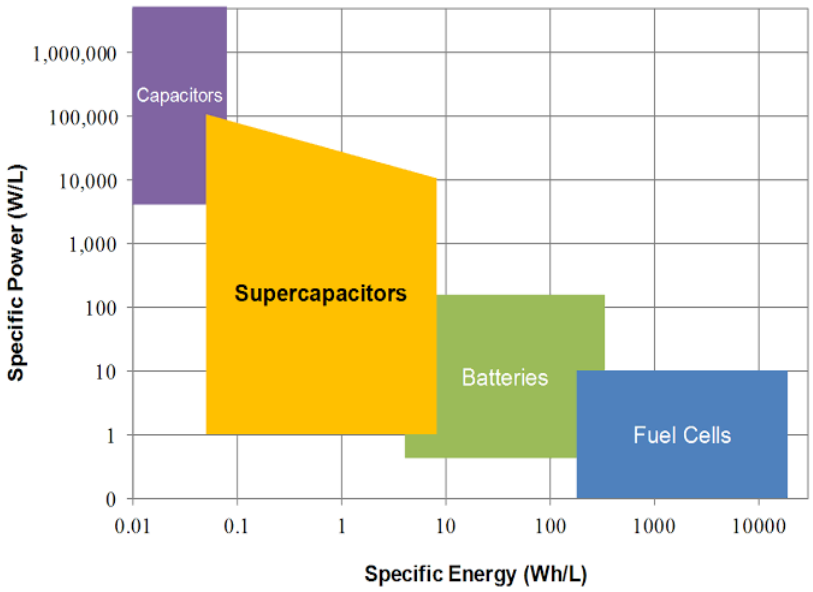

Figure 1.1 Schematic representation for energy storage devices

1.2.1 Batteries

Battery is a device consisting of one or more electrochemical cells which converts stored chemical energy to electrical energy by chemical reduction-oxidation reactions [5]. Battery consist of a negative, positive electrode materials and an electrolyte which helps in the diffusion of ions to move between the electrodes and terminals that allows the flow of charges (current) in an external circuit. Generally, batteries can be divided into three types such as primary and secondary.

Primary batteries are the most common and are designed as single use batteries, to be discarded or recycled after the run out. They have very high impedance, which translates into long life at current loads. The most frequently used primary batteries are carbon-zinc, alkaline, silver oxide, zinc air, and lithium metals (like lithium manganese dioxide and lithium thionyl chloride).

Secondary batteries are rechargeable batteries. These secondary batteries can be charged/discharged several times due to their reversible change in composition of electrode materials [6]. Commonly available secondary batteries are nickel-cadmium, lead-acid, nickel-metal hydride, some lithium metal, and Li-ion. The limitations of secondary batteries include limited life, limited power, low energy-efficiency, and disposal concerns [7].

1.2.2 Fuel cells

Similar to batteries, fuel cells convert the chemical energy of a fuel into electrical energy. Hydrogen is one of the most used fuels in fuel cells. As long as the input fuels are present, these cells produce the energy. An electrochemical process takes place during the conversion of fuel to energy. This electrochemical process of producing energy is clean, simple and highly efficient. These fuel cells are mainly classified based on the fuel used a) direct methanol fuel cell, b) phosphoric acid fuel cell, c) solid oxide fuel cell, d) alkaline fuel cell, e) proton exchange membrane or solid polymer fuel cell, f) molten carbonate fuel cell and g) regenerative fuel cell [8-9].

1.2.3 Capacitors

Capacitors store electrical energy by charge separation as positive and negative charges between two electrodes. Commonly, capacitors are constructed by two conductors, mostly in the form of a sheet, separated by an insulating material. When there is a potential difference across the conductors, static electric field is developed across the dielectric material. The amount of charges stored in the ideal capacitor can be estimated from the following relation,

$$C = \frac{q}{v} \qquad (1)$$

Where, q is charge, C is capacitance, and V is voltage. In case of the classical parallel plate capacitor, containing a dielectric between the plates, the capacity can be estimated from the relation.

$$C = \varepsilon\frac{A}{d} \qquad (2)$$

Where, ε is the dielectric constant of medium, A (cm^2) is the area of the plates and d (cm is the thickness of the dielectric material. the dielectric material. The conventional

capacitor yields capacitance in few picofarads to few thousands of microfarads. This capacitor is useful in timer circuits and filter circuits [10].

To store the electrical energy, battery, capacitor and supercapacitor (also called electrochemical capacitor or ultracapacitor) are essentially used. The energy storing capacity/energy density of battery is high as compared to the capacitors and supercapacitors [7]. On the other hand, capacitors have high charge deliver rate/power density than the batteries and supercapacitors. Supercapacitors fill the gap of batteries and capacitors; which have higher power density than the batteries and higher energy density than the capacitors. Supercapacitors have long cycle life (1000 to 5000 cycles) than batteries and high capacitance (1 to 2700 F g^{-1}) and lower equivalent series resistance (ESR) than the capacitors.

1.3 SUPERCAPACITOR

Supercapacitors, also known as electrochemical capacitors or ultracapacitors,have been studied over the past few decades. They provide an energy storage technology with high power density, long cycling life and high reversibility.

History of supercapacitor

The development of supercapacitors started in the 50s of the 20th century. First experiments started between 50s and 70s and were conducted by US companies General Electric (GE) and Standard Oil of Ohio (SOHIO).

In 1853, the concept of the double-layer capacitance was first described by Hermann von Helmholtz. In 1957, Becker, working for general electric, developed and patented the idea of the first electrochemical capacitor [11]. The device was made of carbon with high specific surface area coated on a metallic current collector in a sulphuric acid solution [12]. In 1962, an energy storage device using porous carbon as an electrode material was patented by the Standard Oil Company, Cleveland, Ohio (SOHIO) and in this patent. It was acknowledged that “the double-layer at the interface behaves like a capacitor of relatively high specific capacity” [13]. SOHIO also patented another disc-shaped capacitor with a carbon paste soaked in an electrolyte in 1970 [14]. In 1971, this double-layer capacitor technology was licensed to the Nippon Electric Company (NEC) by SOHIO, and NEC successfully manufactured the first commercially double-layer capacitor with the name of “supercapacitor”

[15]. From that time on, the industrialization period of the supercapacitor had started with the development of key technologies. These included improving the electrode materials, electrolyte and the manufacturing process. A kind of supercapacitor named “Gold capacitor”, used for memory backup applications, was developed by Panasonic in 1978. The Pinnacle Research Institute (PRI) developed the first high power double-layer capacitors named “PRI Ultracapacitors” by incorporating metal-oxide in the electrode in 1982. In late 70’s and 80’s, Conway et al., made a great contribution to the supercapacitor research, using RuO_2 as the electrode material which showed a high specific capacitance and a low internal resistance [16-17]. The US Department of Energy developed a study in hybrid electric vehicles, in which, the Ultracapacitor Development Program was developed by Maxwell Laboratories in 1992.

Most of today’s supercapacitors have capacity over several thousand Farads and can provide charge-discharge currents in the range from tenths to hundredths of Amperes [18].

Working Principle

In conventional electrochemical capacitor, the electric charges are accumulated at the interface of electrode/electrolyte. The ion with opposite charge is arranged on the electrolyte side and is understood by charge storage mechanism of conventional electrochemical capacitor. The schematic of conventional electrochemical capacitor is shown in figure 1.2 The conventional capacitor stores the electrical charges in the same way; the difference is that the two electrodes are separated by the dielectric material.

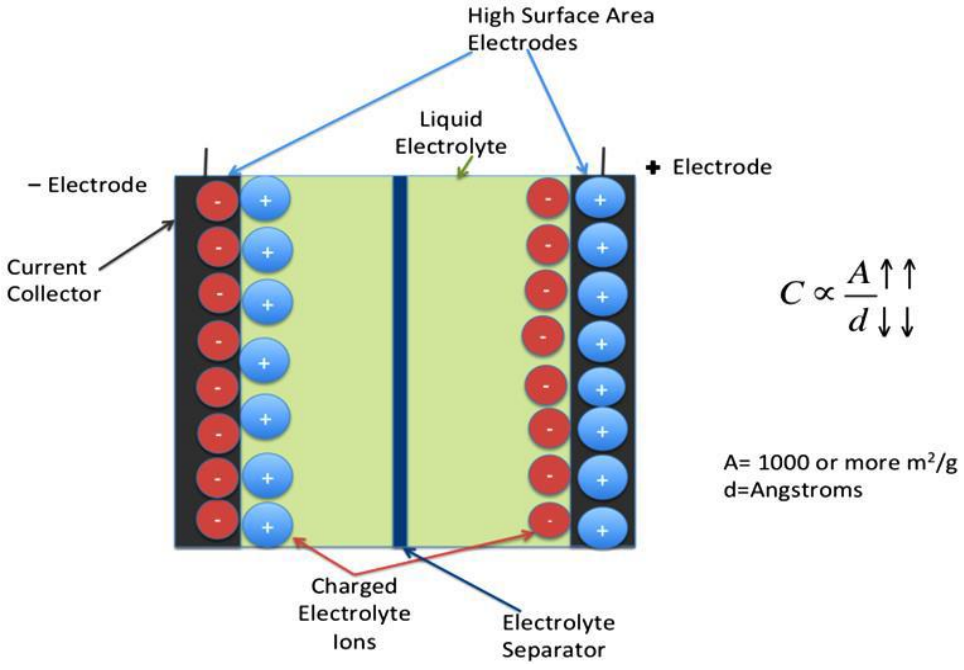

Fig. 1.2 Schematic of conventional electrochemical capacitor

1.4 TYPES OF SUPERCAPACITOR

Supercapacitors can be divided into three general classes: electrochemical double layer capacitors (EDLCs), Pseudocapacitors, and Hybrid capacitors. EDLCs physically store charges through reversible ion adsorption at the electrode-electrolyte interface, while pseudocapacitors chemically store their charges through redox reaction at the near of a few nanometers from the surface. All the supercapacitor can be characterized by unique mechanisms for storing charge, which re electrostatic storage, reversible faradaic redox and a combination of the two. Faradaic processes, such as oxidation-reduction reactions, involve the transfer of charge between electrode and the electrolyte. A non-faradic mechanism, by contrast, does not use a chemical mechanism [19].

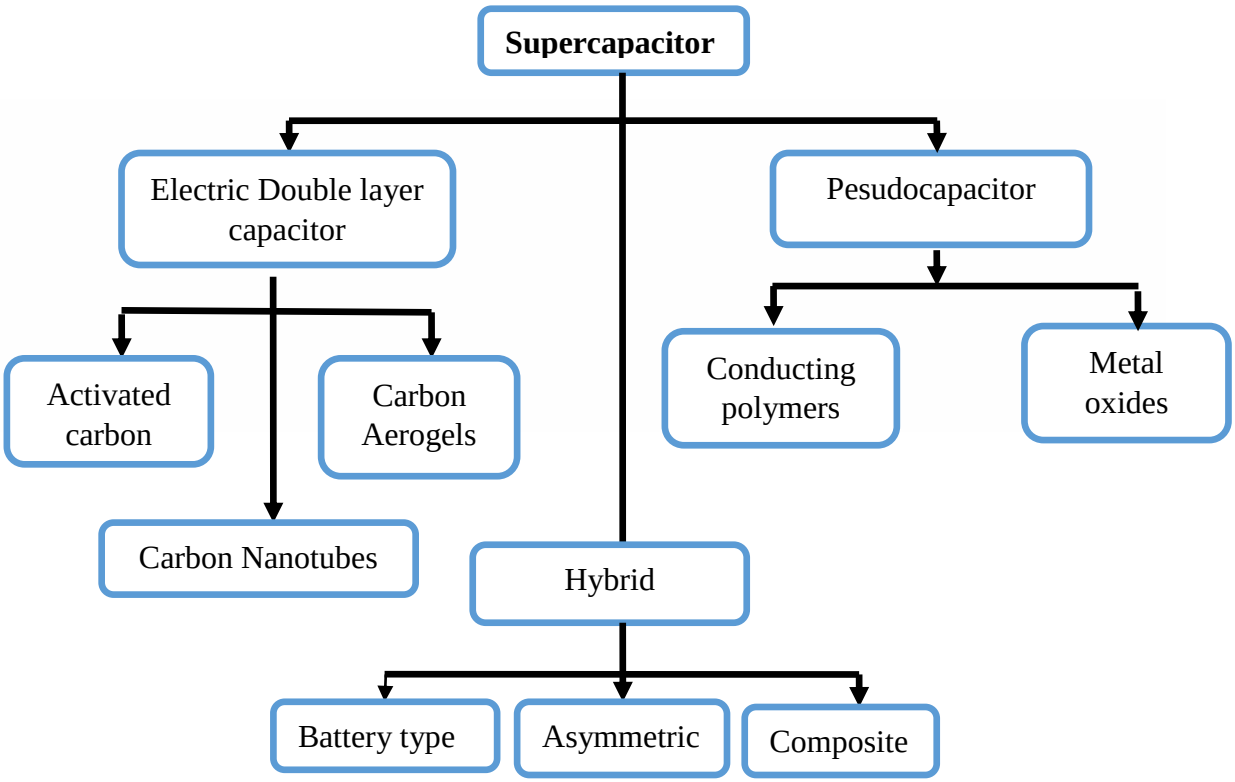

Figure 1.3 Classification of supercapacitors

1.4.1 Electrochemical double layer capacitors (EDLC)

The electrochemical double layer capacitance EDLC, store charges by physical adsorption at the electrode material and the electrolyte interface. This charge accumulation is a non-faradic process responsible for the capacitance of EDLC. During charging of the EDLC, electrons moves from negative electrode to positive electrode and cations in electrolyte move towards negative electrode while anions move towards the positive electrode. During discharge, reverse process takes place [20]. However, due to the electrostatic surface charging mechanism, EDLCs devices experience a limited energy density, which is why today's EDLC research is mainly focused on increasing energy performance and improving temperature range where batteries cannot operate. Carbon electrode materials generally have higher surface area, lower cost, and more established fabrication techniques than other materials, such as conducting polymers and metal oxides [21]. Recently, different kinds of carbon materials that can be used to store charge in EDLC electrodes, such as activated carbons (ACs), carbon aerogels, and carbon nanotubes [22].

Energy storage mechanism in EDLCs

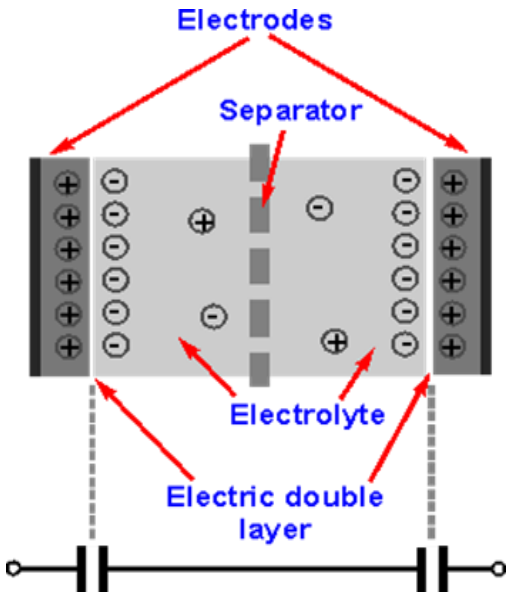

Figure 1.4 Schematic representation of EDLCs

- EDLCs have two electrodes immersed in an electrolyte. Applications of electric potential leads to electrons flowing onto the negative electrode plate from the negative polarity side of sources.

- Electrons that have arrived from the source attract positively charged ions existing in the electrolyte.
- An ionic layer is formed by these separations of positive and negative charges on the negative plate side.
- EDLCs have two electrodes immersed in an electrolyte. Applications of electric potential leads to electrons flowing onto the negative electrode plate from the negative polarity side of sources.
- Electrons that have arrived from the source attract positively charged ions existing in the electrolyte.
- An ionic layer is formed by these separations of positive and negative charges on the negative plate side [23].

1.4.2 Pseudocapacitors

EDLCs store charge electrostatically, while pseudocapacitor store charge by the reversible redox reactions at the surface of active materials. It involves fast reversible faradic reactions like electrosorption, redox reactions and intercalation processes at the electrode/electrolytic interface. The charge-discharge behavior closely resembles a capacitor than a galvanic cell. This pseudocapacitor behavior was first studied by Conwat et al., in 1975. The capacitance arising from such a system is referred to as pseudocapacitance to distinguish it from the double layer capacitance. The pseudocapacitance is related with charge stored (ΔQ) and change of potential (ΔV) as follows,

$$C = \frac{\Delta Q}{\Delta V} \qquad 3$$

In pseudocapacitance, thermodynamic change of potential during charge accumulation has been occurred during the redox process. Pseudocapacitors are known to exhibit better reversibility. Pseudocapacitors exhibit both battery like behaviour with Faradic reaction occurring across the electrochemical double layer, and conventional capacitor behaviour with high reversibility and high power [20]. The following types of redox reactions occur in pseudocapacitors.

1. Reversible surface adsorption of proton or metal ions from the electrolyte at the electrode.
2. Redox reaction of transition metal oxides
3. Reversible electrochemical doping-dedoping in conducting polymers

Energy storage mechanism of pseudocapacitor

There are several faradaic mechanisms that can result in capacitive electrochemical features:

(1) Under potential deposition.

(2) Redox pseudo capacitor (as in RuO_2&H_2O).

(3) Intercalation pseudo capacitor.

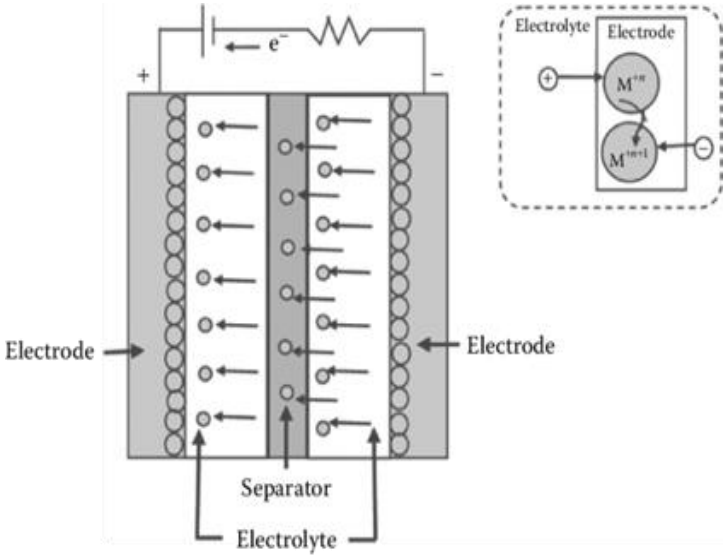

Figure 1.5 Schematic representation of Pseudocapacitor

- Under-potential deposition occurs when metal ions form an adsorbed monolayer at a different metal's surface well above their redox potential. One classic example of under-potential deposition is that of lead on the surface of a gold electrode.

- Redox pseudo-capacitor occurs when ions are electrochemically adsorbed onto the surface or near surface of material with a concomitant faradaic charge-transfer.

- Intercalation pseudo-capacitor occurs when ions intercalate into the tunnels or layers of a redox-active material accompanied by a faradaic charge-transfer with no crystallographic phase change. Intercalation pseudo-capacitor mechanism combines the benefits of a battery material (charge storage within bulk) and a super capacitor material (rapid).

- The nature of the electrolyte and its interaction with the electrode materials has a strong influence on the pseudo capacitive behavior and thus the pseudo capacitor., there are several types of electrochemical processes that can contribute to the pseudo capacitor, including reversible adsorption of ions from the electrolyte, redox reactions involving ions from the electrolyte for some transition metal oxides, reversible electrochemical doping in conductive polymer-based electrodes, and lattice intercalation [24].

1.4.3 Hybrid capacitor

Hybrid electrochemical capacitor which consists of a double layer carbon material and a pseudocapacitance material has attracted signification attentions. EDLCs offer good cyclic stability, good power performance while in the case of pseudo capacitor it offers greater specific capacitance. In the case of hybrid system it offers a combination of both, that is by combining the energy source of battery-like electrode, with a power source of capacitor-like electrode in the same cell

Several combinations have been tested in the past with both positive and negative electrodes in aqueous and inorganic electrolytes. Generally, the faradic electrode results in an increase of energy density at the cost of cyclic stability, which is the main drawback of hybrid devices compared to EDLCs, it is imperative to avoid turning a good super-capacitor into an ordinary battery.

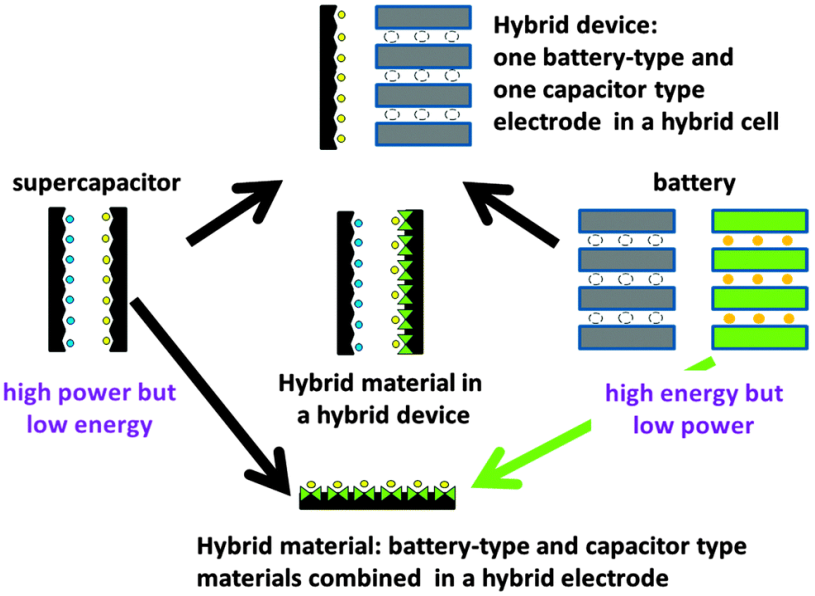

Figure 1.6 Schematic representation of hybrid capacitor

The three main types of hybrid capacitor configurations are as follows:

1. Composite hybrid: Composite electrodes to integrate carbon-based materials with either conducting polymer or metal oxide materials and incorporate both physical and chemical charge storage mechanisms together in a single electrode. The pseudo-capacitive materials are able to further increase the capacitance of the composite electrode through Faradaic reactions.

2. Battery-type: Like asymmetric hybrids, battery-type hybrids couple two different electrodes; however, battery-type hybrids are unique in coupling a super-capacitor electrode with a battery electrode. This specialized configuration reflects the demand for higher energy super-capacitors and higher power batteries, combining the energy characteristics of batteries with the power, cycle life, and recharging times of super-capacitors. Research has focused primarily on using nickel hydroxide, lead dioxide, and LTO ($Li_4Ti_5O_{12}$) as one electrode and activated carbon as the other.

3. Asymmetric, for example; Asymmetric hybrids combine Faradaic and non-Faradaic processes by coupling an EDLC electrode with pseudo-capacitor electrode Activated carbons - $Li_4Ti_5O_{12}$. The intention behind such types of constructive combination is to achieve high energy density of battery electrode to the high power density of super

capacitor electrode. Asymmetric hybrid capacitors that couple these two electrodes mitigate the extent of this tradeoff to achieve higher energy and power densities than comparable EDLCs. Also, they have better cycling stability than comparable pseudo-capacitors [25].

1.5 Components of Electrochemical Supercapacitor

The main components of an electrochemical supercapacitor are electrodes and electrolyte. The role of the electrodes is to provide a connection between conducting part and non-metallic part of the circuit. The voltage generated from a cell depends on the two metals used as electrodes and the concentration of the electrolyte ions. The role of the electrolyte in an electrochemical device is to establish a highly conductive pathway for ions and provide electronic insulation between the electrodes [26].

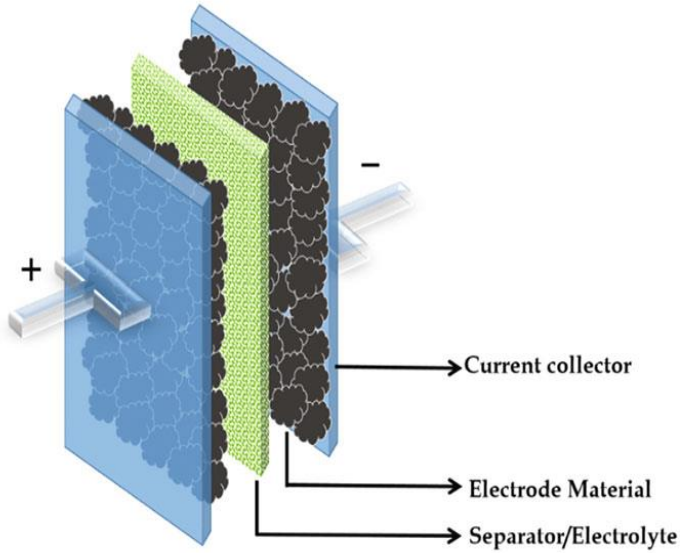

Figure 1.7 Schematic representation components of supercapacitor

1.5.1 Electrode

It is used in electrochemical cell and is referred as either a cathode or anode. At anode (indicated by a minus symbol, "−") the electrons leave the cell and oxidation occurs, and at cathode (indicated by a minus symbol, "+") the electrons enter the cell and reduction occurs. Each electrode converted into the anode or the cathode depending on to the route of current through the cell. A bipolar electrode is an electrode that behaves as the anode for one cell and

the cathode for another cell. Electrochemical double layer capacitors were primarily composed of carbonaceous materials, statically deposit charges within the porous structures of electrodes. Pseudocapacitor, which consists of transitional metal oxide and conducting polymers such ad electrodes, accumulates energy through fast, reversible electrochemical redox reaction on the active surface of the electrodes [27]. Both mechanisms share common qualifications for selecting appropriate materials in electrodes, which include the following:

- Large surface area and porosity
- Good surface wettability
- High electrical conductivity
- Long cycle stability (>10^5 cycles)

EDLCs electrode materials

The EDLCs are distinguished primarily by the form of carnon they use as an electrode material. Carbon electrode materials generally have higher surface area, lower cost, and more fabricated then other materials .

- Activated carbons (AC)
- Carbon aerogels (CNTs)
- Carbon nanotubes
- Graphene

Pseudocapacitors electrode materials

Pseudocapacitor electrodes utilize redox reactions on the surfaces of electroactive materials. The redox reactions are electrode potential dependent and change with charging and discharging. In EDLCs, which store charge electrostatically, pseudocapacitor store charge faradically through the transfer of charge between electrode and electrolyte. This is accomplished through electrosorption, reduction-oxidation reactions, and intercalation processes. These Faradaic processes may allow pseudocapacitors to achieve greater capacitances and energy densities than EDLCs [28].

- Conducting polymers
- Metal oxide

1.5.2 Current collector

The current collectors are metallic connectrd to the external circuit that polarize (positively or negatively). The electrode and electrolyte materials are the active components of supercapacitors, whereas the current collector is a passive component. An Important feature of current collector is its electrical conductivity, which must be high. The collector also has to be inert to the electrolyte [30].

1.5.3 Separator

The separator prevents the occurrence of electrical contact between the two electrodes, but it is ion-permeable, allowing ionic charge transfer to take place. The specific requirements of a separator are low electrical resistance for ion transfer within the electrolyte while having a strong electronic insulating capability, high chemical and electrochemical stabilities in the electrolyte, good mechanical strength to provide device durability and low thickness. Therefore, separators are usually made from thin and highly porous films or membrane. Commonly used separator materials in EDLC are cellulose, polymer membranes, glass fibre, paper, ceramic and polymer electrolyte.

Furthermore, the separator's properties such as chemical composition, thickness, porosity, pore size distribution and surface morphology were found to have a noticeable influence on several EDLC performance indicators including polarizability limits, specific capacitance, equivalent series resistance, specific energy and power densities [31].

1.5.4 Electrolyte

Electrolyte is an important role in overall electrochemical supercapacitor performance. In supercapacitors, the electro-decomposition voltage of the electrolyte determines the operating potential of the device. It is a medium which has free positive and negative ions for current flow. Under normal condition, electrolytes have an equal amount of cations and anions in the form of free electrons or free ions to conduct electricity.

Electrolyte is an ionic conductor but an electronic insulator, and it is practically either a solid or more often a liquid which usually works with porous membrane or gel in electrochemical energy storage devices. The electrolyte is mainly determined by solubility of the electrolytic ions, mobility of the free/dissociated ions, salvation of the free ions, dielectric constant of the bulk solvent, and viscosity of solvent. A liquid electrolyte commonly refers to

a solution comprising salts and solvents, and functional additives, but it can also be a pure liquid salt, such as an ionic liquid or a molten salt. The conductivity of electrolytes is mainly determined by solubility of the electrolytic ions, mobility of the free/dissociated ions, solvation of the free ions, dielectric constant of the bulk solvent, and viscosity of solvent. The electrolyte generally should be the following requirements:

- Wide electrochemical window
- High ionic conductivity
- High chemical and thermal stability
- Chemical inertness to other cell components such separator, electrode substrates and cell packaging materials
- Safe, non-toxic, and economically affordable

Nowadays, electrochemical cells are widely used in various electrochemical applications like in semiconductors, capacitors and electro/optical devices. The use of polymer electrolyte can resolve these difficulties and are predictable to improve the performance of conventional liquid systems. Polymer electrolytes used in electrochemical cell have shown high performance, good ionic conduction and optically transparent. Their researches were focusing interested in developing polymer electrolytes for electrochemical devices which are flexible, movable, biodegradable and economical. These electrolytes can be prepared by using ionic salts, plasticizers, polymers and ceramics [32].

1.6 Types of electrolytes

The electrolyte used in making the supercapacitor is an important component which charges the capacitance of the supercapacitor. Electrochemical supercapacitors using aqueous electrolytes posses both high conductivity and capacitance, but their working voltage is limited by the narrow decomposition voltage of aqueous electrolytes. Although organic electrolytes and ionic liquids can operate at higher voltages, they normally suffer from much lower ionic conductivity. Solid-state electrolytes may avoid the potential leakage problem of the liquid electrolytes, but they also suffer from low conductivity.

Most recently, solid electrolyte or gel electrolyte were obtained from proton conducting polymer electrolyte, which attracted great attention for the fabrication of solid state supercapacitor. The electrolytes can be divided into aqueous, organic, ionic liquids and gel electrolytes. There are varieties of electrolytes that are being employed in supercapacitor devices to validate their overall impact on the capacitive performance. They can be classified into the following broad categories [32].

1.6.1 Liquid electrolytes

The liquid electrolytes are classified into two groups; the aqueous and organic electrolytes Liquid electrolytes may be molten salts or non-aqueous electrolyte Till today, aqueous electrolytes are largely used to develop the supercapacitor, due to its easy preparation, low cost, non–toxic nature and the high ionic conductivity (~10-3 S cm^{-1})**.** But limited operating potential window (1.23 V) of aqueous system kept limit on the performance of supercapacitor. Although the operating potential of organic electrolytes can reaches up to 3 V, but they are associated with safety risks because of the flammability and highly toxic nature. Their practical energy density is also small and most of them are below 5 Wh kg-1. The main reason is that capacitance is not large enough due to the large sizes of the organic molecules (15–20 Å). Both aqueous and organic liquid electrolytes have some common drawbacks. The supercapacitor fabrication with these kinds of electrolytes required high–cost packaging materials and techniques to avoid possible leakage of electrolytes, as most of the electrolytes are highly toxic and corrosive. Secondly, it is quite difficult to fabricate small and Flexible supercapacitor using liquid electrolyte. Another limitation is that the evaporation of liquid electrolyte effectively reduces the energy storing capacity of the supercapacitor. Therefore, it is essential to search new electrolyte system which is more suitable as compared to the liquid electrolyte [33].

1.6.2 Ionic Liquids electrolyte

Ionic liquids (ILs) are another important class of electrolytes for supercapacitors. These ionic liquids are often dissolved in organic solvents or taken in their pure form (solvent free electrolyte) to investigate the overall impact on the performance of a supercapacitor device. The physical and chemical properties of these ionic liquids strongly depend on the type of cation and anion. Their properties of low vapor pressure, high chemical and thermal stability, low flammability, and electrochemical potential range 2 to 6 V, typically about 4.5

V. Usage of ionic liquids is limited by low conductivity value, in the range of mS/cm. Because of this feature ionic liquids are used in supercapacitors which are operated at higher temperatures [34].

1.6.3 Solid state electrolytes

Solid electrolytes are in solid form they possess ionic conductivity in the range of 10^{-6} to10^{-8} S/cm at room temperature. The conductivity in these electrolytes is due to the movement of ions through holes present in crystal lattice. The cations or anions must be allowed to transfer in the arrangement as charge transports. These solid electrolytes have numerous rewards over conventional liquid electrolyte but their conductivity is lower than the mandatory conductivity for device application. On the basis of structural and physical properties, solid electrolytes are classified in four categories:

- Framework crystalline materials
- Amorphous – glassy electrolytes
- Composite electrolytes
- Polymer electrolytes

1.6.4 Framework Crystalline Materials

Crystalline solid electrolytes are those which direct H^+, Li^+, Na^+, K^+, O_2-as well as various bivalent and trivalent cations. They have usually ionic and covalent bonding. The conductivity in such electrolytes is due to the hopping of ions from one site to another site present in crystal structure. The number of sites is generally more than the number of mobile ions present. The mobile ions act as ion conductors as they have dispersion coefficient.

1.6.5 Amorphous Glassy Electrolytes

They have more advantageous properties over crystalline materials like (i) absence of grain boundaries, (ii) high ionic conductivity, (iii) wide range of compositional variability, (iv) preparation into desirable shapes and can be formed in thin film forms. These glassy electrolytes are formed by mixing of three different compositions, $MX\text{-}M_2O\text{-}A_xO_y$, where A_xO_y is the oxide, which can be B_2O_3, P_2O_5, SiO_2 and MoO_3 etc., M_2O is the network modifier e.g., Ag_2O, Li_2O, Cu_2O and Na_2O etc. and MX is the doping salt usually metal halides e.g. AgI, CuI and LiI. Conductivity of these materials can be controlled by varying the

amount of glass former, glass modifier and dopant salt. These glassy materials are usually prepared either by the melt-quench techniques or sol-gel methods.

1.6.6 Composite Electrolyte

Composite electrolytes are basically two phase solid systems in which two or more materials are mixed together to get some desired material properties, particularly enhancement in the ionic conductivity of materials at room temperature. These composite materials are prepared by dispersing sub micrometer size insulating and chemically inert materials (called second phase dispersoids such as Al_2O_3,SiO_2,NiO, GeO_2, Bi_2O_3, ZrO_2, etc.) into a moderate ionically conducting solids (called first phase or host materials).

1.6.7 Polymer Electrolytes

Polymer electrolytes are the composites of polymers and salts/acids, these salts/acids provides ions to the insulating polymer matrix but some polymer electrolytes have their own ion producing groups and known as polyelectrolytes. They act as electrode separator and provide electronic insulation and fast transport of the desired ions between the electrodes. Polymer electrolytes are of great interest to use them in electrochemical devices because of their properties like flexibility, versatility in shape, elasticity, thermal stability, light weight, ease of fabrication, mechanical integrity, good electrode-electrolyte contact, cost effective etc. They possess ionic conductivity in the range of 10^{-5} to ~ 10^{-2} S/cm with solid free-standing consistency. Examples of solid polymer electrolytes are PEO-$AgNO_3$, PEO-$LiCF_3SO_3$, PEO-$LiClO_4$ and PPO-$LiClO_4$.

Electrolytes are finding their place in between the electrodes so they are in close interaction with cathode and anode. For better performance of the device electrolyte should have following essential characteristics:

- Stability toward both the electrode surfaces
- Good ionic conductor and electronic insulator
- Wide electrochemical window
- Strong against electrical, thermal and mechanical spites
- Inert to other cell components

P. V. Wright (1973) discovered first ion conducting polymer electrolyte by using polyethylene oxide (PEO) with alkali salt. Later Armand and co-workers explored the

application of these materials for device application. Since that time, a lot of research activities on the solid state ionic conductors have been carried out around the world to find suitable polymer electrolytes as a substitute of liquid electrolytes. A great number of polymer electrolytes were reported by researchers, using different moveable ions like Li^+, Na^+, H^+, K^+, Ag^+, Zn^+, Cu^+, Mg_2^+ etc., found their applications in different electrochemical devices such as, electrochromic devices, fuel cells, batteries, supercapacitors, dye sensitized solar cells, sensors, etc.

1.6.1.1 Types of polymer electrolytes

The polymer based solid electrolytes for supercapacitor can be grouped into three types:

- Solid polymer electrolytes (SPEs, also known as dry polymer electrolytes),
- Composite polymer electrolytes,
- Gel polymer electrolytes (GPE).

The SPE composed of a polymer (e.g., PEO) and a salt (eg., LiCl), without any solvents (eg., water). The ionic conductivity of SPE is provided by the transportation of salt ions through the polymer. The GPE consists of a polymer host (e.g., PVA) and an aqueous electrolyte (e.g., H_2SO_4) or a conducting salt dissolved in a solvent. Composite polymer electrolytes include high surface area inorganic solids in proportion with a 'dry solid polymer' or 'polymer gel'.

(i) Dry solid polymer electrolytes (SPEs)

The dry solid polymer electrolytes are mostly based on high molecular weight polymers like poly (ethylene oxide) (PEO) and/or poly (propylene oxide) (PPO) as they typically form stable dry complexes and exhibit higher ionic conductivity than other solvating polymers when complexes with different Li^+ ion salts. These polymers have tendency to make complexes with numerous ionic salts /acids due to the occurrence of polar groups like –O–, –H–, and –C–H– in the polymer chain and persist in a single phase. The development of polymer – salt/acid complex is also governed by solvation energy and lattice energies of the polymers and inorganic salts. The lower standards of both the parameters; namely lattice energy of salt and cohesive energy of the polymer, allows the formation of stable polymer-salt complex.

The ionic conductivity in these polymer electrolytes is mostly depends on the occurrence of these inorganic ionic salts or acids. As a common trend the conductivity reduces

as the salt concentration increases. The reason behind the reduction in conductivity is the interference in the motion of ion transportation as well as the creation of ion pairs which effects in the decrease in the number of free ions exists for the conduction. Though, the ion transportation in these SPEs is owing to local moderation as well as segmental motion of the polymer chains, which happens at high degree of amorphicity in the host polymer. The major disadvantage of these dry polymer electrolytes is their low ionic conductivity (10^{-6} to10^{-8} S/cm) at room temperature which is due to the crystalline nature of polymer host. PEO shows crystalline nature below 70^{o}C but above this temperature, it occurs in the amorphous state. Hence, a basic valuable conductivity (~10^{-4} S/cm) is easily attainable in the temperature series of 70–90^{o}C [36].

(ii) Composite Polymer Electrolytes (CPEs)

Composite polymer electrolytes (CPEs) are simply prepared by dissolving a small portion of micro/nanosize inorganic (ceramic)/organic filler particles into the conventional SPE host. CPEs are produced by dispersing small amount of organic or inorganic fillers into the polymer electrolytes. These CPEs offer some advantages such as good interfacial contact at electrode– electrolyte region, high flexibility, improved ion transport, high ionic conductivity and excellent thermodynamic stability towards lithium and other alkali metals.

Weston and Steele in 1982 was the first to show the consequence of dissolving inert α-alumina filler in the PEO system. CPEs containing nano metre grain size fillers are also known as nano composite polymer electrolytes (NCPEs). It was observed that the adding of fillers improved the ionic conductivity, mechanical stability and the interfacial activity of SPEs. It was further found that the size of the filler particles plays a significant role in improving the physical properties, mechanical and electrochemical properties of the composite polymer electrolyte systems. Depending on the conduction processes, ceramic fillers are of two types namely; active and passive fillers. The one which is actively participating in the conduction processes (Li_3N, γ-$LiAlO_2$ etc.) are called as active fillers whereas the inactive fillers (Al_2O_3, SiO_2, MgO, NiO, TiO_2, and ZrO_2etc.) which do not involves in the conduction process is called as passive fillers [37-38].

(iii) Gel polymer electrolytes (GPEs)

Gel polymer electrolytes (GPEs) are also termed as ‘polymer hybrids’ or ‘gelionics’. GPEs are formed when the polymer host and doping salt are dissolved in polar and high

dielectric constant organic solvents or plasticizer. They are generally formed by adding a huge amount of liquid plasticizer and/or solvent(s) to polymer matrix. Hence, GPEs possess both cohesive property of solids and the diffusive property of liquids. Usually, the plasticizers which are used in gel electrolytes are low-evaporation solvents, like, propylene carbonate (PC), ethylene carbonate (EC), dibutyl phthalate (DBP), diethyl carbonate (DEC) and high dielectric constant solvent such as N,N–dimethyl formamide (DMF) and γ–butyrolactone are widely used as main components of GPEs. They show high ionic conductivity but reduced mechanical strength as compared to the solvent-free SPEs.

The organic solution remained trapped within the polymer matrix and lead to the formation of gels with a very high ionic conductivity. A gel electrolyte is a mixture of polymer, salt and the solvent. Various polymers such as polyvinyl alcohol (PVA), poly (ethylene oxide) (PEO), poly (methyl methacrylate) (PMMA), poly (pacrylonitrile) (PAN), poly (vinylidene fluoride) (PVdF) and poly (vinylidene fluoride-hexafluoroproplene) (PVdF-co- HFP) have been used for making gel electrolytes. It have been created which showed the ionic conductivity values in the order of$\sim 10^{-4}$ to 10^{-3} S/cm at room temperature as well as shows good electrochemical constancy, and free standing nature. It has been detected that the use of plasticizer increases the degree of amorphicity of the polymer hosts which results in increase in ionic mobility and hence increases the ionic conductivity. However, the occurrence of liquid plasticizers in extreme quantity in the polymer matrix diminishes the mechanical integrity of GPEs, as well as number of problems commonly faced in liquid electrolytes. The volatile nature of the organic solvents/plasticizers reduces the conductivity of the gel in the long run. High volume of liquid phase in the gels restricts their temperature range of stable performance.

GPEs have many inherent properties, for instance low interfacial resistance, decreased reactivity towards the electrode materials, improved safety and exhibit better shape flexibility as well as significant increase in ionic conductivity with a small portion of plasticizers.

Gel polymer electrolyte has the advantage of being safe and flexible without the need of any separator [38].

Solid electrolytes encompasses investigations of physical and chemical behavior of the solids with fast ion movement within the bulk as well as their technological aspects. These solid electrolytes are also called as the ‘superionic solids’ or ‘fast ion conductors’. The solid

electrolytes show tremendous scope to develop all–solid–state mini/micro electrochemical devices viz. batteries, fuel cells, supercapacitors,, etc. The solid electrolytes have the following characteristics;

- High ionic conductivity in the range of 10^{-2} to 10^{-4} S cm^{-1}
- Ions are the principle charge carriers
- High thermal and electrochemical stability.

1.7 Natural polymer based electrolytes

Natural polymers have shown great interest in the production of devices for generating and storing energy at low cost. Natural polymers are cost effective and eco-friendly derived from renewable sources and become a promising replacement for synthetic polymers. There are a wide variety of natural polymers used for making polymer electrolytes like- agar-agar, cellulose, chitosan, gelatin, pectin, starch, etc. In these natural polymers based electrolytes glycerol and water are widely used as plasticizer. The ionic conductivity has been found in the order of 10^{-4} S/cm at room temperature. They can be used in different electrochemical devices applications like smart windows, electronic and optical devices, capacitors.

- Cellulose membrane Electrolytes
- Agar membrane Electrolytes
- Pectin membrane Electrolytes
- Starch membrane Electrolytes
- Chitoson membrane Electrolytes
- Cellulose membrane Electrolytes

Cellulose is important as they have good viscosimetric, emulsifying, stabilizing, dispersing and agglutinant properties. They are highly soluble in some organic solvents and water. They also have ability to form films with desirable mechanical strength. These characteristics make them appropriate for applications in ink, paper, food, pharmaceutical, cosmetic, ceramic, textile and agricultural products. Some researchers also used cellulose and its derivatives for making SPEs by doping different salts and obtained conductivity in the range of 10^{-6} to 10^{-4} S/cm at room temperature.

Cellulose is the most abundant biopolymer in excellent chemical stability, good water solubility, non-toxic nature, and is renewable, sustainable and environmentally friendly. Among all of the materials (biopolymer), one shows potential aspirant to act as polymer host for proton-conducting biopolymer electrolytes (BEs) is carboxymethyl cellulose (CMC). Recently, due to the good biocompatibility and biodegradable CMC attracts more attention as representative water-soluble polysaccharide in many research fields. CMC contains a hydrophobic polysaccharide backbone and many hydrophilic carboxyl groups, and hence shows amphiphilic characteristics. The substitution of CH_2- COONa group is in homogeneous in both substituted position and degree, which increases the complexity of hydrogen bondste. CMC has been serving as an electrode material, binder and gel electrolytes in energy storage systems which include lithium ion batteries, fuel cells and supercapacitors [38].

1.8 Advantages of supercapacitor

- Extremely low internal resistance or effective series resistance and consequently high efficiency.
- The energy storage mechanism of super-capacitor is a highly reversible process. The process moves charge and ions only. It does not make or break chemical bonds. It is therefore, capable of hundreds of thousands of complete cycles with minimal change in performance.
- Super-capacitor is of rapid action. They charge/discharge the current in much faster manner than the batteries.
- Super-capacitors are ideal when a quick charge is needed to fill a short-term power need; whereas batteries are chosen to provide long-term energy.
- It works in a broad range of temperature.
- High current capability. Super-capacitor is designed with a very low equivalent series resistance (ESR), allowing it to deliver and absorb very high current. Commonly, the charge/discharge current can be up to 1000A.
- Wide temperature range. Super-capacitor can operate in temperature range -40° C-70° C, greatly wider than that of batteries.

- High specific power up to 17kW/kg.
- Extremely low internal resistance.
- Reduce battery size, weight and cost.

1.9 Limitations of supercapacitor

- Super-capacitors have low specific energy.
- Expensive in terms of cost per watt.
- Linear discharge voltage prevents using the full energy spectrum.
- High self-discharge; higher than batteries.
- Low cell voltage; requires serial connections with voltage balancing.

1.10 Applications of supercapacitor

- Supercapacitors have found applications in household appliances, electronic tools, mobile telephones, cameras etc.
- Electrochemical capacitors are increasingly reliable devices which can work with turbines or photovoltaic cell.
- Super-capacitors are most effective to bridge power gaps lasting from a few seconds to a few minutes and can be recharged quickly. Eg. Flywheel.
- Other applications are to start backup generators during power outages and provide power until the switch-over is stabilized.
- The virtue of ultra-rapid charging during regenerative braking and delivery of high current on acceleration makes the super-capacitor ideal as a peak-load enhancer for hybrid vehicles as well as for fuel cell applications.
- Backup power system in missiles.
- Power sources for laptops, flash in cameras.
- Used in diesel engine start up in submarines and tanks.

- Today small size super-capacitors as for example gold caps from Tokin are widely used as maintenance-free power sources for IC memories and microcomputers [36].

OBJECTIVES:

- To prepare a membrane using natural products with high conductivity for the application of supercapacitor

METHODOLOGY

- To optimize the ratio of CMC:BB membrane without salt and identify a best ratio for standalone membrane formation
- To add electrolytic salts at varied concentrations in the selected membranes to improve electrolytic conduction

CHAPTER-II

REVIEW OF LITERATURE

Membrane electrolyte based on natural polymers, such as cellulose derivatives, chitosan, starch etc. are to be investigated due to their natural abundance, low price and environmentally friendly nature. The potential of cellulose based solid polymer electrolytes (SPEs) can be studied extensively by means of electrical conductivity property due to their applications in solid state electrochemical cells, fuel cells, batteries and electro chromic devices.

3.1 Cellulose based Membrane Electrolytes

Cellulose and its derivatives are important as they have good viscosimetric, stabilizing, and dispersing properties. They are highly soluble in some organic solvents and water. They also have ability to form films with desirable mechanical strength. These characteristics make them appropriate for applications in ink, paper, food, pharmaceutical, cosmetic, ceramic, textile and agricultural products. Some researchers also used cellulose and its derivatives for making membrane electrolytes by different salts and obtained conductivity in the range of 10^{-6} to 10^{-4} S/cm at room temperature.

3.2. Gelatin based Membrane Electrolytes

Gelatin is a form of protein and was the first materials to be used in the production of movies. This protein is very promising in the area of development of new materials, since it is abundantly available, has low cost, good film-forming properties, nontoxic and forms transparent solutions with high viscosity. Gelatin films are generally obtained by solubilization, heat and dehydration of collagen, which leads to a distortion of a partial triple helix of this macromolecule. However to improve its functional properties formaldehyde and glutaraldehyde are used as crosslinking agents. It is observed that in SPEs based on gelatin the conductivity lies in between 10^{-5} to 10^{-4} S/cm.

3.3 Starch based Membrane Electrolytes

Starch is an interesting natural polymer. It is abundantly present in nature in various forms and can be obtained from various renewable sources. It is the major reserve material of many plant storage tissues. Starch is a mixture of two units; linear amylose and highly

branched amylopectin. It is soluble in some organic solvents and hot water. It has an ability to form film with good mechanical strength.

3.4 Chitosan based Membrane Eletcrolytes

Chitosan is a derivative of chitin and one of the most studied natural polymers. It is a poly cationic polymer due to the existence of one amino group and two hydroxyl groups in its repeating units. Chitosan has been extensively studied due to its specific properties, such as biocompatibility and bioactivity. It is widely used in pharmaceutical and industrial applications. Chitosan also constitutes a polymer host for electrolytes because it is able to dissolve ionic salts and promote ionic conductivity.

3.5 Natural Gum based Membrane Electrolytes

Natural gums are polysaccharides of natural origin. They can increase the viscosity of the solutions even at small concentration. They are used as thickening agents, gelling agents, emulsifying agents, and stabilizers. Most often these gums are found in the woody elements of plants or in seed coatings. They are classified according to their origin as well as they are categorized as uncharged and ionic polymers or polyelectrolytes. For example gum arabica and gellan gum are polyelectrolytes whereas xanthan and guar gums are uncharged.

S. No	Reported by	Electrolyte materials	Conductivity (S/cm)	Refrences
1.	Diogo F. Vieira and Agnieszka Pawlicka, (2010)	Gelatin - $LiBF_4$ Gelatin - lithium perchlorate ($LiClO_4$)	2.29×10^{-5} 1.5×10^{-5} – 4.9×10^{-4}	[39]
2.	Rozali, et al., (2012)	Carboxymethyl cellulose (CMC)-Salicylic acid (SA)	9.50×10^{-8}	[40]
3.	Rita Leones, et al., (2012)	Gelatin – $(C_2mim)(OAc)$ Agar - $[C_2mim][C_2SO_4]$ $[C_2mim][OAc]$	1.18×10^{-4} 2.25×10^{-5}	[41]

		[Ch][OAc]		
4.	Raphael, et al., (2012)	Agar - $LiClO_4$	6.5×10^{-5}	[42]
5.	Pawlicka, et al., (2012)	Xanthum gum – Acetic acid (AA), glutaraldehyde (GA) and ethylene glycol (EG)	7.26×10^{-5} - 3.92×10^{-4}	[44]
6.	Y.N. Sudhakar and M. Selvakumar, (2012)	Chitosan (CS) – Starch lithium perchlorate ($LiClO_4$)	3.7×10^{-4}	[45]
7.	K. H. Kamarudin and M. I. N. Isa, (2013)	CMC- ammonium nitrate (AN)	7.71×10^{-3}	[46]
8.	M. F. H. Abd El-Kader and H. S. Ragab, (2013)	Starch/methylcellulose	0.41×10^{-7}	[47]
9.	Mohd Saiful Asmail Rani, et al., (2014)	CMC-CH_3COONH_4	5.77×10^{-4}	[48]
10.	Rahul Singh, et al., (2014)	Starch - Potassium iodide (KI)	3.41×10^{-4}	[49]
11.	Sudhakar, et al., (2014)	Guar gum (GG) - $LiClO_4$	2.2×10^{-3}	[50]
12.	Shukur, et al., (2014)	Starch - LiOAc	$(2.07 \pm 0.53) \times 10^{-5}$ - $(1.04 \pm 0.10) \times 10^{-3}$	[51]
13.	Yusof, et al., (2014)	Corn starch- Chitosan Ammonium iodide (NH_4I)	$(3.04 \pm 0.32) \times 10^{-4}$	[52]
14.	Ramlli M.A and Isa M.I.N, et al., (2014)	Carboxyl methyl cellulose (CMC) – Ammonium Fluoride	2.68×10^{-7}	[53]

		(NH_4F)		
15.	Sohaimy and M. I. N. Isa, (2015)	CMC-$(NH_4)_2CO_3$	7.71×10^{-6}	[54]
16.	Przemyslaw Ledwon, et al., (2015)	HPC- dichloromethane	3.5×10^{-3}	[55]
17.	Sudhakar, et al., (2015)	HEC-Phosphoric acid(H_3PO_4)	4.19×10^{-3}	[56]
18.	Teoh, et al., (2016)	Corn Starch - $LiClO_4$ and ($BaTiO_3$)	1.28×10^{-2}	[57]
19.	M. N. Chai and M. I. N. Isa, (2016)	CMC- Oleic acid-Glycerol	1.64×10^{-4}	[58]
20.	Ahmad and Isa , (2016)	CMC-NH_4Cl	1.43×10^{-3}	[59]
21.	Shikha Gupta and Pradeep K .Varshney, (2017)	HEC- lithium tetraborate (Li_2B4O_7)	4.6×10^{-3}	[60]
22.	N. Suganya and V. Jaisankar, (2017)	CMC -co-polyacrylamide (PAAm)/polyaniline	2.71×10^{-4}	[61]
23.	Anna Railanmaa, et al., (2017)	Starch and gelatin - NaCl	10^{-4} - 10^{-5}	[62]
24.	Mohd. Khalid and Ana M. B. Honorato, et al., (2017)	Gum Arabic (GA)-ortho-phosphoric acid (H_3PO_4)	17.9 mS cm^{-1}	[63]
25.	Jagdish Kumar Chauhan, et al., (2017)	Starch- Sodium perchloride ($NaClO_4$)	$>10^{-3}$	[64]

26.	Zainuddin, et al., (2018)	CMC- Kappa Carrageenan (KC)	3.91×10^{-7}	[65]
27.	A.S. Samsudin, and M.A. Saadiah, (2018)	CMC- ammonium bromide (NH_4Br)	1.12×10^{-4}	[66]
28.	Nwanya, et al., (2015)	Agar- ($LiClO_4$) Agar- ($K\ ClO_4$) Agar-(CH3COOH)	3.53×10^{-8} 2.24×10^{-8} 9.12×10^{-8}	[67]

CHAPTER-III

MATERIALS AND METHODS

3.1 INTRODUCTION

This chapter gives the description of various materials and the method of preparing of natural product based electrolytic membranes studied in this thesis and respective experimental techniques used for their characterization. Selection of materials depend on various parameters like its abundance, efficiency, cost effectiveness, environmental friendly nature; easy synthesis process etc., membrane electrolyte is one of the most important classes of polymeric materials due to their potential application in different electrochemical devices like batteries, fuel cells and supercapacitors. Mostly, the membrane electrolytes posses' ionic conductivity of the order of 10^{-3} S cm^{-1}, which is quite acceptable from device fabrication point of view, but it lacks in its mechanical strength due to its gelly nature.

3.2 MATERIALS

- Carboxymethyl cellulose (CMC)
- Bovine bone (BB) gelatin
- Potassium hydroxide (KOH)
- Lithium hydroxide (LiOH)

3.3 PREPARATION OF POLYMER ELECTROLYTE

The Sodium Carboxymethyl cellulose (CMC) based membrane films are prepared by dissolving distilled water (10 ml) and simultaneously, Bovine Bone (BB) in 5 ml distilled water. The CMC and BB is separately homogenized using magnetic stirrer. The different concentrations of KOH and LiOH are taken in appropriate weight percentage (wt %) ratio and added to the solution of CMC-BB. The mixture is stirred continuously for 1hr at 40°C until it

gets homogenized. Inner surface of the petri dish is swapped with glycerol. Then the homogeneous solution mixture is poured in petri dishes and left to dry for 12hrs at room temperature to obtain the membrane. They are peeled out. Due to the environmental concern the toxic solvents are replaced by using non toxic solvents such as (water, ethanol *etc.,).*

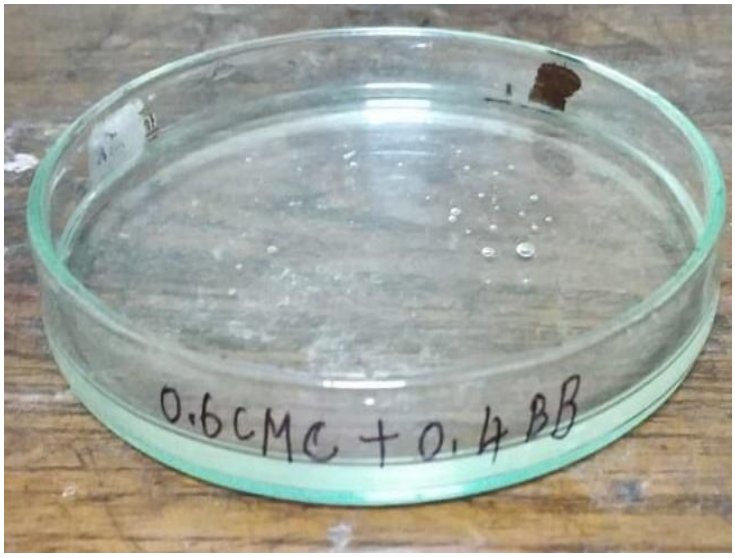

Figure 3.1 Prepared solution poured into the petridish

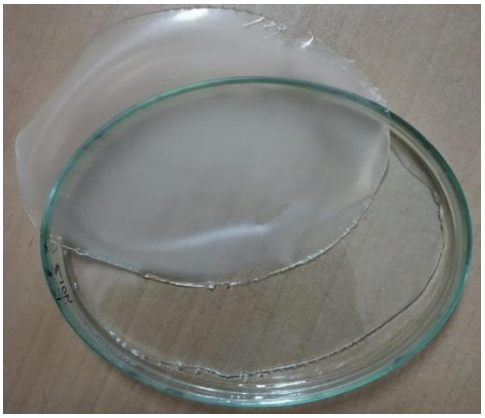

Figure 3.2 Peeled CMC:BB membrane

Initially the membrane films are prepared using different ratio of CMC and BB. To standardize the film forming capacity and conduction testing. The details of the concentration of the constituents are given in the Table 3.1 and Table 3.2

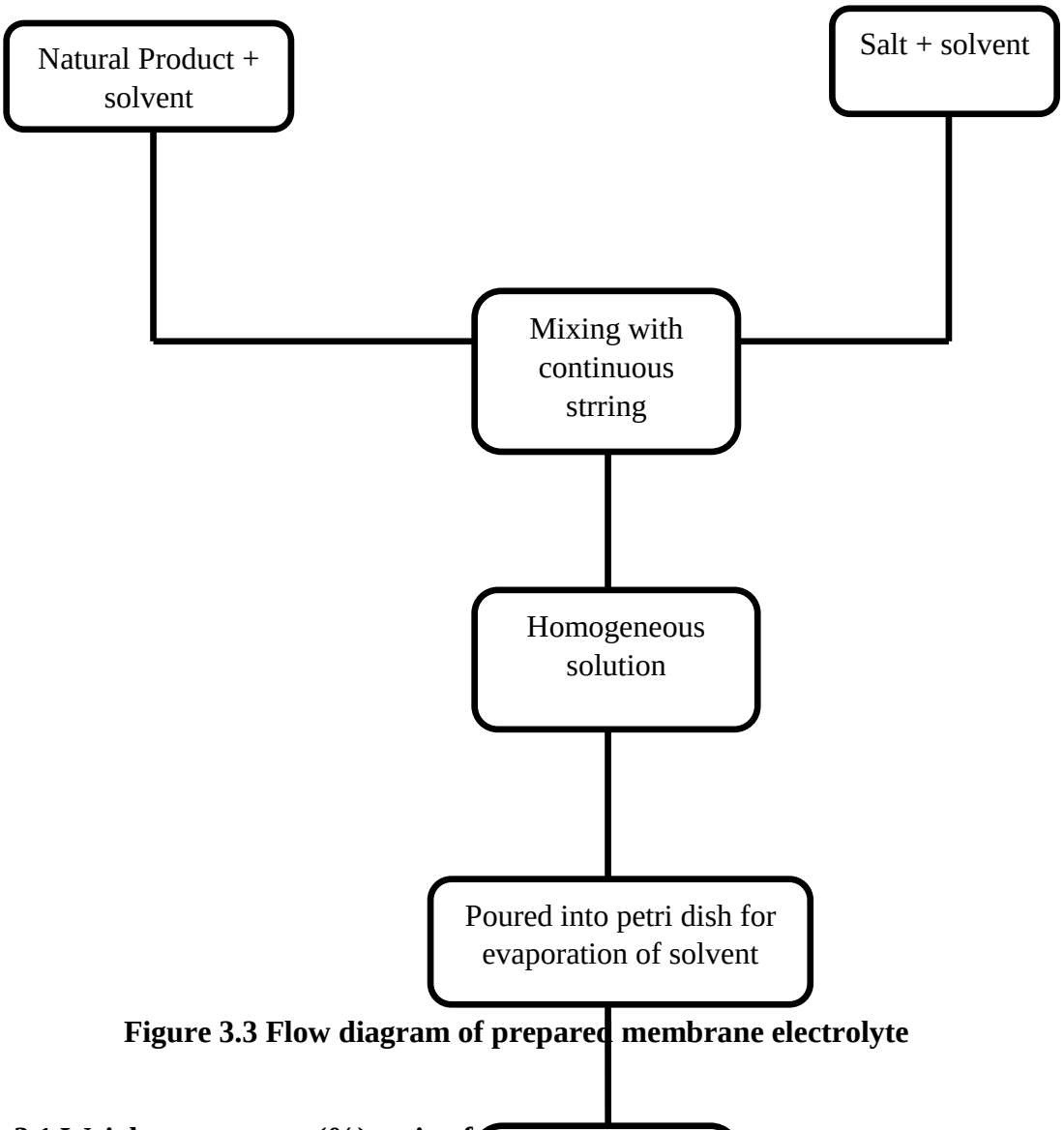

Figure 3.3 Flow diagram of prepared membrane electrolyte

Table 3.1 Weight percentage (%) ratio of

S.No	Rati	
	CMC	BB
1	10	90
2	20	80

3	30	70
4	40	60
5	50	50
6	60	40
7	70	30
8	80	20
9	90	10

Table 3.2 Composite of KOH and LiOH electrolyte

S. No	Ratio of CMC-BB	KOH-LiOH (g)
1	1:9 5:5 9:1	0.01
2		0.03
3		0.05
4		0.07
5		0.09

3.4 CHARACTERIZATION

Ionic conductivity and dielectric constant was analyzed by electrochemical impedance spectroscopy (EIS). The vibrational spectral analysis was characterized by Fourier Transform Infrared Spectroscopy (FTIR).

3.4.1 ELECTROCHEMICAL IMPEDANCE SPECTROSCOPY (EIS)

3.4.1.1 INTRODUCTION

The electrochemical impedance method was developed in the 1950s, based on earlier studies of dielectric systems. In the early 1980s frequency response analyzers came into the market. Meanwhile, ac impedance spectroscopy belongs to the routine techniques in

electrochemistry. By imposing potential sweeps, potential steps or current steps, the electrochemical cell is generally driven to a condition far from equilibrium, and a transient response signal is observed [68]. The ac impedance method perturbs the cell with an alternating signal of small magnitude.

3.4.1.2 IMPEDANCE

Impedance spectroscopy (IS) is used to evaluate different electrical and electrochemical properties in wide frequency domain due to electrode/electrolyte interfacial reactions and the migration of ions within electrolyte or ion conducting solids. The terms resistance and impedance both denote an opposition to the flow of electrons or current. In direct current (dc) circuits, only resistors produce this effect. However, in alternation current (ac) circuits, two other circuit elements, capacitors and inductors, impede the flow of electrons. Impedance can be expressed as a complex number, where the resistance is the real component and the combined capacitance and inductance is the imaginary component. The total impedance in a circuit is the combined opposition of all its resistors, capacitors, and inductors to the flow of electrons. The opposition of capacitors and inductors is given the same name reactance, symbolized by X and measured in ohms. Since the symbol for capacitance is C, capacitive reactance is symbolized by XC. Similarly, since the symbol for inductance is L, inductive reactance is symbolized by XL. Capacitors and inductors affect not only the magnitude of an alternating current but also its time-dependent characteristics or phase. When most of the opposition to current flow comes from its capacitive reactance, a circuit is said to be largely capacitive and the current leads the applied voltage in phase angle. When most of the opposition to current flow comes from its inductive reactance, a circuit is said to be largely inductive and the current lags the applied voltage in phase angle. The more inductive a circuit is, the closer the difference in phase angle approaches 90 degrees.

It’s sometimes easier to perform calculations using admittance, the reciprocal of impedance. Admittance is symbolized by Y and measured in siemens (S). Like impedance, admittance can be expressed as a complex number, where the conductance, the reciprocal of resistance, is the real component, and the susceptance, the reciprocal of reactance, is the imaginary component.

3.4.1.3 IMPEDANCE PARAMETERS

In general electrical characterizations can be done by DC and AC measurement techniques. Though the DC measurement technique is straightforward, it cannot be implemented for solid electrolytes for the following reason:

As the DC field is applied to the electrolyte, the material gets polarized and ionic conductivity ceases giving only electronic conductivity. It is difficult to find an electrode material compatible with the solid electrolyte that does not give polarization effects at electrode-electrolyte interface. Therefore for solid electrolytes, AC measurement of electrical conductivity is done to avoid polarization of the sample.

On applying a sinusoidal voltage $V=V_{max}\sin\omega t$, where ω ($2\pi f$) is the angular frequency, a current will flow within the electrolyte with identical frequency to that of applied voltage. Due to capacitive and inductive effects, however the current is typically out of phase with voltage.

$$I=I_{max} \sin(\omega t+\theta) \quad (1)$$

Where

I_{max} is the maximum current and θ is the phase angle.

The relationship between applied voltage and resultant current can be written as:

$$Z=V_{max}/ I_{max} \quad (2)$$

where,

- V_{max} is maximum voltage.
- Z is the total impedance or opposition to the charge flow within electrolyte.

The admittance, the ease of charge flow through the material can be written as:

$$Y=1/Z = I_{max}/ V_{max} \quad (3)$$

With a phase difference between V_{max} and I_{max}, the impedance and admittance are vector quantities, processing magnitude and phase and as such may be represented in the

vector plane. Similarly both quantities may be represented in the complex plane, where X and Y axes are designated as the real and imaginary components respectively.

$$Z = Z'_{real} - jZ''_{imaginary} \quad (4)$$

$$Y = Y'_{real} - jY''_{imaginary} \quad (5)$$

However to obtain a more accurate characterization of the material under study is often necessary to use two other formalisms, closely related to those mentioned above; i.e., the complex electric modulus and complex permittivity. They are given by

$$M = M''_{real} - M''_{imaginary} = j\omega C_0 Z \quad (6)$$

$$\varepsilon = \varepsilon'_{real} - \varepsilon''_{imaginary} = (j\omega C_0)^{-1} Y \quad (7)$$

where C_0 is the vacuum capacitance of the cell.

3.4.1.4 NYQUIST PLOT OR COLE-COLE PLOT

In the electrochemical impedance analysis, an AC potential is applied to a solid electrolyte and the current through the sample is measured. The response to this potential is an AC current signal containing the excitation frequency and harmonics. By observing the current response, the resistance within different frequencies can be examined. The electrochemical impedance is measured from this small excitation signal and the data can be represented as Nyquist plot.

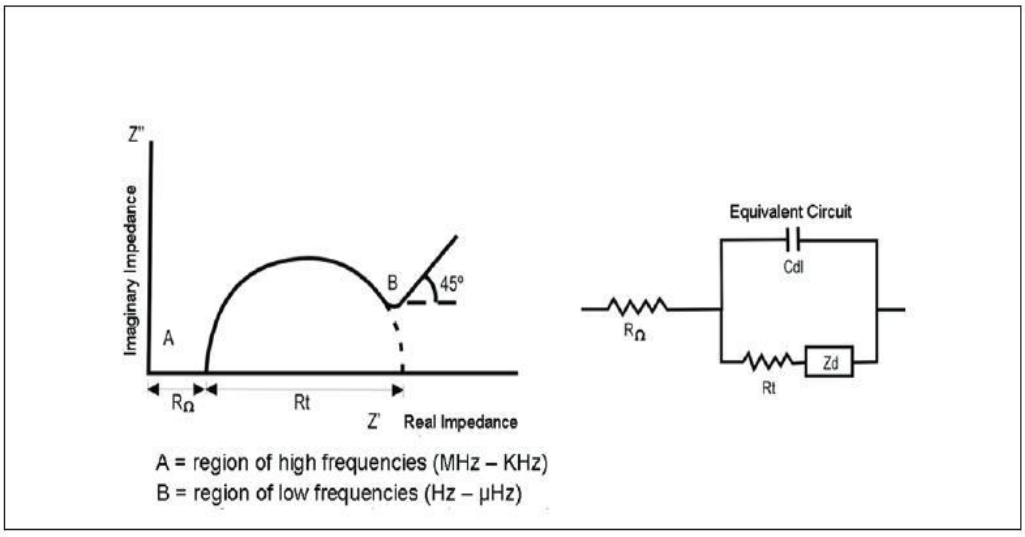

Figure 3.4 Schematic representation for Nyquist plot

On the Nyquist plot the impedance can be represented as a vector (arrow) of length |Z|. The angle between this vector and the X-axis, commonly called as the "phase angle", f (=arg Z). Another common representation is Bode plot where impedance is plotted with log frequency on the X-axis and both the absolute values of the impedance (|Z|=Z0) and the phase-shift on the Y-axis.

Equivalent circuit modeling of EIS data is used to extract physically meaningful properties of the electrochemical system by modeling the impedance data in terms of an electrical circuit composed of ideal resistors (R), capacitors (C) and inductors (L). The generalized Constant Phase Element (CPE) and Warburg Element (Z_W) are also used to represent the diffusion or mass transport impedances of the cell.

The ionic conductivity of membrane electrolyte is an important parameter which can be calculated by the help of A.C impedance spectroscopy and expressed as:

$$\sigma = t/R_bA$$

Where,

t is the thickness of the sample,

R_b is the bulk resistance and

A is the area of the sample.

The bulk resistance can be determined from the Nyquist plot where the semicircles intercept on the Z‟ axis. Hence by using Nyquist plot, the values of the relasxation time, the bulk capacitance of the sample can also be obtained [69].

3.4.2 FOURIER TRANSFORMATION INFRARED SPECTROSCOPY (FTIR)

3.4.2.1 INTRODUCTION

FTIR (Fourier Transform Infra-Red) spectrometer obtains a infrared spectra by first collecting an interferogram of a sample signal using an interferometer, then performs a Fourier Transform on the interferogram to obtain the spectrum.

An interferometer is an instrument that uses the technique of superimposing (interfering) two or more waves, to detect differences between them. The FTIR spectrometer uses a Michelson interferometer.

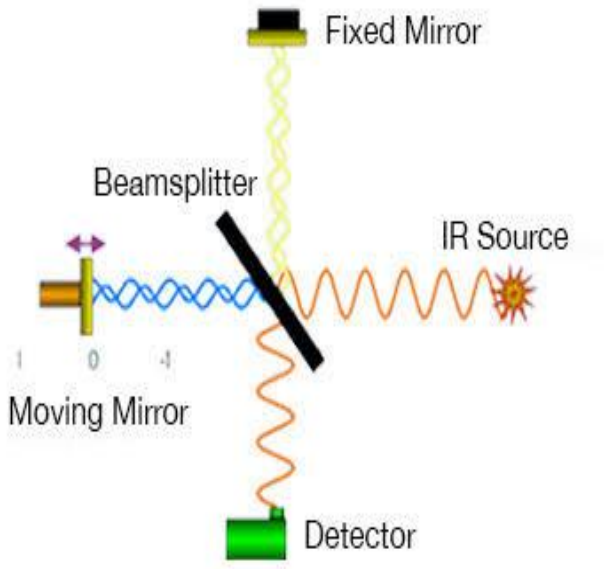

Figure 3.5 Schematic representation of Michelson Interferometer

3.4.2.2 WORKING PRINCIPLE

- The optical system in an FTIR spectrometer is very simple: the interferometer requires two mirrors, an infrared light source, an infrared detector, and a beam splitter.
- The beam splitter is the heart of the interferometer. Essentially a half-silvered mirror, the beam splitter reflects about half of an incident light beam while simultaneously transmitting the remaining half.
- One half of this split light beam travels to the interferometer's moving mirror while the other half travels to the interferometer's stationary mirror.
- The two mirrors reflect both beams back to the beam splitter where each of the two beams is again half reflected and half transmitted. Two output beams result: one travels to the detector as the other travels to the source.
- When the two beams return to the beam splitter, an interference pattern, or interferogram, is generated. This interference pattern varies with the displacement of the moving mirror, that is, with the difference in path length in the two arms of the interferometer.
- The interference pattern, detected by the infrared detector as variations in the infrared energy level, is what ultimately yields spectral information [70].

Figure 3.6k Photograph of Fourier Transform Infrared Spectrometer

3.4.2.3 SAMPLE ANALYSIS PROCESS

- The source
- The interferometer
- The sample
- The detector

(i) The Source

Infrared energy is emitted from a glowing black body source. This beam passes through an aperture which controls the amount of energy presented to the sample (and, ultimately, to the detector). The two common sources are

- **Nernst filament**-It consists of a spindle of rare earth oxides about 1 inch long and 0.1 inch diameter. The Nernst requires to be pre-heated before it conducts electricity, but once red-heat is reached the temperature is maintained by the current.
- **Globar filament**-It consists of a rod of carborandum, somewhat thicker and longer than the Nernst.

(ii) The Interferometer

The beam enters the interferometer where the "spectral encoding" takes place. The resulting interferogram signal then exits the interferometer.

(iii) The Sample

The sample is held between plates of polished mineral salt rather than glass. Pure liquids studied in thickness of about 0.01mm, while solutions are usually 0.1-10 mm thick, depending on the dilution.

- Gas samples at pressure of about 1 atm or greater are usually contained in glass cells either 5 to 10cm long, closed at their ends with rock salt windows.
- Solid samples are more difficult to examine because the particles reflect and scatter the incident radiation and transmittance is always low.

(iv) The Detector

The beam finally passes to the detector for final measurement. The detectors used are specially designed to measure the special interferogram signal. There are two types of detector which are in common use. One is sensing the heating effect of the radiation, the other depends on the photoconductivity. The greater the effect at a given frequency, the greater is the transmittance of the sample at that frequency.

- Pyroelectric detectors such as deuterated triglycine sulphate (DTGS) are commonly used in FT spectrometers. As they are also thermal detectors they are sensitive across the whole IR range, but have the rapid signal response needed in interferometry.

- Photoconductive detectors in common use are Indium antimonide (InSb) which can be used above 1400 cm-1 and Mercury cadmium telluride (MCT) are used above 700 cm These detectors operate at liquid nitrogen temperature.

(v) The Computer

The measured signal is digitized and sent to the computer where the Fourier transformation takes place. The final infrared spectrum is then presented to the user for interpretation and any further manipulation.

3.4.2.4 SAMPLE PREPARATION

IR spectra can be measured using liquid, solid, or gaseous samples that are placed in the beam of infrared light. A drop of a liquid can be placed as a thin film between two salt plates made of NaCl or KBr, which are transparent to infrared light at most important frequencies. A solid can be ground with KBr and pressed into a disk that is placed in the light beam. Alternatively, a solid sample can be ground into a pasty mull with paraffin oil. As with a liquid, the mull is placed between two salt plates.

Solids can also be dissolved in common solvents such as CH_2Cl_2, CCl_2, or CS_2 that do not have absorptions in the areas of interest. Gases are placed in a longer cell with polished salt windows. These gas cells often contain mirrors that reflect the beam through the cell several times for stronger absorption [70].

CHAPTER-IV

RESULTS AND DISCUSSION

4.1 INTRODUCTION

The present work aims to prepare and study the electrical properties of the membranes for supercapacitors application. A first time attempt is made to synthesize various ratios of CMC and Bovine bone with different concentrations of electrolytic salts KOH and LiOH. The membranes are prepared by solution casting method and intended towards the application as an electrolyte cum separator for supercapacitor. The prepared films are characterized by Electrochemical Impedance Analysis and Fourier Transform Infrared spectroscopy (FTIR) and the results are discussed in this chapter.

4.2 ELECTROCHEMICAL IMPEDANCE SPECTROSCOPY (EIS) ANALYSIS

Electrochemical spectroscopy is used to study charging and transport phenomena in ion-conducting and conjugated matrix. Clearly, the impedance plot of the samples comprises a broadened semicircle in the high frequency region followed by a spike in the lower frequency region. The incomplete semicircle at higher frequencies can be attributed to the formation of double layer capacitance at the electrode/electrolyte interface. The impedance spectra measurement are carried out for the determination of conductivity and dielectric properties of the prepared membranes. The evaluation is made throughout large range of frequencies from 10 kHz to 1mHz where the prepared membranes are cut into preferred size of 2x2 cm^2 which is sandwiched between two copper electrodes and connected to the measurement leads of the instrument. The impedance measurements for all the prepared membranes are made in the instrument Biologic SP-150 in the two-electrode configuration.

4.2.1 CONDUCTIVITY MEASUREMENTS

The Nyquist plot consists of a high-frequency semicircle and low frequency spike as shown in the Figure 4.1. In general, the high-frequency semicircle is due to the parallel combination of solution/electrolytic resistance (migration of carriers, mostly ions due to the electrolytic nature of the membrane, through the host matrix) and bulk capacitance (due to immobile or insulating matrix). The low frequency spike can be attributed to the effect of blocking electrode which means that the conducting species in the electrolyte gets terminated

at the interface of electrolyte and the electrode. They do not diffuse into the electrode and hence are readily available during reversibility. The bulk resistance or the electrolytic resistance of the samples can be calculated from the low frequency intercept of semicircle and the high frequency intercept of spike on the real axis.

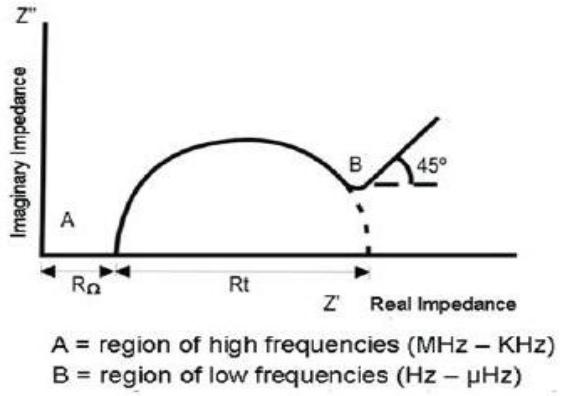

Figure 4.1 Illustration of the Impedance spectra

The interpretation of the EIS measurement is usually done by the correlation between the impedance data and the equivalent circuit representing the physical processes taking place in the system under investigation.The complex impedance plots otherwise known as Nyquist plot reveals the behavior of solution conduction, interfacial capacitance and the electrode-electrolyte interface phenomena.

The DC conductivity of the samples has been determined by fitting the experimental data using Z-view software and the experimental data fitted with the equivalent circuits. The solid circle indicates the experimental data and the line represents the fitted data. The value of the resistance can be calculated from the equivalent circuit. This equivalent circuit is a combination of resistance, capacitance, as well as a few specialized electrochemical elements such as constant phase element (CPE) and Warburg diffusion element.

The conductivity values of the sample can be measured using

$$\sigma = t / R_b . A \qquad (1)$$

where,

- **σ** is the conductivity (S cm^{-1}),
- t is the thickness of electrolytic membrane ,
- R_b is resistance (solution/ solution-matrix / interfacial) of electrolyte membrane and
- A is the area of the analysis of the film (cm^2).

4.2.1.1 Impedance measurements of CMC: BB membrane:

The electrolytic membranes based on Na- carboxymethyl cellulose (Na-CMC) and Bovine bone (BB) is prepared and electrolytic salts such as KOH and LiOH are incorporated. Figure 4.2 shows the schematic diagram of the prepared electrolytic membranes with different ratios of CMC, BB and KOH/LiOH.

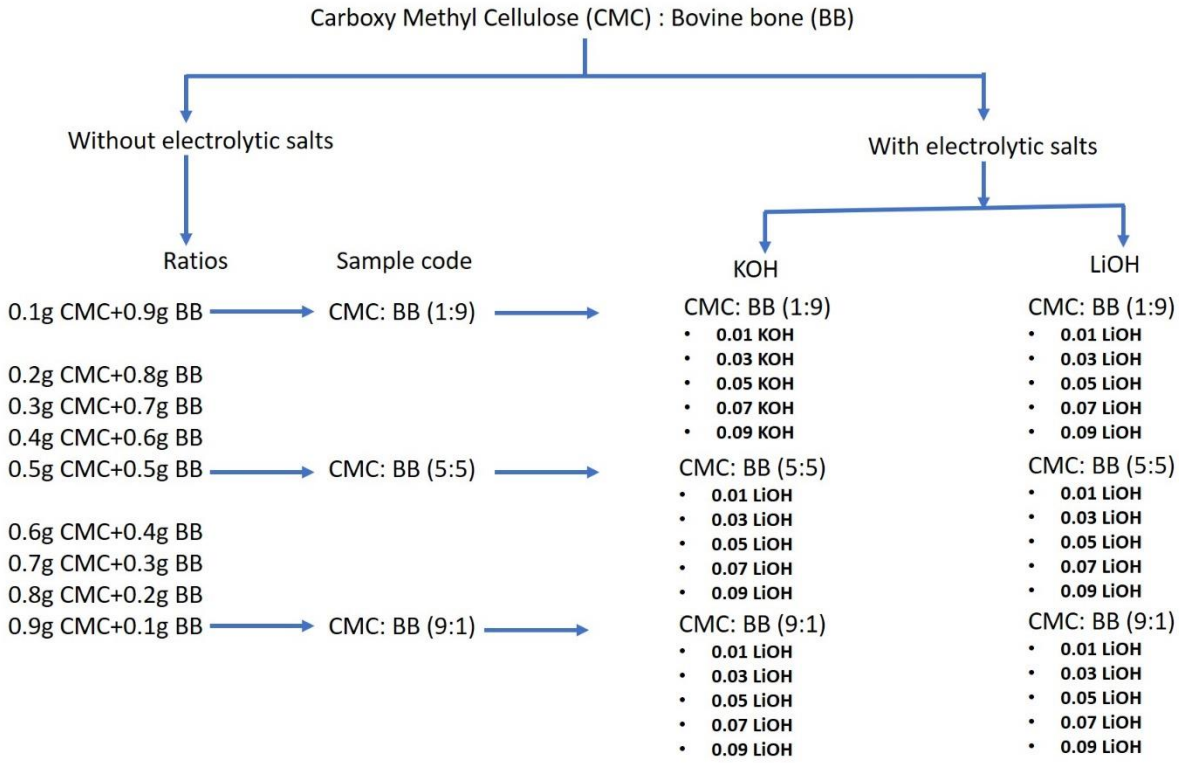

Figure 4.2 (a) Schematic diagram of the prepared electrolytic membranes

Figure 4.3 (a) shows the Nyquist plot of CMC: BB membranes of different compositions, in the frequency range of 10 kHz to 1mHz, with a sinusoidal amplitude of 10mV. A smaller voltage of 10mV is applied along with the ac sinusoidal frequency so that

the invasive technique of ac impedance shows prominent variations and also at the same time does not interfere with the natural resistance of the membrane.

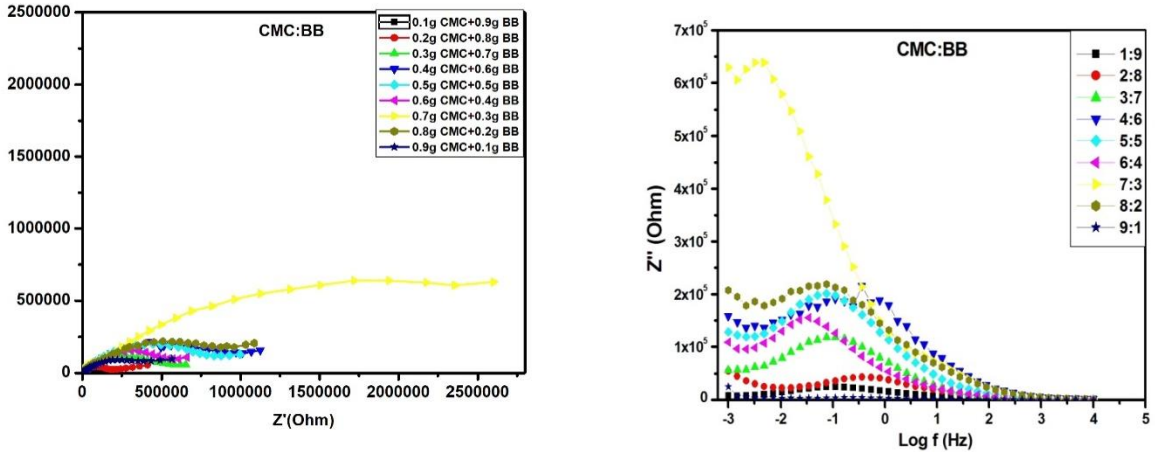

(a) **(b)**

Figure 4.3 (a & b)Comparison of Nyquist and Bode plot of imaginary impedance of all ratiosof CMC: BB without salt

Figure 4.4 (a-i) shows the best fit for the corresponding impedance plot and equivalent circuit confirms that there is an absolute agreement between the experimental and fitted results. The fitted data consists of series resistance with two parallel circuits with combination of constant phase element and resistance. It should be noted that the best fit of experimental data to the single time constant model was obtained using a constant phase element (CPE) rather than an ideal capacitor which is attributed to inhomogeneity in the conducting medium.

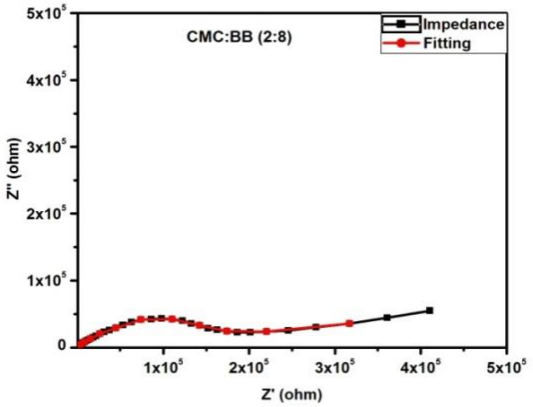
CMC:BB (2:8)
Impedance
Fitting
Z'' (ohm)
Z' (ohm)

(a)

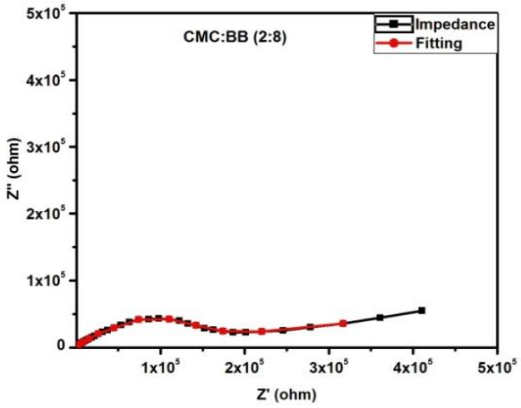
CMC:BB (2:8)
Impedance
Fitting
Z'' (ohm)
Z' (ohm)

(b)

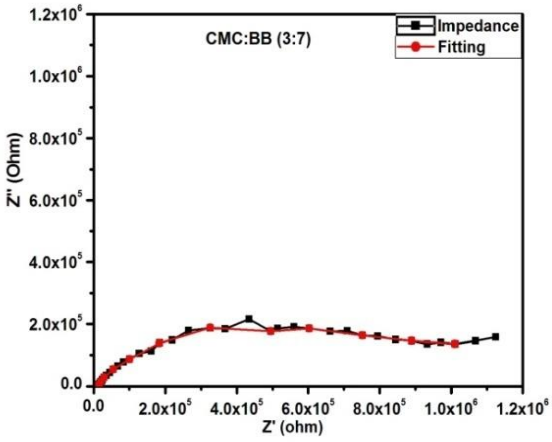
CMC:BB (3:7)
Impedance
Fitting
Z'' (Ohm)
Z' (ohm)

(c)

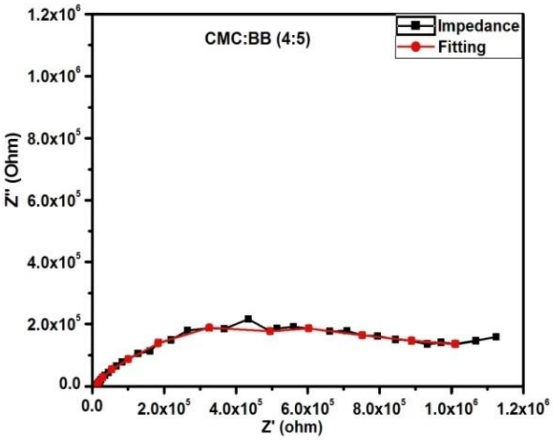
CMC:BB (4:5)
Impedance
Fitting
Z'' (Ohm)
Z' (ohm)

(d)

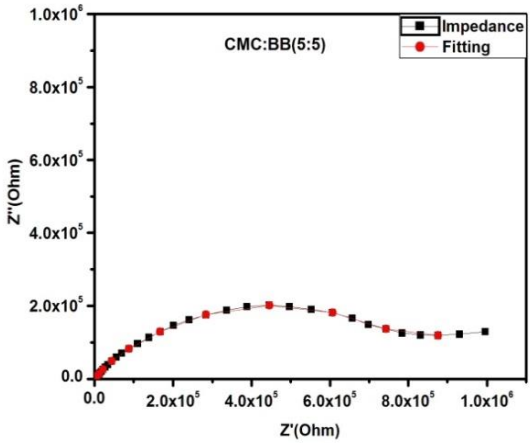
CMC:BB(5:5)
Impedance
Fitting
Z''(Ohm)
Z'(Ohm)

(e)

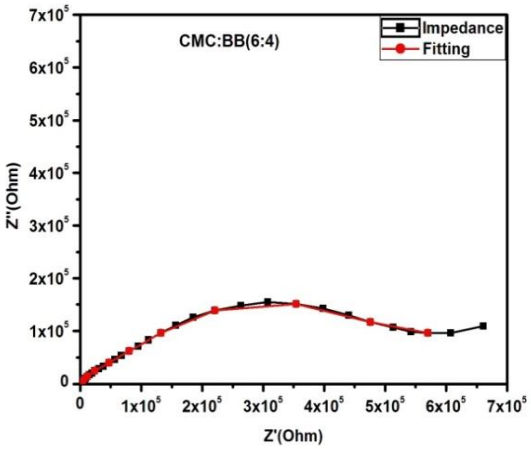
CMC:BB(6:4)
Impedance
Fitting
Z''(Ohm)
Z'(Ohm)

(f)

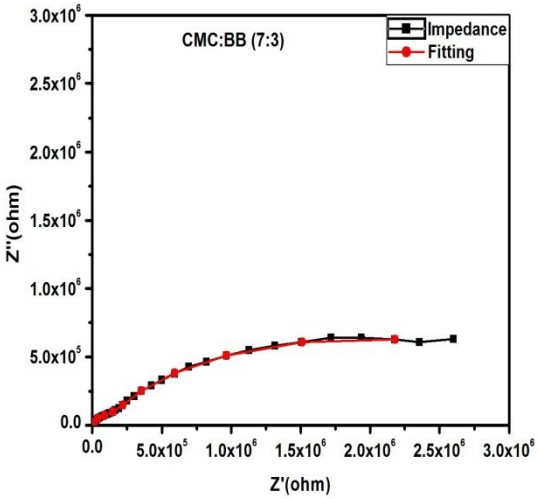

(g)

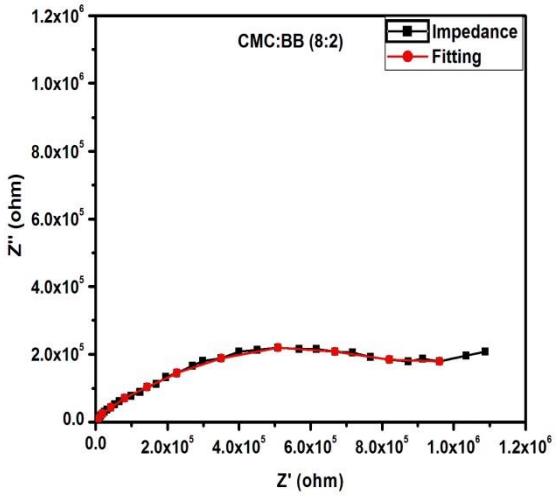

(h)

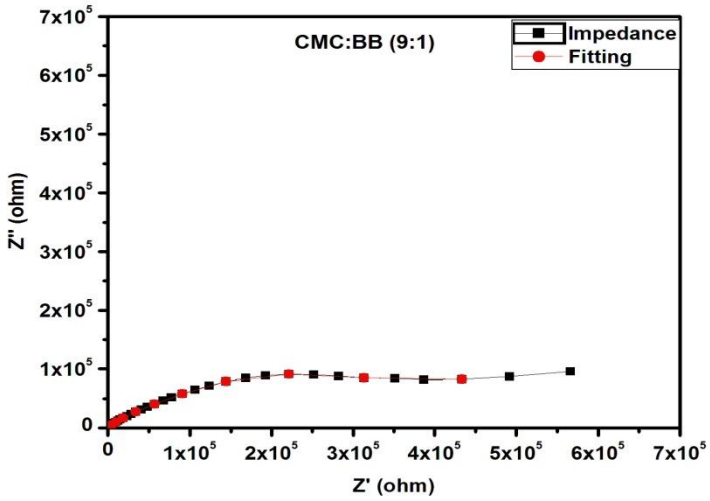

(i)

Figure 4.4 (a-i) Nyquist plot of different ratios of CMC:BB

Table 4.1 Comparison of CMC:BB membrane of different ratios and fitted data of equivalent circuits

S.No	Ratio of CMC : BB	Equivalent circuit	R_1 (Ω)	R2 (Ω)	R_3 (Ω)	CPE1-T (micro Farad)	CPE1-P	CPE2-T (micro Farad)	CPE2-P
1.	1 : 9	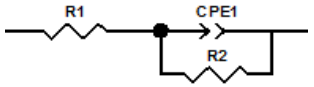	206.7	114090	-	9.9072	0.54	-	-
2.	2 : 8	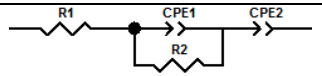	11.6	208790	-	3.7181	0.51	0.9531	0.45
3.	3 : 7	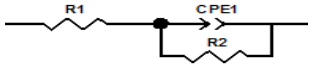	69.3	518900	-	2.3317	0.63	-	-
4.	4 : 6	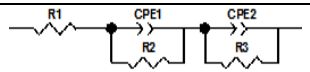	10655	566100	577870	0.89940	0.58	6.3739	0.61
5.	5 : 5	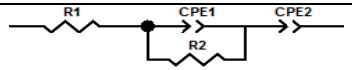	4.47	722550	-	1.6841	0.59	0.2539	0.34
6.	6: 4	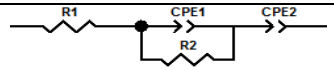	66.02	602310	-	3.6106	0.54	0.0222	0.53
7.	7 : 3	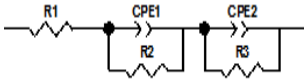	1573	2714100	95593	2.0488	0.57	0.2430	0.88
8.	8 : 2	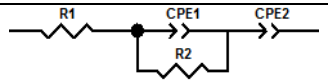	10.6	721090	-	1.0837	0.54	0.2051	0.33
9.	9 : 1	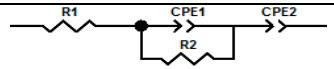	10	439260	-	5.3964	0.51	0.0882	0.73

Figures 4.3 (a & b) shows the comparison of all ratios of Nyquist plot, Bode plot of the imaginary impedance for the CMC: BB membranes of ratios 1: 9, 2:8, 3:7, 4:6, 5:5, 6:4,7:3, 8:2 and 9:1 respectively. The Bode plot of the CMC:BB Membrane of ratio 1:9 shows a relaxation at the frequency 106mHz indicating that the charge is discharged periodically after accumulation of charges in the electrode – electrolyte interface. The total resistance appears to depend on the ratio of CMC until the 5:5 ratios however, higher than this inconsistent change is observed which may be due to the poor homogenizing capacity of BB as the ratio of BB is smaller in these membranes. It is to be noted that the ratio of 8:2 is almost similar to 4:6 and 5:5 which proposes that the homogeneity plays a role. While the 9:1 shows extremely smaller resistance compared to the 5:5 but not smaller enough as 1:9. Thus, it is understood that by compositing the CMC and BB, a rational behaviour is expected only upto 5:5. However, as 9:1 have behaved peculiar further analyses are made on this composition also. The Bode plots of imaginary resistance of the ratios indicate the relaxation frequencies to be 358mHz, 106mHz, 346mHz, 75mHz, 357mHz, 4.8mHz, 23mHz for the compositions 2:8, 3:7, 4:6, 5:5, 6:4,7:3, 8:2 and 9:1 respectively. All the relaxations are in the mHz range and hence it is understood that the relaxation is caused only in the electrode electrolyte interface due to the blocking of charge carriers at the electrode interface. Hence, the matrix conduction is extremely through for incorporating electrolytic salt for improvisation of conduction. Table 4.1 shows the equivalent circuit and consolidated data of CMC and BB membranes of various ratios. The table includes the values of solution or electrolytic resistance (R1), resistance due to the insulating matrix (R2), Resistance due to the electrode electrolyte interface (R3) and the values of Constant Phase Element (CPE-T, CPE-P) due to the dispersion of conduction caused. The CPE1 corresponds to the capacitive component caused due to the insulating matrix with the conducting charge carrier and CPE2 refers to the polarization effects in the electrode electrolyte interface.

From the Table 4.1, among all the samples, 5:5 ratio of CMC and BB exhibit the lowest value of R1 (solution/electrolytic resistance) value 4.47 Ω. The electrolytic conduction is in the order of 5:5 < 9:1< 8:2< 2:8< 6:4< 3:7 <1:9 < 7:3 <4:6. Among all the last two ratios given above exhibits exorbitantly higher resistance whilst all the other have a meagre difference of few tens which need not be looked into very seriously. Looking into the CPE values, the ratios 1:9 and 3:7 did not exhibit the relaxation at the interface of electrode and

electrolyte. All the ratios exhibited the matrix to carrier relaxation. The order of capacitance of matrix to carrier relaxation is 4:6<8:2< 5:5 <7:3 <6:4 <2:8 < 9:1 <1:9. The dispersion component of the Constant Phase element is almost the same for all these capacitances. The capacitance caused due to the interface blocking is of the order of 7:3< 4:6 < 2:8 < 5:5< 8:2< 9:1 < 6:4. Overall view of all the three factors indicate that the more suitable ratio considering optimal electrolytic resistance, charge carrier capacitance due to the insulating matrix and the interfacial capacitive component is with 5:5.

4.2.1 Conductivity Measurements of CMC:BB Membranes withDifferent Concentrations of Electrolytic salt KOH and LiOH

To increase the conductivity of CMC: BB membranes, electrolytic salts can be composited with the membrane. Hence, in this work, various concentrations of KOH and LiOH (0.01g 0.03g, 0.05g, 0.07g, 0.09g) are added to the three ratios of CMC: BB Membrane namely 1:9, 5:5 and 9:1 ratios. The three are chosen on the following basis (i) 5:5 is chosen for the reasons stated already in the previous section such as this ratio exhibits an optimal electrolytic conduction, and their electrical properties are studied (ii) 1:9 is chosen as the membrane did not show any interfacial relaxation and (iii) 9:1 as it has all the three components, namely electrolytic resistance, resistance and relaxation due to the insulating matrix and also the interfacial relaxation, prominent.

4.2.1.1. Conductivity Measurements of CMC:BB (1:9) Membranes with different concentrations of Electrolytic salt KOH

Figures 4.3 (a &b) shows the comparison of Nyquist plot, Bode plot of the imaginary impedance of CMC:BB membrane of ratio 1:9 incorporated with 0.01, 0.03, 0.05, 0.07 and 0.09 g of KOH. Figure 4.4 (a-i) shows the Nyquist plot of all the concentrations of CMC: BB-KOH. The concentrations of KOH shows relaxation in the Bode Plot at frequencies 275mHz, 10mHz, 718mHz, 34mHz and 78mHz for the NaCl concentrations of 0.01,0.03,0.05,0.07 and 0.09g respectively. As all the frequencies are in mHz of relaxation, it is clear that the relaxation originates from the electrode electrolyte interfacial polarization and not due to the insulating matrix to the electrolytic salt included in the matrix. The order of the electrolytic resistance is 0.01g < 0.09g < 0.05g < 0.07g < 0.03g.

4.2.1.2 Impedance measurements of CMC: BB with KOH

(i) CMC: BB (1: 9)- KOH

The Nyquist plot of CMC: BB (1:9) with different concentrations of KOH alkaline salt is shown in figure 4.5(a). The dependence of conductivity on the salt concentration provides information on the specific interaction between the salt and the membrane matrix. The conductivity varies with a wide range of factors, such as cation and anion types, salt concentration, temperature, etc. In this case, the conductivity and other elements of CMC: BB ratios shows variation with respect to salt concentration. From the graph, it is seen that addition of different concentrations of salt with CMC: BB strongly influences the electrochemical impedance properties. Figure 4.5 (b) shows the bode plot of CMC: BB (1:9) with different concentrations of KOH. From the bode plot observed, there is relaxation in all the bode plots indicating that there is only one time constant related to the relaxation in all the concentrations of KOH. The peak frequencies shift to lower frequencies indicating that the interfacial layer gets thicker with higher concentrations of KOH. The Nyquist plot of 0.07gKOH shows very high resistance but in the Bode plot, the same frequency of relaxation is observed indicating that the interfacial resistance is not altered but there may be some agglomerations of KOH in this sample which may be the reason for such large resistances in the membrane.

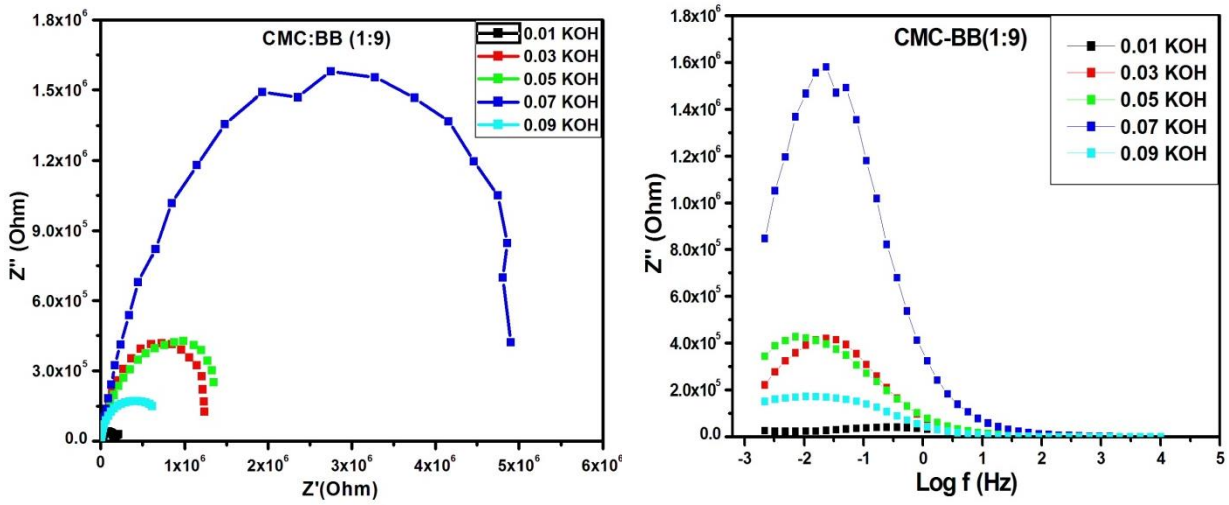

(a) **(b)**

Figure 4.5 (a & b) Comparison of Nyquist and Bode plot of imaginary impedance of all ratiosof CMC: BB- KOH (1:9)

Figure 4.6(a-e) shows the best fit for the corresponding impedance plot and equivalent circuit confirms that there is an absolute agreement between the experimental and fitted results.

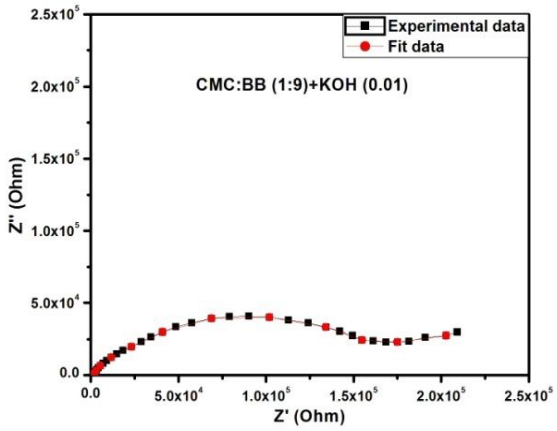

(a)

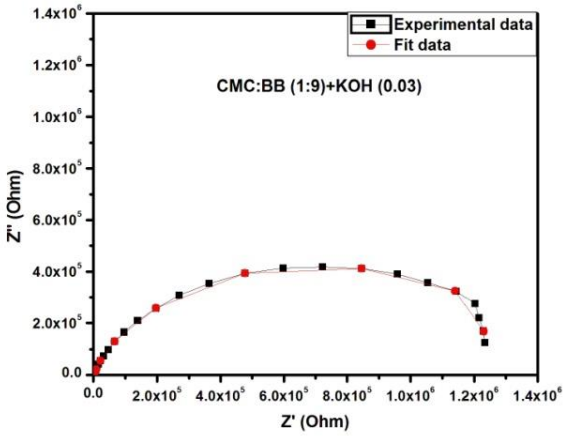

(b)

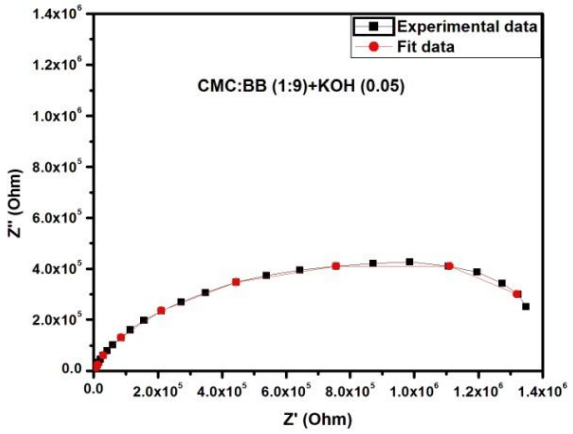

(c)

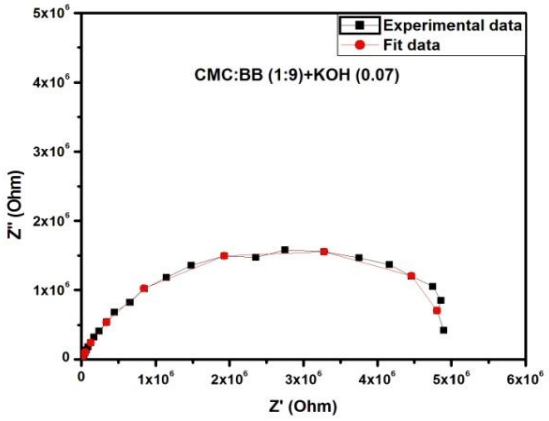

(d)

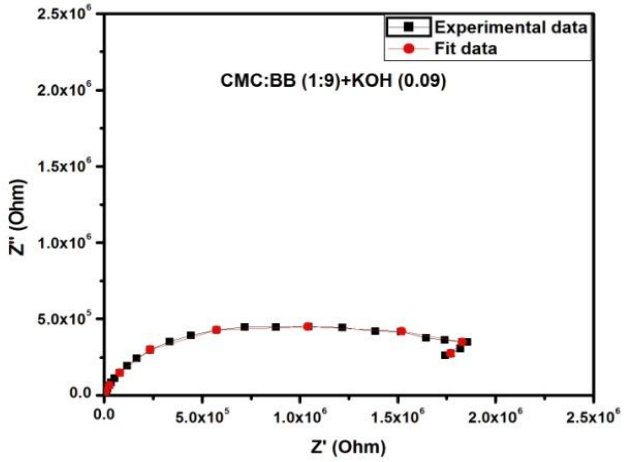

(e)

4.6 (a-e) Nyquist plot for CMC: BB (1:9)-KOH-0.01, 0.03, 0.05, 0.07, 0.09g

Table 4.2 shows the equivalent circuit along with the fitted values of CMC: BB (1: 9) with KOH salt. The Nyquist plot of CMC: BB with different ratios of KOH concentrations are fitted with corresponding equivalent circuit. Among all the CMC: BB membranes with different concentrations of KOH. CMC: BB (1:9)-0.01g KOH shows the highest value of $2.0463\times10^{-6}\Omega$. The different concentrations of KOH with CMC:BB shows the DC conductivity in the range of 10^{-4} S/cm to 10^{-7}S/cm. The increased dc conductivity is observed only when the value of R2 is decreased. The element CPE-P shows a lower value of 0.53 due to which the ion conductiontakes place. The CMC: BB (1:9)-KOH 0.09g showsa next highest value of R2 with the CPE-P value of 0.79 and hence the DC conductivity value of $0.521\times10^{-6}Sm^{-1}$. The electrolytic resistance is moderate952Ω in this sample. And the lowest DC conductivity value is observed for CMC: BB (1:9)-KOH 0.07g where the R1 value is high from all the other samples and the value of R2 as 4.78×10^{6} Ω. The element CPE-P shows a value of 0.73 and hence the lowest DC conductivity value of 0.069×10^{-6} Ω is observed. From the results obtained for the membrane casted with KOH in CMC: BB (1:9), the ratio of 0.01 shows higher value DC conductivity.

The Nyquist plot of CMC: BB (5:5) with different concentrations of KOH is shown in Figure 4.7(a). The dependence of ionic conductivity on the salt concentration provides information on the specific interaction between the salt and the membrane matrix. The conductivity varies with a wide range of factors, such as cation and anion types, salt

concentration, temperature, etc. The equivalent circuit contains series resistance, one parallel circuit with combination of constant phase element and resistance. From the graph, it may be concluded that the addition of different concentrations of salt with CMC:BB, strongly influences the electrochemical impedance properties. From Figure 4.7b, it is understood that there is only one relaxation time constant involved in the conduction process. As the peak frequency changes inconsistently with the concentration, it is evident that the interfacial thickness does not depend on the salt concentration but on probably other factors such as humidity, consistency of liquid while casting etc. The factors are not probed in this work as the focus is to identify a good conducting concentration only. Table 4.3 shows the comparison ratios of CMC: BB (5:5) at different concentrations of KOH salt. The DC conductivity for these samples range between $10^{-4}$and 10^{-9} S/cm. All the concentrations except 0.09g show low solution resistance but the resistance of insulating matrix with the electrolytic conductor is too high. The value of R_1 is 241.7Ω for CMC: BB (5:5) - KOH 0.09 and the other ratios exhibit the same R_1 value of 10 Ω and R_2 value 4.3020×10^5 Ω and a higher DC conductivity value is obtained as 2.5655×10^{-7} Sm^{-1}. And the ratio CMC: BB (5:5) -KOH 0.05 shows the higher DC conductivity value of 0.74112×10^{-6} Sm^{-1}.The interfacial resistance is too high in all the concentrations except for 0.05g which is 1342Ω. Hence, among the 5:5 ratio 0.05g of KOH have better conduction. Whereas, with 1:9 ratio, 0.01g loading had the higher conduction with single interface. With 5:5 double layers is seen one in the insulating matrix side and one in the electrode electrolyte interface which contributed two time constants in the 5:5 samples.

Table 4.2 Comparison of CMC: BB (1:9) membrane with different concentrations of KOH

KOH Concentration (g)	Equivalent circuit	R_1 (Ohm)	R_2 (Ohm)	CPE-T (Micro Farad)	CPE-P	DC Conductivity (Sm^{-1})
0.01	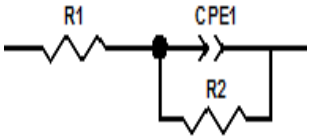	225	2.1004×10^{6}	4.702	0.53	2.046×10^{-6}
0.03	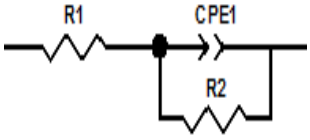	502.3	1.2316×10^{6}	2.5829	0.80	0.2591×10^{-6}
0.05	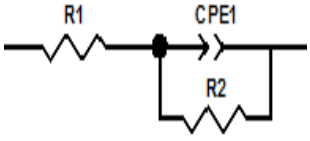	2477	1.385×10^{6}	2.7529	0.73	0.289×10^{-6}
0.07	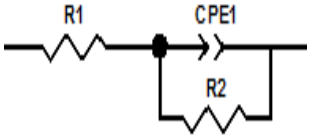	3000	4.783×10^{6}	6.5686	0.73	0.069×10^{-6}
0.09	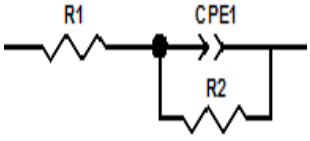	952	0.47767×10^{6}	4.4907	0.79	$0.527\text{x}10^{-6}$

(ii) CMC: BB(5: 5)- KOH

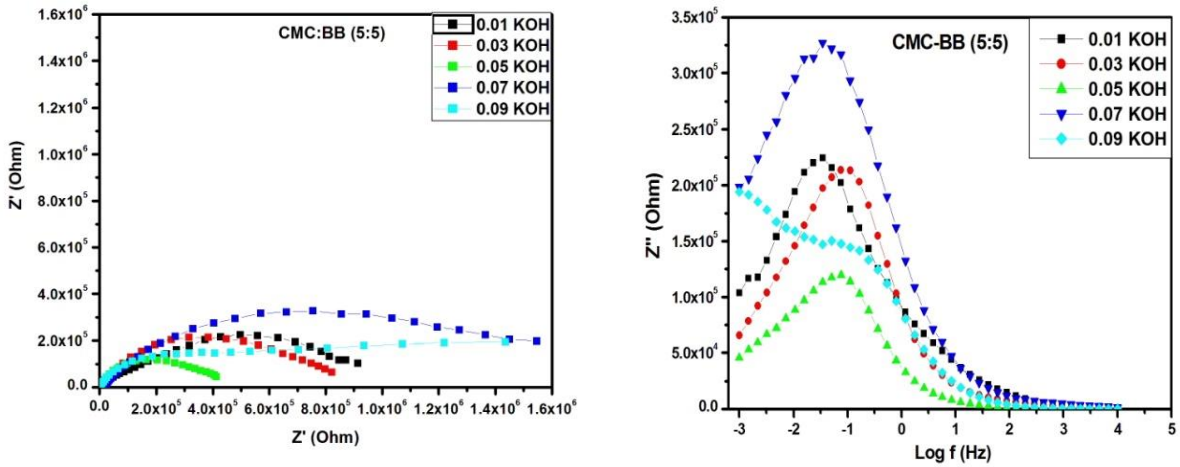

(a) **(b)**

Figure 4.7 (a & b) Comparison of Nyquist and Bode plot of imaginary impedance of all ratiosof CMC: BB- KOH (5: 5)

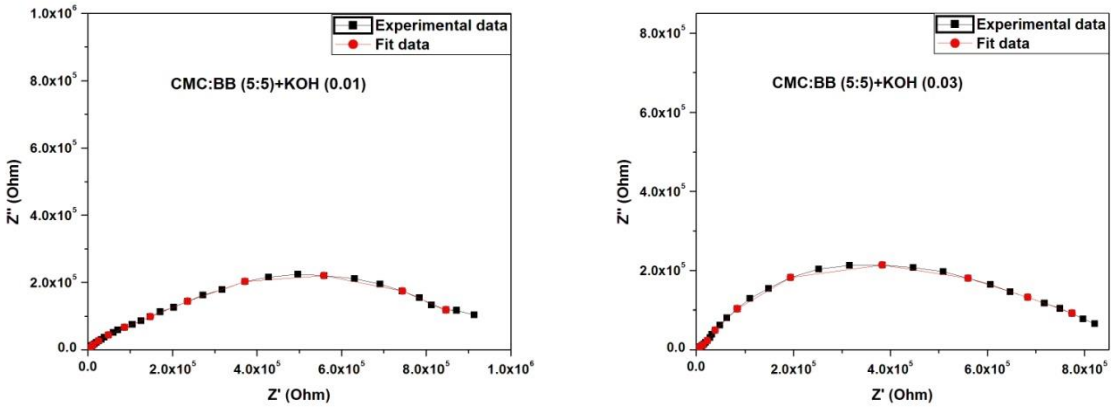

(a) **(b)**

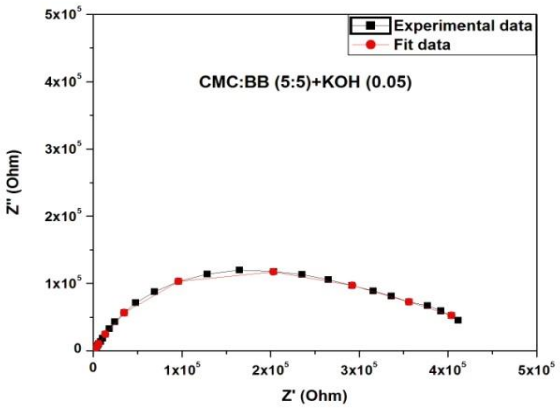

(c)

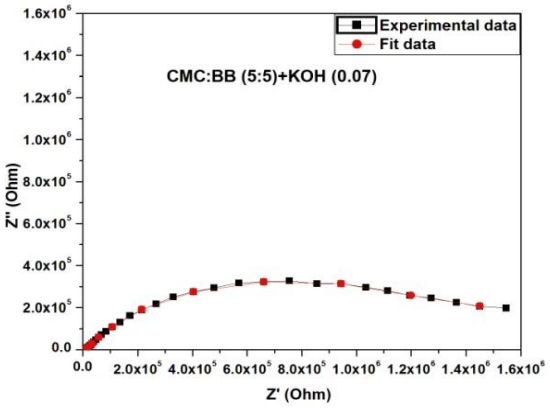

(d)

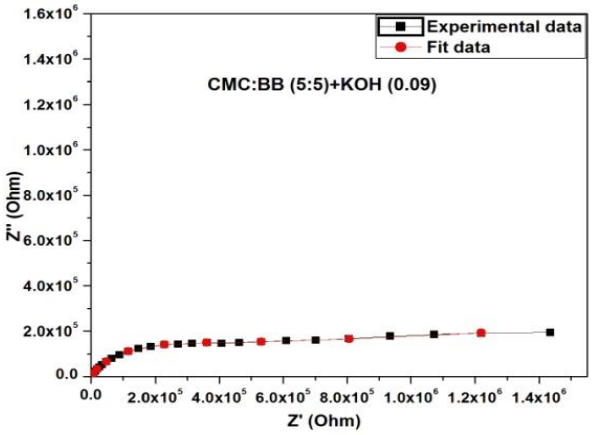

(e)

Figure 4.8 (a-e) Nyquist plot for CMC: BB (5:5)-KOH-0.01, 0.03, 0.05, 0.07, 0.09

Table 4.3 Comparison of CMC: BB (5:5) membrane with different concentrations of KOH

KOH concentra-tions (g)	Equivalent circuit	R_1 (Ohm)	R_2 (Ohm)	R_3 (Ohm)	CPE-T		CPE-P		DC conductivity (Sm^{-1})
					CPE-1 (Micro Farad)	CPE-2 (Micro Farad)	CPE 1	CPE 2	
0.01	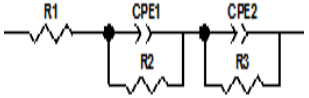	10	1.0283×10^6	20635	0.158	2.3633	0.6061	0.5044	0.262×10^{-6}
0.03	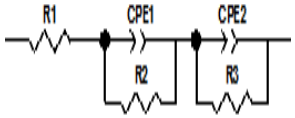	10	7.9091×10^5	289080	0.4346	2.3722	0.2424	0.6694	0.025×10^{-6}
0.05	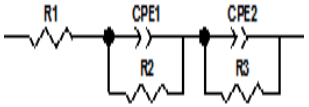	10	3.9669×10^5	1342	0.1138	5.8670	0.6443	0.7406	0.714×10^{-6}
0.07	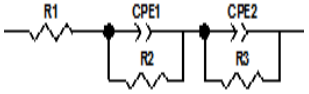	10	1.5063×10^6	10818	0.1.024	1.0745	0.6956	0.5790	0.232×10^{-6}
0.09	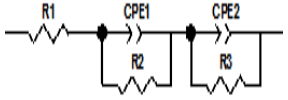	241.7	4.3020×10^5	699940	2.0261	0.29877	0.7387	0.8999	0.219×10^{-6}

(ii) CMC: BB (9:1)- KOH

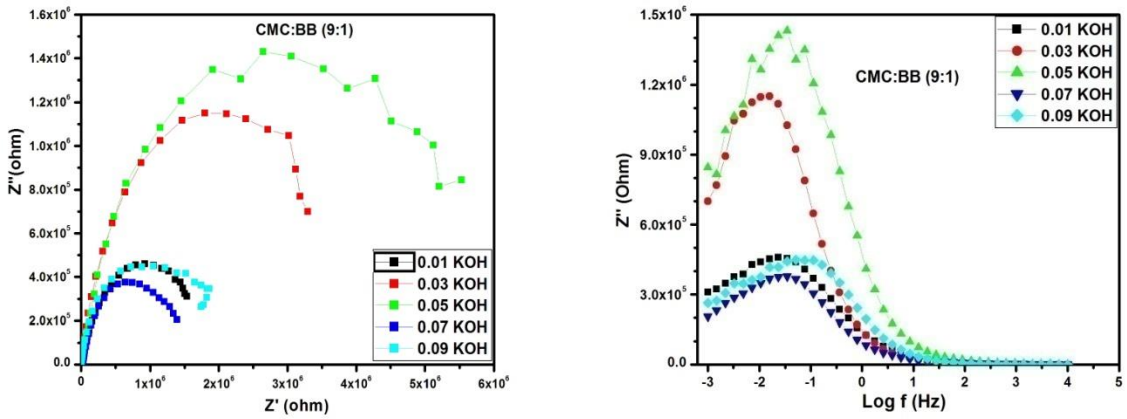

(a) **(b)**

Figure 4.9 (a & b) Comparison of Nyquist and Bode plot of imaginary impedance of all ratiosof CMC: BB- KOH (9: 1)

The Nyquist plot of CMC: BB (9:1) with different concentrations of KOH is shown in Figure 4.9(a). Figure 4.9 (b) shows the bode plot of CMC: BB (5:5) with different concentrations of KOH. From the observed bode plot there is only one time constant but the peaks are not sharp but broad indicating that the dispersion caused in the conduction is lower than in the case of 1:9 ratio samples. Compared to the all the different ratios, CMC: BB (9: 1)-KOH 0.01g shows a larger conduction but less than that of 0.01g KOH in 1:9 CMC:BB membrane. Figure 4.10 (a-e) shows the fitted results of the Nyquist plots of CMC:BB 9:1 with different concentrations of KOH.

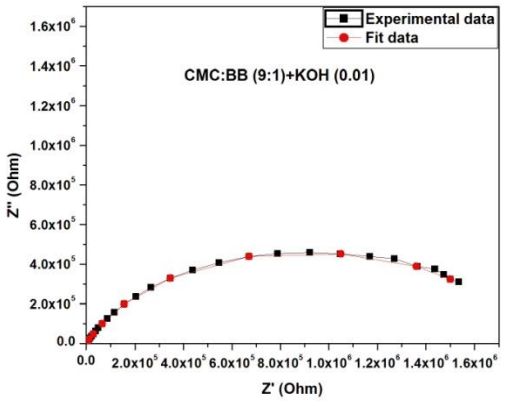

(a)

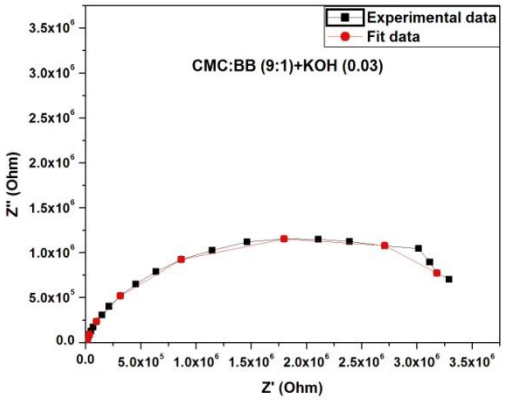

(b)

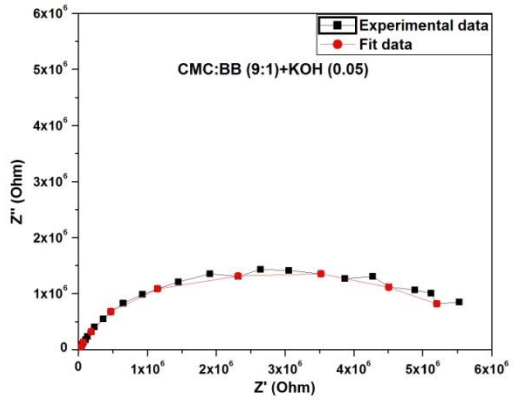

(c)

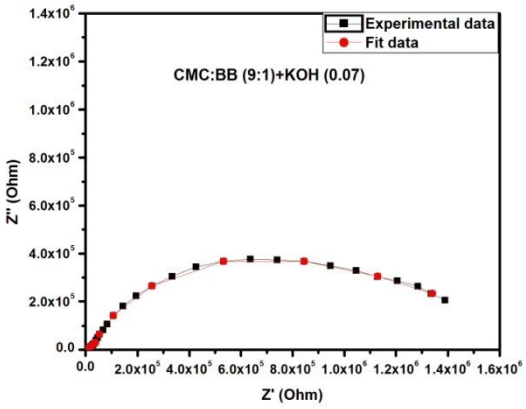

(d)

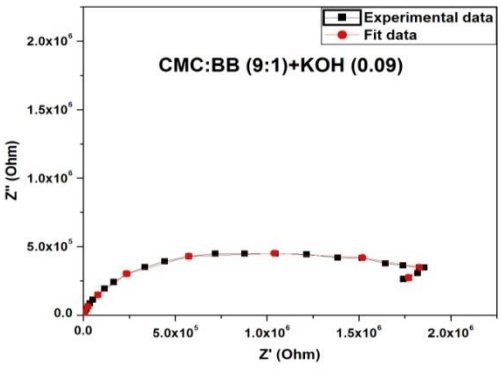

(e)

Figure 4.10 (a-e) Nyquist plot for CMC: BB (9:1)-KOH-0.01, 0.03, 0.05, 0.07, 0.09g

Table 4.4 Comparison between the different ratios of CMC: BB (9: 1) membrane with different concentrations of KOH

Concentration of KOH	Equivalent circuit	R_1 (Ohm)	R_2 (Ohm)	CPE-T (Micro Farad)	CPE-P	DC conductivity (Sm^{-1})
0.01	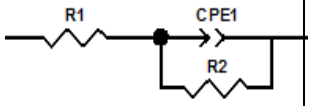	228.3	1.8×10^{6}	1.8851	0.65	0.398×10^{-6}
0.03	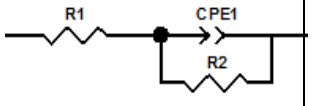	100	3.4169×10^{6}	1.5438	0.78	0.220×10^{-6}
0.05	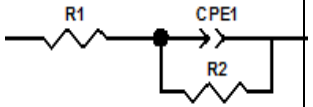	5513	5.9962×10^{6}	0.53985	0.67	0.106×10^{-6}
0.07	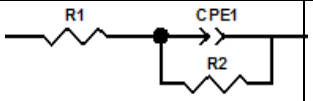	7970	1.5116×10^{6}	2.4819	0.59	0.278×10^{-6}
0.09	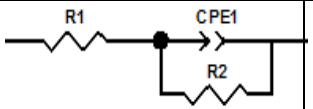	192.2	1.7148×10^{6}	8.9778	0.79	0.264×10^{-6}

Table 4.4 shows the comparison between the different ratios of CMC: BB(9:1)- KOH salt.. In these concentrations, 0.03, 0.09 and 0.01 g of KOH yield comparable electrolytic resistance. Out of the three, 0.09 and 0.01g of KOH shows almost similar interfacial resistance but for 0.03g this resistance is exorbitantly larger making this sample of not much use towards the application. Hence, Among all the CMC: BB ratios of 1:9, 5:5 and 9:1, with five different concentrations of KOH s, CMC:BB with 1:9 ratio having 0.01g of KOH is having highest DC conduction of value $2.046 \times 10^{-6} Sm^{-1}$ with lower dispersion in the capacitance which is preferably a good host material to be used as a electrolyte cum separator in supercapacitor application.

4.2.1.3 Impedance measurements of CMC: BB with LiOH

(i) CMC: BB (1: 9)- LiOH

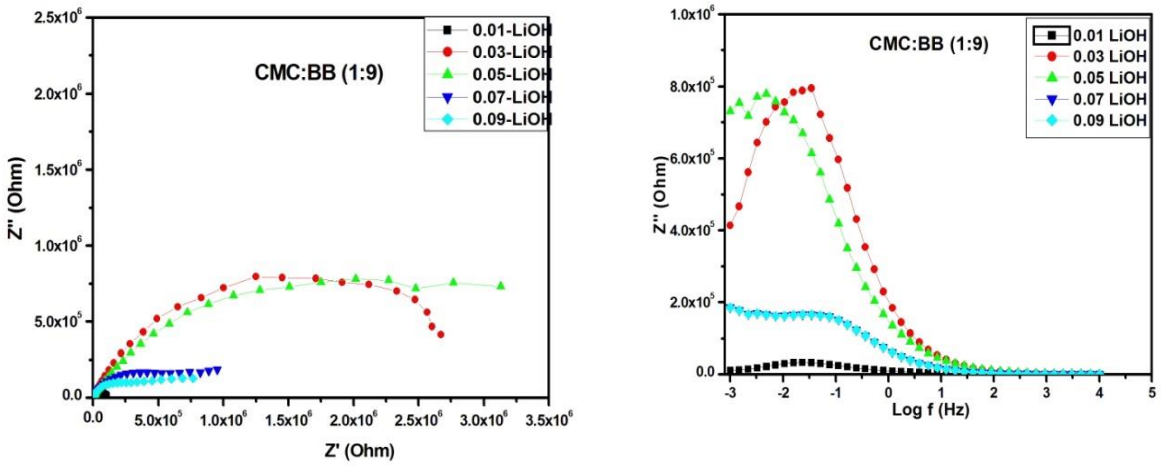

(a) **(b)**

Figure 4.11 (a & b) Comparison of Nyquist and Bode plot of imaginary impedance of all ratiosof CMC: BB- LiOH (1:9)

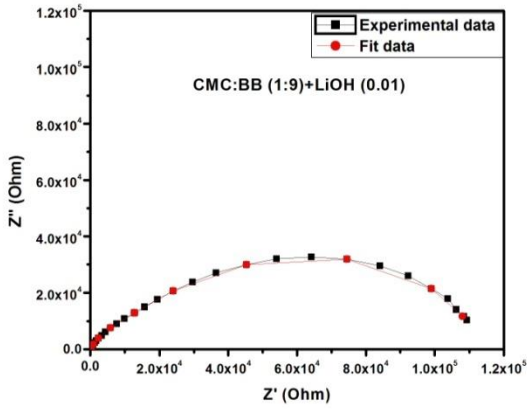

(a)

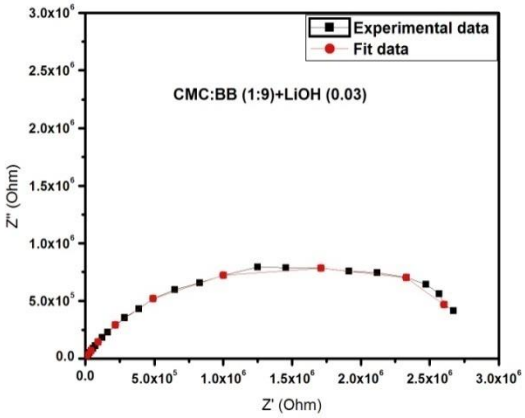

(b)

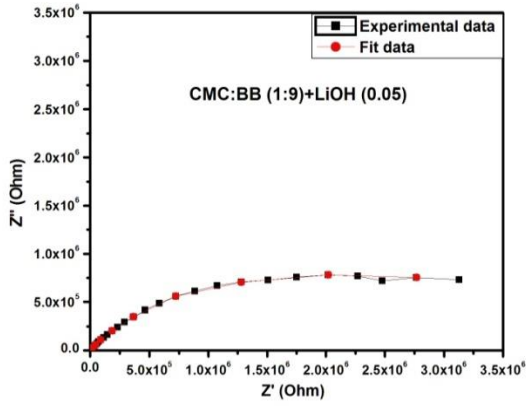

(c)

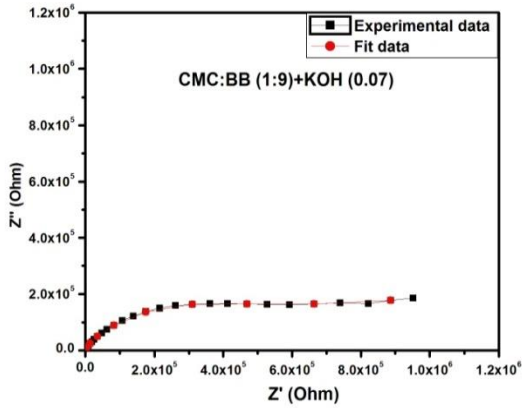

(d)

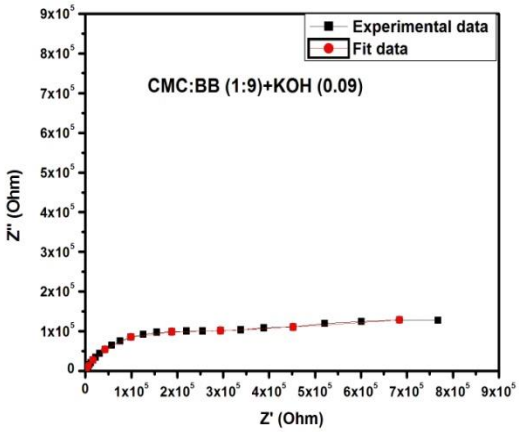

(e)

4.12 (a-e) Nyquist plot for CMC: BB (1:9)-LiOH-0.01, 0.03, 0.05, 0.07, 0.09g

Table 4.5 Comparison between the different ratios of CMC: BB (1: 9) membrane with different concentrations of LiOH

Concentr-ation of LiOH (g)	Equivalent circuit	R_1 (Ohm)	R_2 (Ohm)	R_3 (Ohm)	CPE-T		CPE-P		DC conductivity (Sm^{-1})
					CPE 1(Micro Farad)	CPE-2(Micro Farad)	CPE 1	CPE 2	
0.01	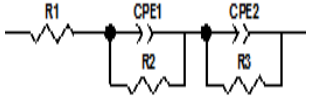	18.72	4690	1.1241×10^{6}	0.1914	0.2979	0.96	0.67	2.701×10^{-6}
0.03	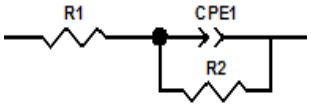	10	2.9107×10^{6}	-	1.3086	-	0.65	-	0.125×10^{-6}
0.05	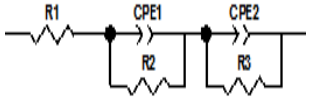	2932	3.1594×10^{5}	1.1646×10^{6}	2.8416	7.4392	0.83	0.78	0.166×10^{-6}
0.07	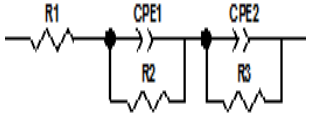	10	1.548×10^{5}	8.4435×10^{5}	3.6293	0.8209	0.82	0.63	0.673×10^{-6}
0.09	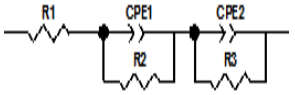	10	4.6522×10^{5}	2.1628×10^{5}	0.3876	5.4406	0.80	0.75	0.815×10^{-6}

Figure 4.11 (a & b) shows the Nyquist and bode plot of imaginary impedance of CMC: BB (1: 9) with different concentrations of LiOH. Figure 4.12 (a-e) shows the fitted results of the Nyquist plots of CMC: BB 1:9 with different concentrations of LiOH. From the Bode plot, it is evident that the peak frequency changes inconsistently with respect to concentration and it does not depend on the interfacial thickness. Table 4.5 shows the comparison between the different ratios of CMC: BB (1:9) – LiOH. A small DC conductivity value of $0.125x10^{-6}$ $Sm^{-1}$is observed for CMC: BB- 0.03g of LiOH and it do not show the electrode/ electrolyte interfacial resistance. Among all these concentrations, 0.01, 0.03, 0.07 and 0.09 g of LiOH yield comparable electrolytic resistance whereas 0.05g shows a higher value of 2932 Ω.A higher DC conductivity value is observed for the concentration of 0.01g of LiOH in the CMC: BB membrane which is equal to $2.701x10^{-6}$ $Sm^{-1}$and is comparatively higher than 0.01g of KOH incorporated CMC: BB membrane.

(ii) CMC: BB (5: 5)- LiOH.

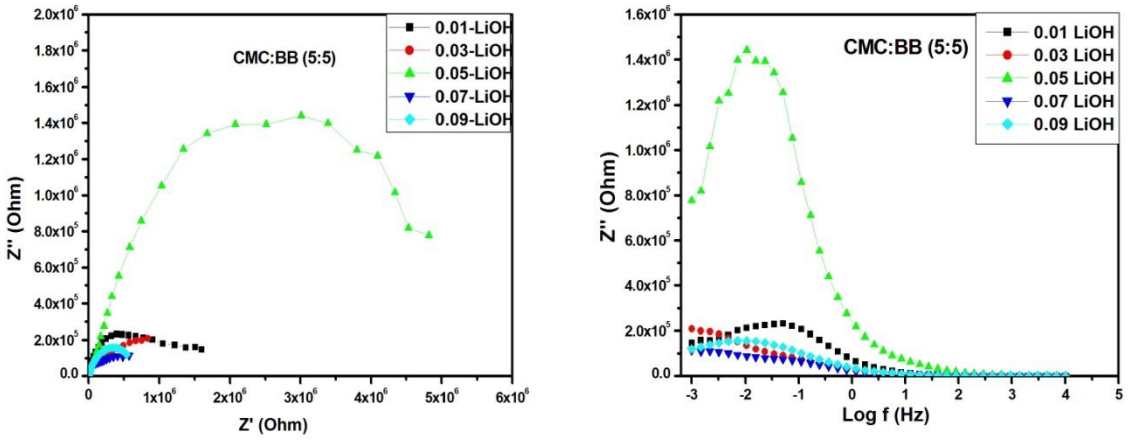

(a) **(b)**

Figure 4.13 (a & b) Comparison of Nyquist and Bode plot of imaginary impedance of all ratiosof CMC: BB- LiOH (5: 5)

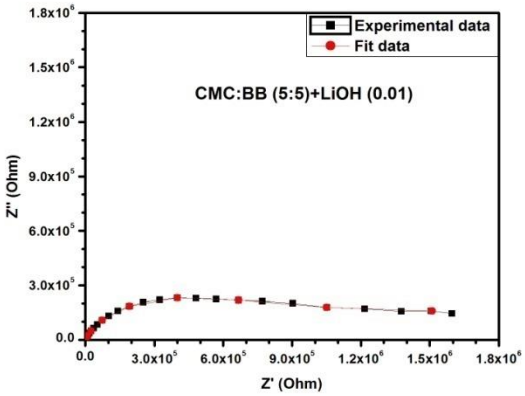

(a)

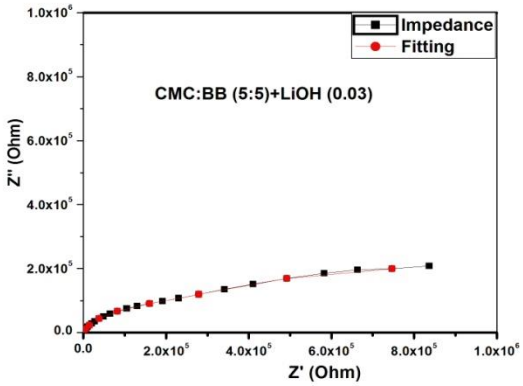

(b)

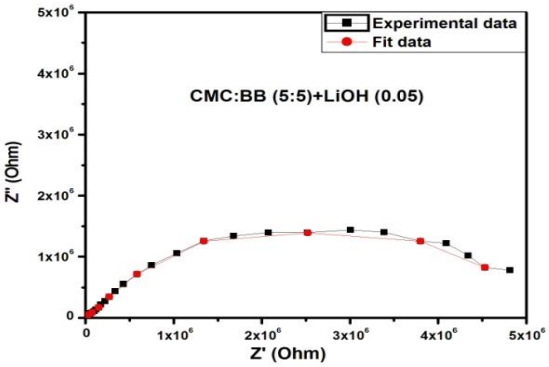

(c)

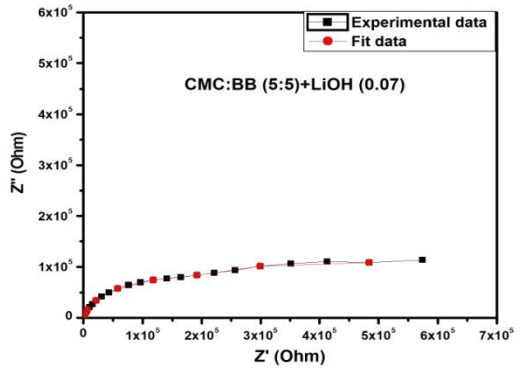

(d)

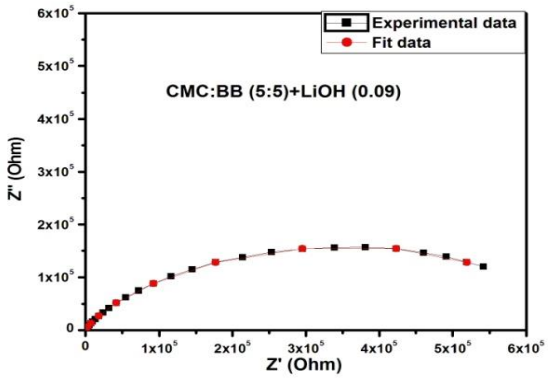

(e)

4.14 (a-e) Nyquist plot for CMC: BB (5:5)-LiOH-0.01, 0.03, 0.05, 0.07, 0.09g

Table 4.6 Comparison between the different ratios of CMC: BB (5: 5) membrane with different concentrations of LiOH

Concentr-aions of LiOH (g)	Equivalent circuit	R_1 (Ohm)	R_2 (Ohm)	R_3 (Ohm)	CPE-T		CPE-P		DC conductivity (S/m)
					CPE-1(Micro Farad)	CPE-2 (Micro Farad)	CPE 1	CPE 2	
0.01	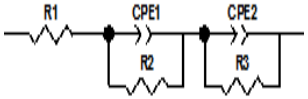	150	4.2655×10^{5}	9.5157×10^{5}	0.3014	0.141	0.78	0.82	0.385×10^{-6}
0.03	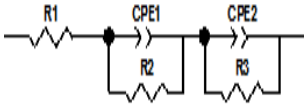	12.93	1.0842×10^{5}	6.7185×10^{5}	6.6515	0.1998	0.79	0.77	0.964×10^{-6}
0.05	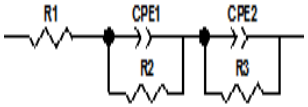	110.2	2.4804×10^{5}	4.071×10^{6}	60.506	1.3044	0.69	0.86	0.075×10^{-6}
0.07	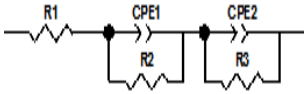	9.885	1.1921×10^{5}	3.8573×10^{5}	9.0053	0.4887	0.84	0.80	0.743×10^{-6}
0.09	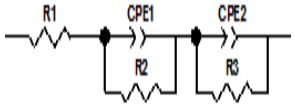	9.866	84448	5.0574×10^{5}	7.1041	0.1338	0.76	0.71	0.700×10^{-6}

Figure 4.13 (a & b) shows the Nyquist and bode plot o f imaginary impedance of CMC: BB (1: 9) with different concentrations 0.01g, 0.03g, 0.05g, 0.07g, 0.09g of LiOH. Figure 4.14 (a-e) shows the Nyquist plot for CMC: BB (5:5)-LiOH-0.01, 0.03, 0.05, 0.07, 0.09g. Table 4.6 shows the comparison of varied concentrations of LiOH. A similar electrolytic resistance value is observed for the concentrations 0.03, 0.07 and 0.09g of LiOH and a higher value of 110.2Ω is observed for the concentration of 0.05g and also it exhibits the smaller DC conductivity value of $0.075x10^{-6}$ Sm^{-1}. A higher interfacial resistance of $9.515x10^{5}$ Ω is observed for 0.01g of LiOH and this do not render any effect on choosing this concentration of LiOH for further application as electrolyte. A higher DC conductivity value of $0.964x10^{-6}$ $Sm^{-1}$is observed for 0.03g of LiOH. This value is relatively higher than that of CMC: BB -KOH (5: 5)-0.05g. It shows a better result in the ratios 1:9 and 5:5 while adding LiOH into the CMC: BB membrane.

(ii) CMC: BB (9: 1)- LiOH

The comparison of Nyquist plot and Bode plot of imaginary impedance for different concentrations namely., 0.01g, 0.03g, 0.05g, 0.07g and 0.09g of CMC: BB (9:1) is shown in the Figure 4.15 (a & b).

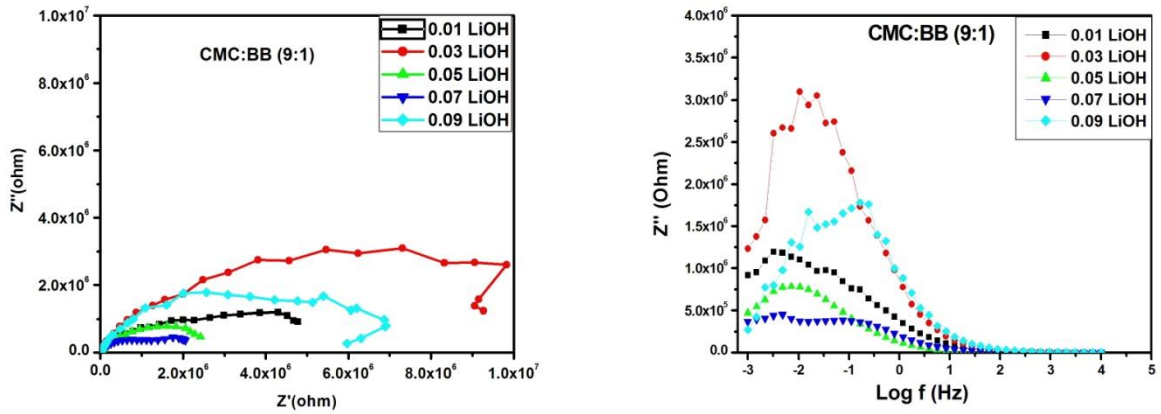

(a) **(b)**

Figure 4.15 (a & b) Comparison of Nyquist and Bode plot of imaginary impedance of all concentration of CMC: BB- LiOH (9: 1)

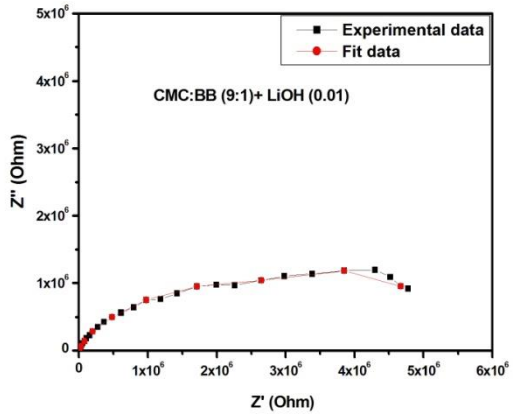

(a)

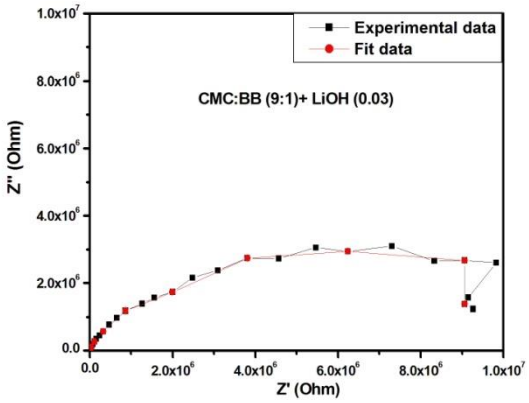

(b)

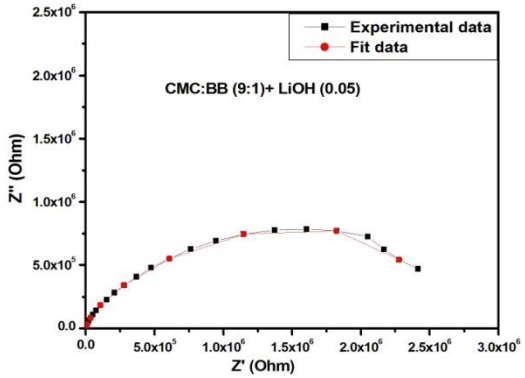

(c)

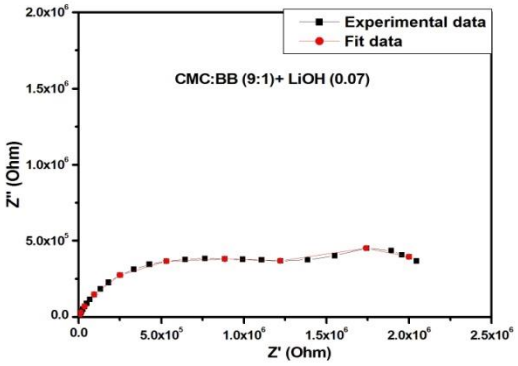

(d)

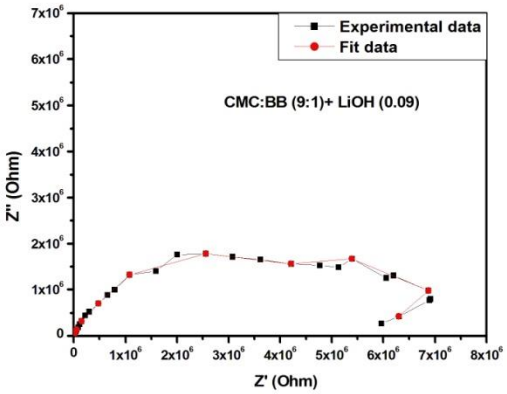

(e)

4.16 (a-e) Nyquist plot for CMC: BB (9:1)-LiOH-0.01, 0.03, 0.05, 0.07, 0.09g

Table 4.7 Comparison between the different ratios of CMC: BB (9: 1) membrane with different concentrations of LiOH

Concentr-aions of LiOH (g)	Equivalent circuit	R_1 (Ohm)	R_2 (Ohm)	R_3 (Ohm)	CPE-T		CPE-P		Ionic conductivity (Sm^{-1})
					CPE 1	CPE-2	CPE 1	CPE 2	
0.01	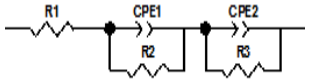	100	1.6786×10^{6}	2.8505×10^{6}	40.889	4.3484	0.7439	0.8762	0.076×10^{-6}
0.03	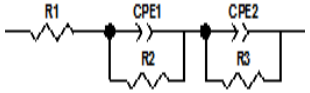	324	1.5804×10^{6}	8.5731×10^{6}	27.571	60.586	0.8351	0.7808	0.062×10^{-6}
0.05	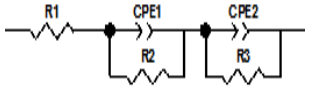	40	3.5026×10^{5}	2.1437×10^{6}	2.0205	4.4403	0.8626	0.8189	0.186×10^{-6}
0.07	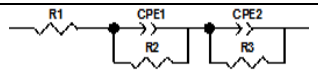	40	7.4975×10^{5}	1.8066×10^{6}	1.061	4.9778	0.8045	0.5884	0.302×10^{-6}
0.09	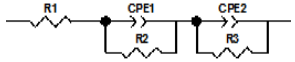	100	2.8694×10^{6}	4.2198×10^{6}	24.297	73.584	0.7836	0.6792	0.053×10^{-6}

Figure 4.16 (a-e) shows the fitted data of Nyquist plot for CMC: BB (9:1)-LiOH-0.01, 0.03, 0.05, 0.07, 0.09g. Table 4.4 shows the comparison between the different ratios of CMC: BB (9:1)- LiOH. A smaller electrolytic resistance value of 40Ω is obtained for 0.05 and 0.07g of LiOH. The resistance due to the insulating matrix is also observed to be higher as $7.4974 \times 10^{5}\Omega$ in the concentration of 0.07g of LiOH. A higher DC conductivity value of 0.302×10^{-6} $Sm^{-1}$is obtained for 0.07g of LiOH. There is not much difference of value from KOH to LiOH in 9:1 ratio of concentration 0.01g.

Hence, among all the CMC: BB ratios of 1:9, 5:5 and 9:1, with five different concentrations of LiOH, CMC:BB with 1:9 ratio having 0.01g of LiOH exhibits the highest DC conductivity of value of 2.701×10^{-6} Sm^{-1}. The CMC:BB (1:9) - incorporated with 0.01g of both KOH and LiOH shows the higher value of DC conductivity. For KOH incorporated CMC: BB membranes, a higher value of interfacial resistance of $2.100 \times 10^{6}\Omega$ than LiOH is obtained and it do not exhibit an interfacial resistance. Whilst, the CMC:BB (1:9)-0.01g of LiOH is having the component of resistance due to the insulating matrix. Though, there exists an interfacial resistance, since the dispersion values is nearly 0.96, it cannot be impeding the mobility of carriers much. Thus it may result in higher conduction. Hence, the CMC: BB membranes with 1:9 ratio having 0.01g of KOH and LiOH acts as a good host material to be used as a electrolyte cum separator in supercapacitor application.

4.2 Dielectric studies

Dielectric study is performed to confirm the enhancement of ionic conductivity due to increase in available number of mobile charge carriers. The dielectric constant (ε') represents charge stored by a electrolytic material while dielectric loss (ε") represents the amount of energy loss due to the movement of ions when the polarity of the electric field reverses rapidly. The value of ε' and ε" were calculated from the equations:

$$\varepsilon = \varepsilon' - j\varepsilon'' \qquad (1)$$

where,

ε' is real part of dielectric constant,

ε" is imaginary part of dielectric loss

Figure 4.2 (a) and (b) shows the shows the dielectric constant (ε') and dielectric loss (ε") as a function of logarithmic ratio of CMC: BB at room temperature.

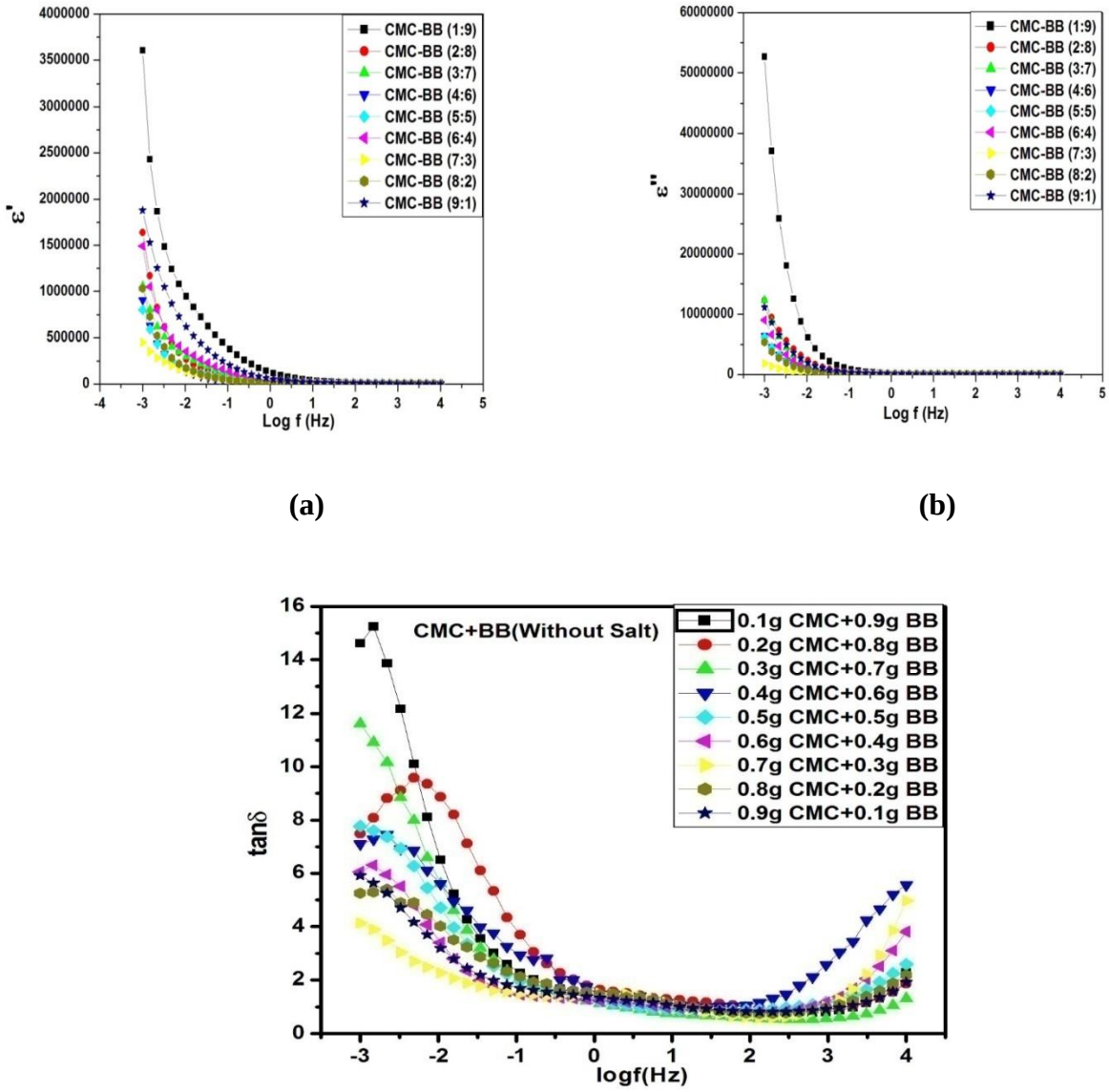

Figure 4.17 (a-c) Dielectric constant (ε'), Dielectric loss (ε'') and tan *δ* for different ratios CMC:BB membrane.

It is observed from the figure that the dielectric constant value and dielectric loss value increases rapidly at lower frequency region, due to the movement of dipoles along the electric field, which enhances the charge- carrier density. The contribution of the charge carriers increases towards the dielectric constant (ε). The dipoles move along the electric field at low frequencies. At high frequencies due to the high periodical reversal of the applied field, the dipoles cannot move along the electric field resulting in a constant value (**ε'**) at low frequencies. This results in increase in the storage of the dipole electric charges per unit volume at lower frequency. From the Figure 4.2(a), it

is evident that in comparison with 1:9 ratio of CMC: BB to other ratio, exhibits high dielectric constant at lower frequency region. This is attributed to the high contribution of charge accumulation at the electrode/ electrolyte interface. These results are good in agreement with impedance results.

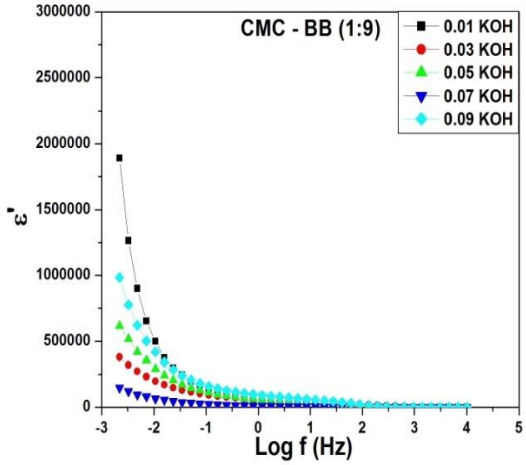

(a)

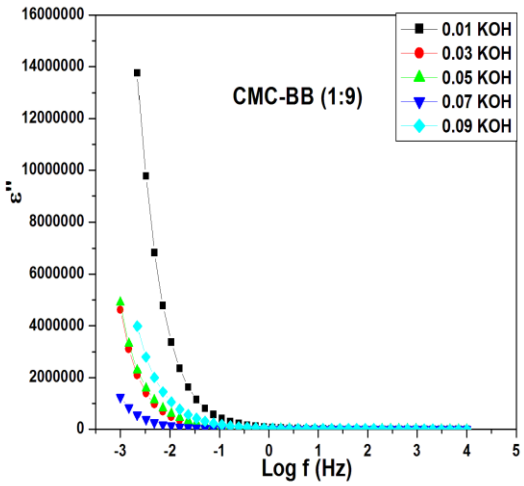

(b)

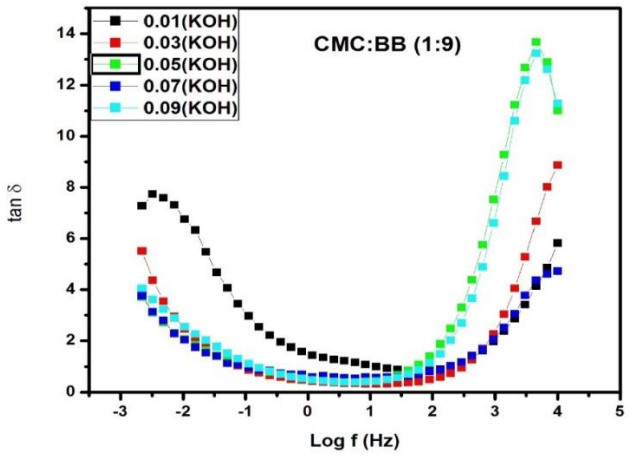

(c)

Figure 4.18 (a-c) Dielectric constant (ε'), Dielectric loss (ε'') and tan *δ* for different ratios of CMC : BB (1:9) membrane with different concentration of KOH

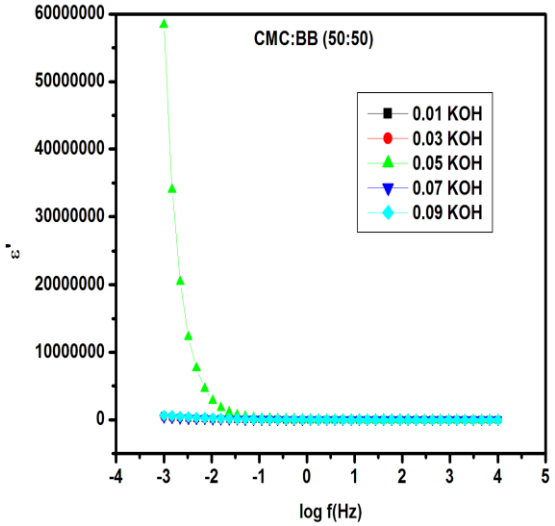

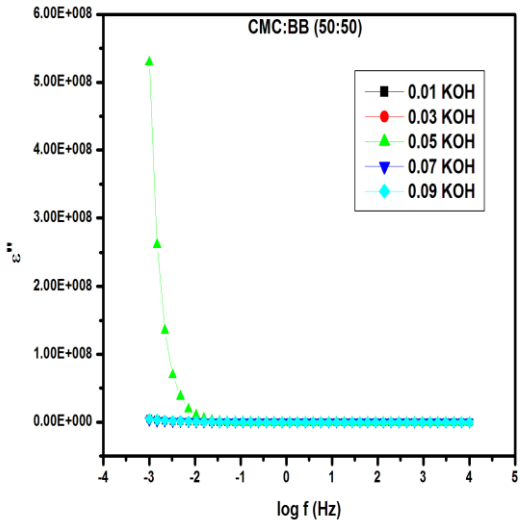

(a) **(b)**

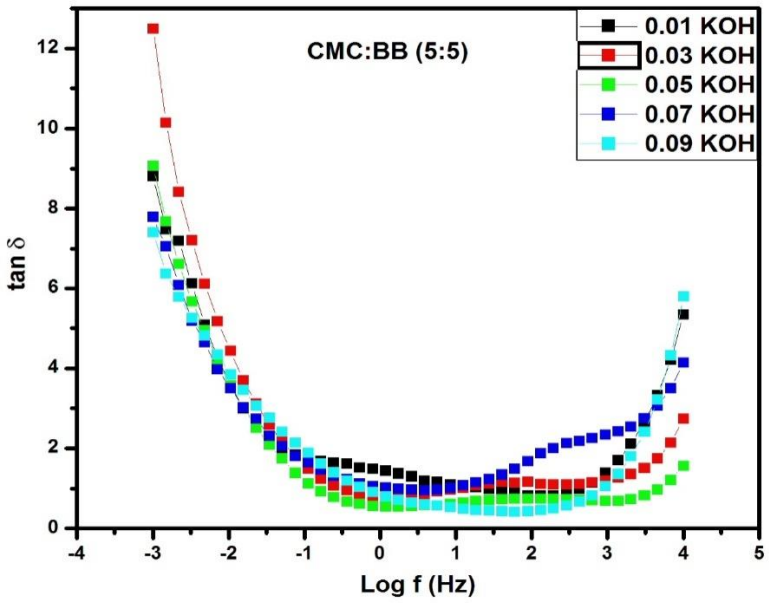

Figure 4.19 Dielectric constant (ε'), Dielectric loss (ε'') and tan δ for different ratios of CMC : BB (5:5) membrane with different concentration of KOH

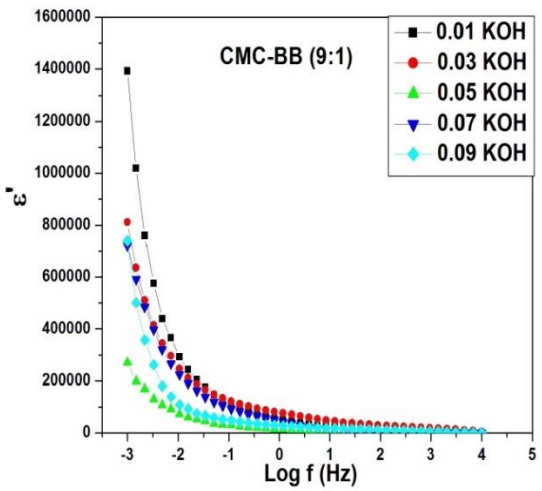

(a)

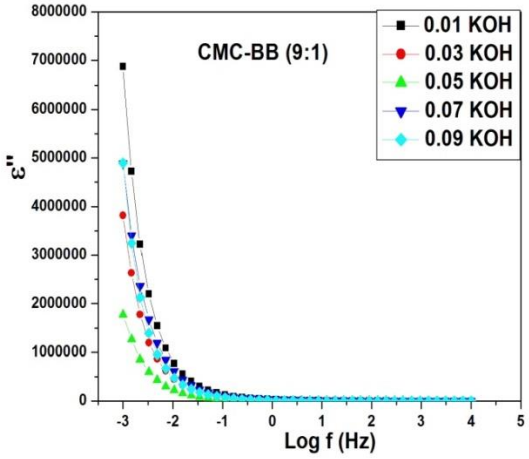

(b)

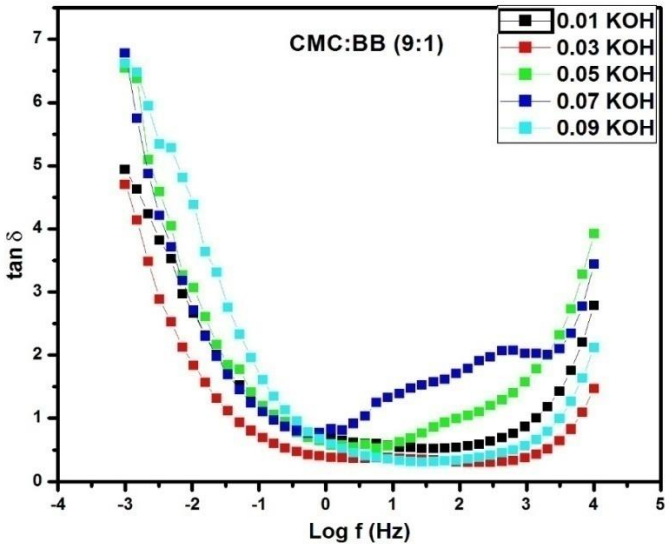

(c)

Figure 4.20 (a-c) Dielectric constant (ε'), Dielectric loss (ε'') and tan *δ* for different ratios of CMC : BB (9:1) membrane with different concentration of KOH

Figure 4.3 (a-f) compares the variation of dielectric constant (ε') and dielectric loss (ε'') with frequency for different KOH concentration at various ratio of electrolytic membranes CMC:BB (1:9), (5:5) and (9:1). The high value of dielectric constant (ε') and dielectric loss

(ε") at low frequency is due to the free charge motion within the materials. The decrease of (ε') with increase in frequency may be attributed to the electrical relaxation processes, but at the same time the material electrode polarization cannot be ignored, as the samples ofour investigation are electrolytic conductors. The electrode interface polarization gets superimposed with other relaxation processes at low frequencies. It is seen that with addition of KOH salt concentration, ε' value increases in the lower frequency. The addition may result in more localization of charge carriers along with mobile ions causing higher ionic conductivity. This may be the reason for higher and strong lower frequency dispersion on KOH concentration at electrolytic membrane.

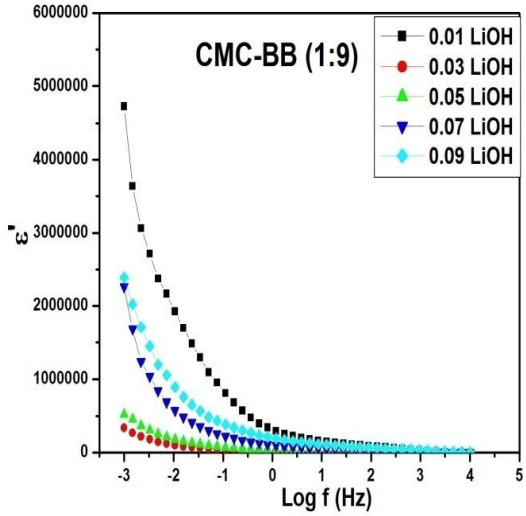

(a)

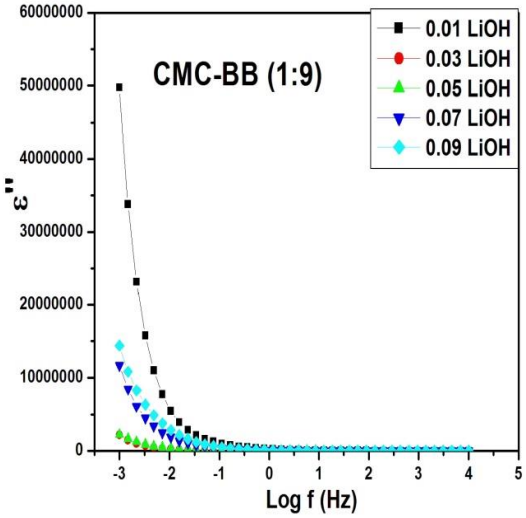

(b)

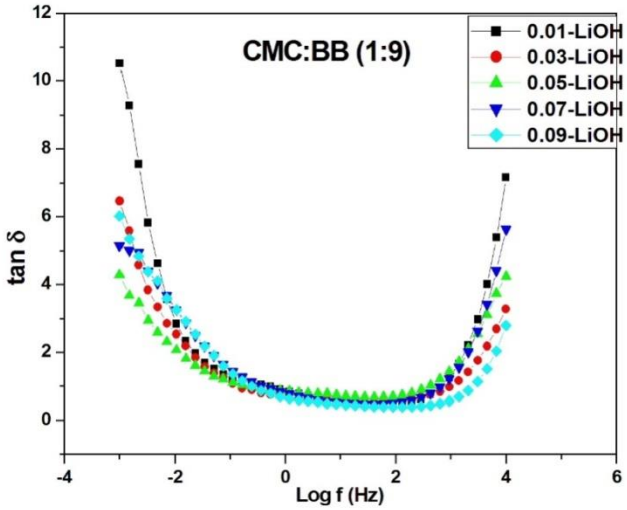

(c)

Figure 4.21 (a-c) Dielectric constant (ε'), Dielectric loss (ε'') and tan δ for different ratios of CMC : BB (1:9) membrane with different concentration of LiOH

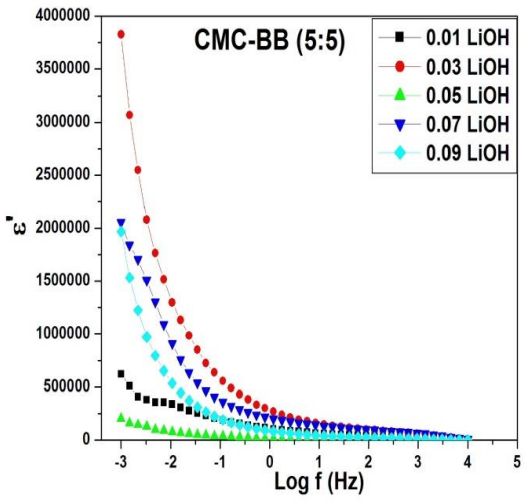

(a)

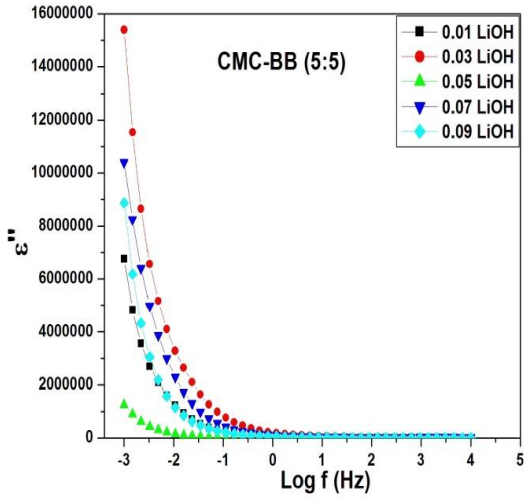

(b)

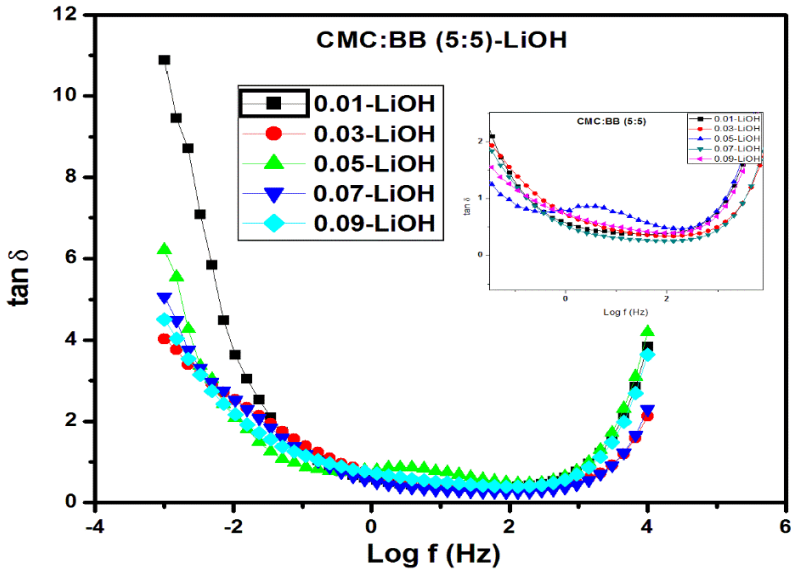

(c)

Figure 4.22 (a-c) Dielectric constant (ε'), Dielectric loss (ε'') and tan *δ* for different ratios of CMC : BB (5:5) membrane with different concentration of LiOH

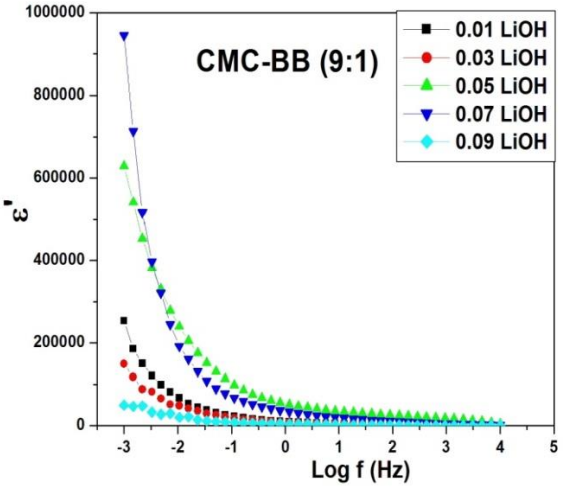

(a)

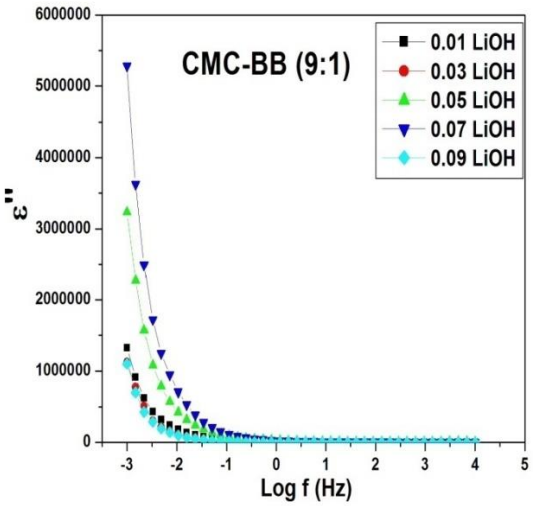

(b)

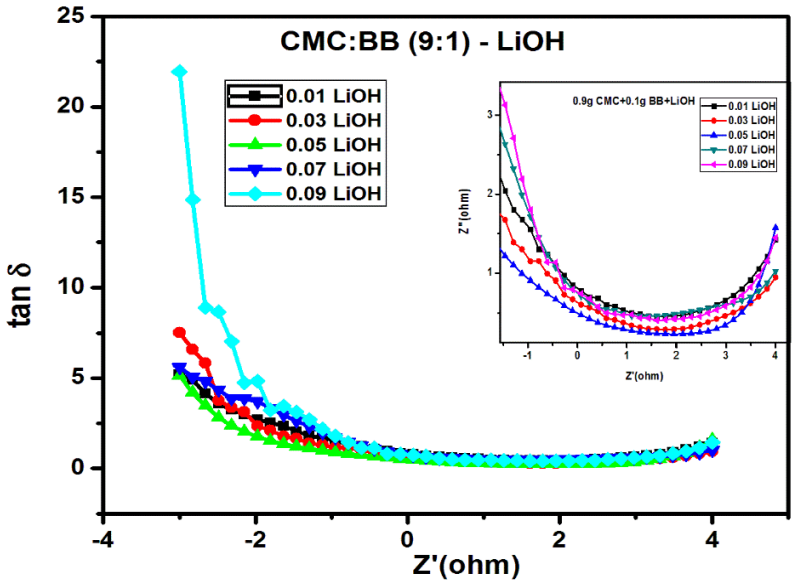

(c)

Figure 4.23 (a-c) Dielectric constant (ε'), Dielectric loss (ε'') and tan *δ* for different ratios of CMC : BB (9:1) membrane with different concentration of LiOH

Figure 4.4 (a-f) compares the variation of dielectric constant (ε') and dielectric loss (ε'') with frequency for different LiOH concentration at various ratio of electrolytic membranes CMC:BB (1:9), (5:5) and (9:1). The higher value of dielectric constant (ε') and dielectric loss (ε'') at low frequency is due to the free charge motion within the materials. The low frequency dispersion of the LiOH and KOH included CMC:BB matrix indicates that there is a blocking electrode and the charge transfer from the electrolyte to electrode is between two different charge carriers namely from ionic to electronic probably [71-72].

4.2 FOURIER TRANSFORM INFRARED SPECTROSCOPY (FTIR)

Fourier Transform Infrared Spectroscopy (FTIR) provides the specific information about the vibrational modes of chemical bonding and molecular structures. FTIR spectra, Figure 4.3.1, of CMC, BB, CMC:BB with 0.01g of KOH alkaline salt and CMC:BB with 0.07g of KOH electrolyte salt is analysed. FTIR vibrational assignments are given in Table 4.8. The ftir spectra of CMC and BB are taken individually for comparison and are given in the figure. The peaks corresponding to 1200 to 1400cm^{-1} got well suppressed in the case of

KOH but not suppressed in the case of LiOH. However, peaks are quiet prominent in this region when LiOH concentration is higher. Otherwise, there is no much variation in the peaks except of slight shifting due to the membrane formation. The peaks shifted in the membrane compared to the pristine CMC and BB indicates that there is a possibility of molecular binding between these functional groups of CMC and BB which makes the membrane to possible stand alone. The membranes show dominant peaks of CMC in the region of 1200 to 1500 cm^{-1} and from 400 to 1200 cm^{-1} to that of BB in all the ratios of CMC:BB. This indicates that the functional groups of CMC and BB coexist in the membrane without getting tampered or chemically reacted to form product [73-74].

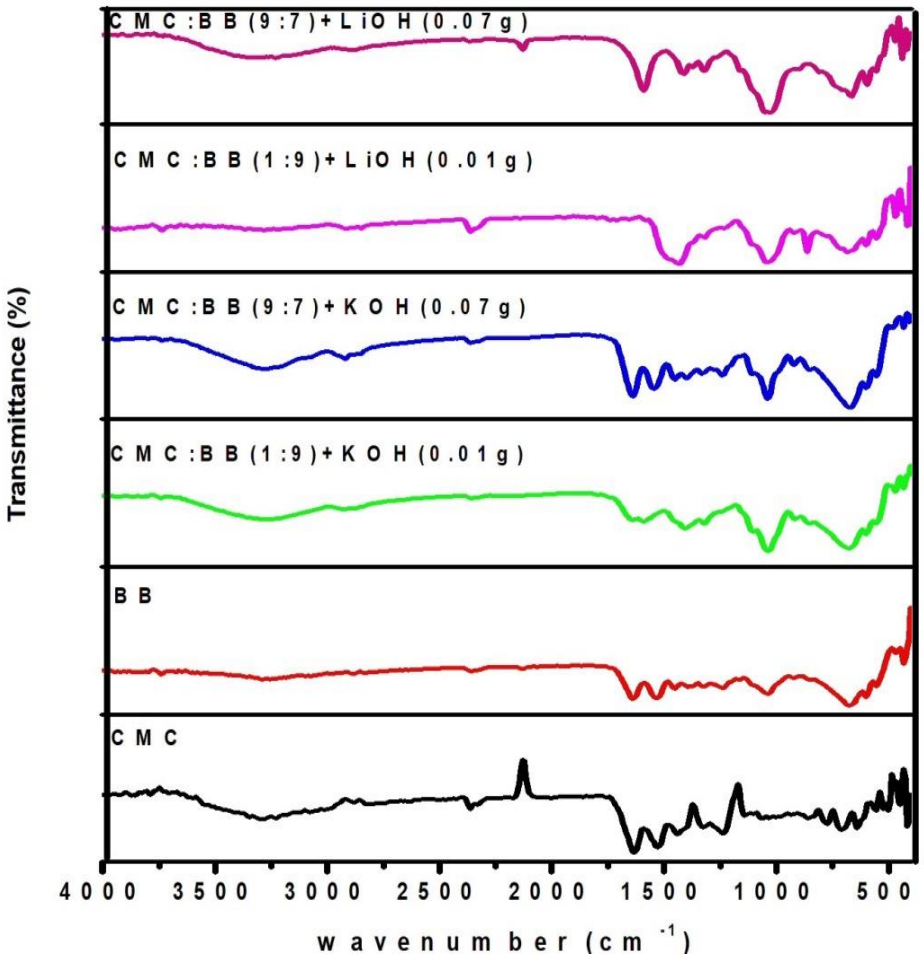

Figure 4.3.1 FTIR spectra of CMC:BB and KOH-LiOH

Table 4.8 FTIR peaks assignment for CMC:BB and KOH-LiOH

S. No	Wave number (cm^{-1})	Assignment/ Vibrations					
		CMC	**BB**	**CMC:BB (1:9) + KOH (0.01)**	**CMC:BB (9:1) + KOH (0.07)**	**CMC:BB (1:9) + LiOH (0.01)**	**CMC:BB (9:1) + LiOH (0.07)**
1.	592	-	V_4 phosphate	-	-	-	-
2.	631	-	V_4 phosphate		-	-	-
3.	671 - 674	Bonding of C-H in the molecule	-	-	-		-
4.	703-785	-	Bonding of C-H in the molecule	-		-	-
6.	871	-	Assigned carbonate				
7.	919		V_1 phosphate				
8.	1031-1038	-	V_3 phosphate		C-O stretching	C-O stretching	C-O stretching
9.	1042-1044	$-OCH_2COO-$ cellulose molecule		$-OCH_2COO-$ cellulose molecule			

S No.	Wave number (cm^{-1})	Assignment/ Vibrations					
		CMC	**BB**	**CMC:BB (1:9) + KOH (0.01)**	**CMC:BB (9:1) + KOH (0.07)**	**CMC:BB (1:9) + LiOH (0.01)**	**CMC:BB (9:1) + LiOH (0.07)**
12.	1244	-	-	C-N stretching vibration and N-H deformation	-		-
13.	1329-1333	-OH in plane bonding	-	-C-O stretching	C-O stretching	-	-
15.	1383-1399	$-OCH_2COO-$ cellulose molecule	-	CH_2 asymmetric stretching	-	CH_2 asymmetric stretching	-
17.	1411	-	V_3 phosphate	-	CH_2 asymmetric stretching		
18.	1422-1425	CH_2 asymmetric stretching	-	-	-		CH_2 asymmetric stretching
20.	1444 1453	-	-	C-H bending	-	C-H bending	-
22.	1532 - 1534	-	Amide II in plane N-H bending and C-N stretching vibration				-

S No.	Wave number (cm^{-1})	Assignment/ Vibrations					
		CMC	**BB**	**CMC:BB (1:9) + KOH (0.01)**	**CMC:BB (9:1) + KOH (0.07)**	**CMC:BB (1:9) + LiOH (0.01)**	**CMC:BB (9:1) + LiOH (0.07)**
23.	1545	C=O carbonyl group				in plane N-H bending and C-N stretching vibration	
24	1586	C-O stretching	-	-	C=O stretching vibrations of carboxyl group	-	-
25.	1637	-	C=O Aromatic carbonyl group		C=O stretching vibrations of carboxyl group	C=O stretching vibrations of carboxyl group	-
26	2120	C ≡ N vibrational group	-			-	-
27.	2132			-	C ≡ N vibrational group		-
28.	2352	-	-	C ≡ N vibrational group		-	-

S No.	Wave number (cm^{-1})	Assignment/ Vibrations					
		CMC	**BB**	**CMC:BB (1:9) + KOH (0.01)**	**CMC:BB (9:1) + KOH (0.07)**	**CMC:BB (1:9) + LiOH (0.01)**	**CMC:BB (9:1) + LiOH (0.07)**
29.	2356	C ≡ N vibrational group	-		-	C≡N vibrational group	
30.	2880-2881	C-H stretching mode	-	C-H stretching mode	-	-	-
32.	2914	C-H stretching mode	-	-	-	-	C-H stretching mode
33.	2921	CH stretching of CH_2 and CH_3 groups	CH_2 asymmetric stretching CH3 symmetric stretch	-	-	C-H stretching mode	
34.	3357-3866	-	-	OH-Hydroxyl group	OH-Hydroxyl group	OH-Hydroxyl group	OH-Hydroxyl group

CHAPTER-V

SUMMARY AND CONCLUSION

The membranes formation of carboxy methyl cellulose (CMC) and bovine bone (BB) by casting method is optimized for different concentrations of CMC and BB. The ratios of 1:9, 2:8,3:7,4:6,5:5, 6:4, 7:3, 8:2 and 9:1 are casted and standalone films are prepared successfully. Two different electrolytic salts are chosen to disperse towards the increment of conductivity in these insulating membranes. Five different concentrations namely 0.01g, 0.03g, 0.05g, 0.07g and 0.09g of LiOH and KOH are included separately in three chosen ratios of CMC: BB membranes namely 1:9, 5:5 and 9:1. The conductivity of CMC:BB ratios analysed using the impedance analysis showed that 5:5 showed optimal electrolytic conduction, 1:9 had no interfacial relaxation and 9:1 has all the three components such as electrolytic resistance, resistance due to insulating matrix and interfacial resistances. All these three ratios are incorporated with the electrolytic salt and the impedance studies are conducted. Among the various samples analysed the high total conductivity occurred with 0.01g of LiOH in CMC:BB (1:9) membrane. Also, the 0.01g of KOH in CMC:BB (1:9) showed comparable results but KOH samples had no resistance on insulating matrix. But the interfacial resistances were severe thus increasing the total resistance of the sample. The dielectric data of all the samples are also analysed and found that there is only one relaxation component due to the electrode-electrolyte interface and no other components due to the resistance of insulating matrix occurs. All the samples showed only low frequency dispersion except for few samples which were discarded and found unsuitable for the application of supercapacitor. The FTIR analysis is made to see whether the alkali salts are agglomerated to yield specific vibrational bands and no such bands was observed in all the samples of interest. Hence, only the CMC:BB membranes with dispersed alkali hydroxides exist in the membrane and the results are quiet reliable towards the employment of these membranes in the supercapacitor application. Thus, the more suitable membrane of CMC:BB (1:9) with 0.01g of LiOH or KOH is identified in the present work.

REFERENCE

1. **G Wang, L Zhang and J Zhang,** A review of electrode material for electrochemical supercapacitors, Royal society of chemistry, Volume 41, Page 797-828, 2012.
2. **T. Tooming, T. Thomberg, H. Kurig, A. Jänes, E. Lust,** High power density supercapacitors based on the carbon dioxide activated d-glucose derived carbon electrodes and 1-ethyl-3-methylimidazolium tetrafluoroborate ionic liquid, J. Power Sources, Volume-280, Page No. 667-677, 2015.
3. **Q. Hu, Z. Gu, X. Zheng, X. Zhang,** Three-dimensional Co3O4@NiO hierarchical nanowire arrays for solid-state symmetric supercapacitor with enhanced electrochemical performances, Chem. Eng. J. Volume 304, Page No. 223-231, 2007.
4. **M. Winter and R. J. Brodd,** What are Batteries, Fuel Cells, and Supercapacitors, Chem. Rev, Volume 104, Pages 4245, 2004.
5. **Ralph J. Brodd Broddarp of Nevada**, Inc., 2161 Fountain Springs Drive, Henderson, Nevada 89074, Volume 104, Pages 10, 2004.
6. **Sibo Wang, Tongzhen Wei, Zhiping Qi;**Supercapacitor Energy Storage Technology and its Application in Renewable Energy Power Generation System, Pages 2806, 2007.
7. **F. Beguin and E. Frackowiak**, eds., Supercapacitors {Materials, systems, and applications. Weinheim, Germany: Wiley-VCH Verlag GmbH & Co. KGaA, 2013.
8. **B.E. Conway**, Electrochemical Supercapacitors: Scientific Fundamentals and Technological applications. New York: Kluwer Academic/Plenum Publishers; 1999.
9. **M. Jayalakshmi, K. Balasubramanian**, Simple Capacitor to Supercapacitors-An Overview, Internatiomal Journal of Electrochemical Science, Volume 3, Page 1196-1217, 2008.
10. **D. Linden, T.B. Reddy**, Handbook of Batteries, Third edition, McGraw-Hill, 2001.
11. **D.Linden**, Mathematical Model and Experiment of Temperature Effect on Discharge of Lead-Acid Battery for PV Systems in Tropical Area, Energy and Power Engineering., Handbook of Batteries, 2nd ed., McGraw-Hill, New York, Volume 8, pages 2.1-24, 1995
12. **Gamby, J., P. L. Taberna,** Studies and Characterizations of Various activated Carbons used for carbon/carbon Supercapacitors, Journal of Power Sources, Volume 1, Page No.101, 2001.

13. **D. Y. and H. Shi**, Studies of Activated Carbons used in Double-Layer Capacitors, 1998, Journal of Power Sources, Volume 1, page 74.
14. **Amit Kumar Mittal, M. Jagadesh kumar,** Electrochemical Double-Layer Capacitors Featuring, Carbon Nanotubes, 2011, Volume 13, Page 263-271.
15. **Augustyn, Veronica and Simon, Patrice and Dunn, Bruce,** Pseudo capacitive oxide materials for high-rate electrochemical energy storage. Energy & Environmental Science, Volume7, 2014, Pages 1597-1614.
16. **Conway, B. E. and W. G. Pell,** "Double-layer and pseudo capacitance types of electrochemical capacitors and their applications to the development of hybrid devices." Journal of Solid State Electrochemistry, 2003, Volume 7, pages 637-644.
17. **Sibo Wang, Tongzhen Wei, Zhiping Qi;** Supercapacitor Energy Storage Technology and its Application in Renewable Energy Power Generation System, 2007, pages 2806.
18. **R. Kötz, M. Carlen,** Principles and applications of electrochemical capacitors, Electrochimica Acta, (2000), Volume 45, Page 2483–2498.
19. **Burke,** Ultracapacitors: why, how, and where is the technology, Journal of Power Sources, (2000), Volume 91, Page 37–50.
20. **J. R. Miller and P. Simon,** Materials science. Electrochemical capacitors for energy management, Science. 321 (2008) 651–652.
21. **A.J. Bard, L.R. Faulkner**, Electrochemical Methods: Fundamentals and Applications, Second Edition, Wiley & Sons, 2000**.**
22. **H. I. Becker**, Low voltage electrolytic capacitors. U.S., Patent 2800616 (1957).
23. **R. A. Rightmire**, Electrical energy storage apparatus. U.S., Patent 3288641 (1966)
24. **Hadjipaschalis I, Poullikkas A and Efthimiou V,** Overview of current and future energy storage technologies for electric power applications, Renew Sustain Energy, 2009, Volume 13, Page 1513–1522.
25. **Sarangapani S, Tilak BV, Chen C.P,** Materials for electrochemical capacitors: theoretical and experimental constraints. J Electrochem Soc, 1996, Volume 143, Page 3791–3799.
26. **Raccichini R, Varzi A, Passerini S, Scrosati B,** The role of graphene for electrochemical energy storage, Nature Materials, 2015, Volume 14, Page 271–279.

27. **Xiang F, Zhong J, Gu N et al**, Far-infrared reduced graphene oxide as high performance electrodes for supercapacitors, Carbon Nanotubes, 2014, Volume 75, Page 201–208.
28. **Tõnurist K, Thomberg T, Jänes A et al**, (2012) Specific performance of electrical double layer capacitors based on different separator materials in room temperature ionic liquid. Electrochemistry Communications, 2012, Volume 22, Page 77–80.
29. **Zhong C, Deng Y, Hu W et al**., A review of electrolyte materials and compositions for electrochemical supercapacitors, Chemical Society Reviews, 2015, Volume 44, Page 7484–7539.
30. **Samantara AK, Maji S, Ghosh A et al.,** Good's buffer derived highly emissive carbon quantum dots: excellent biocompatible anticancer drug carrier, Journal of Material Chemistry Volume 4, Page 2412–2420.
31. **Shi M, Kou S, Yan X,** Engineering the electrochemical capacitive properties of grapheme sheets in ionic-liquid electrolytes by correct selection of anions, Chemphychem, 2014, Volume7, Page 3053–3062.
32. **R.C. Agraeal and G.P. Pandey**, Solid polymer electrolytes: materials designing and all-solid-state battery applications: an overview, 2008, Journal of Physics D: Applied physics, Volume 41, Page 223001.
33. **Jacob M M E, Hackett E and Giannelis E P,** From nanocomposite to nano gel polymer electrolytes, Journal of Material Chemistry**,** 2003, Volume 13, Page 1-5.
34. **Michel Armand,** Polymer with Ionic conductivity, Advanced Materials, 1990, Volume 2, Page 278-286.
35. **J. M. Tarascon, A. S. Gozdz, C. Schmutz, F. Shokoohi, and P. C. Warren,** Perfoemance of Bellocore's plastic rechargeable Li-ion batteries**,** Solid State ionics, 1996, Volume 86-88, Page 49-54.
36. **W. Wieczorek, K. Such, J. Pryluski, and Z. Florianczyk,** Blend- based and composite polymer solid electrolytes, 1991, Volume 45, Page 373-383.
37. **Saikia.D and Kumar A,** Ionic conduction in P(VDF-HFP)/PVDF-(PC + DEC)-$LiClO_4$ polymer gel electrolytes, Electrochemica Acta, 2004, Volume 49, Page 2581–2589.
38. **Cesar Sequeira and Diogo Santos**, Polymer electrolytes Fundamentals and applications, Woodhead Publishing Series in Electronic and Optical Materials, 2010, Page 95-10.

39. **Diogo F. Vieira and Agnieszka Pawlicka**, Optimization of performances of gelatin/LiBF4-based polymer electrolytes by plasticizing effects, Electrochemica Acta, Volume 55, Page No. 1489-1494, 2010.
40. **M. L. H Rozali, A. S. Samsudin and M. I. N. Isa**, Ion Conducting Mechanism of Carboxy Methylcellulose Doped With Ionic Dopant Salicylic Acid Based Solid Polymer Electrolytes, International Journal of Applied Science and Technology, Volume 2, Page No. 4, 2012.
41. **R. Leones, F. Sentanin, L. C. Rodrigues, I. M. Marrucho, J. M. S. S. Esperança, A. Pawlicka, M. M. Silva**, Investigation of polymer electrolytes based on agar and ionic liquids, Express Polymer Letters, Volume 6, Page No. 1007-1016, 2012.
42. **E. Raphael, C. O. Avellaneda, M. A. Aegerter, M. M. Silva and A. Pawlicka,** Agar-based Gel Electrolyte for Electrochromic Device Application, Molecular Crystals and Liquid Crystals, Volume 554, Page No. 264-242, 2012.
43. **Pawlicka, F.C. Tavares, D.S. Dörr, C.M. Cholant, F. Ely, M.J.L. Santos, C.O. Avellaneda,** Dielectric Behavior and FTIR Studies of Xanthan Gum-based Solid Polymer Electrolytes, Electrochimica Acta, Volume 19, Page No. 30458, 2012.
44. **Y.N. Sudhakar and M. Selvakumar**, Lithium perchlorate doped plasticized chitosan and starch blend as biodegradable polymer electrolyte for supercapacitors, Electrochimica Acta, Volume 78, Page No. 398-405, 2012.
45. **K. H. Kamarudin and M. I. N. Isa,** Structural and DC Ionic conductivity studies of carboxy methylcellulose doped with ammonium nitrate as solid polymer electrolytes, International Journal of Physical Sciences, Volume 8, Page No. 1581-1587, 2013.
46. **M. F. H. Abd, El-Kader and H. S. Ragab,** DC conductivity and dielectric properties of maize starch/methylcellulose blend films, Ionics, Volume 19, Page No. 361-369, 2013.
47. **Mohd Saiful Asmal Rani , Siti Rudhziah, Azizan Ahmad and Nor Sabirin Mohamed,** Biopolymer Electrolyte Based on Derivatives of Cellulose from Kenaf Bast Fiber, Polymers, Volume 6, Page No. 2371-2385, 2014.
48. **Rahul Singha, Jaya Baghela, S. Shuklaa, B. Bhattacharyaa, Hee-Woo Rheeb and Pramod K. Singh**, Detailed electrical measurements on sago starch biopolymer solid electrolyte, Phase Transitions, Volume Page No. , 2014.

49. **Y.N. Sudhakar, M. Selvakumar, and D. Krishna Bhat,** Tubular array, dielectric, conductivity and electrochemical propertiesof biodegradable gel polymer electrolyte, Materials Science and Engineering B**,** Volume 180, Page No. 12-19, 2014.
50. **M.F. Shukur, R. Ithnin, and M.F.Z. Kadir**, Electrical characterization of corn starch-LiOAc electrolytes and application in electrochemical double layer capacitor, Electrochimica Acta, Volume 136, Page No. 204-216, 2014.
51. **Y M Yusof, M F Shukur, H A Illias and M F Z Kadir,** Conductivity and electrical properties of corn starch–chitosan blend biopolymer electrolyte incorporated with ammonium iodide, Physics Scripts, Volume 89, Page No. 35701, 2014.
52. **Ramlli M.A. and Isa M.I.N,** Conductivity study of Carboxyl methyl cellulose Solid biopolymer electrolytes (SBE) doped with Ammonium Fluoride, Research journal of Recet Sciences, Volume 3, Page No. 59-66, 2014.
53. **M. I .H Sohaimy and M. I. N Isa**, Conductivity and dielectric analysis of cellulose based solid polymer electrolytes doped with ammonium carbonate (NH_4CO_3), Applied Mechanics and Materials, Volume 719-720, Page No. 67-72, 2015.
54. **Przemyslaw Ledwon, Juliana R. Andrade , Mieczyslaw Lapkowski, Agnieszka Pawlicka,** Hydroxypropyl cellulose-based gel electrolyte for electrochromic devices, Electrochimica Acta, Volume 159, Page No. 227-233, 2015.
55. **Y. N. Sudhakar, M. Selvakumar and D. Krishna Bhat,** Preparation and characterization of phosphoric acid-doped hydroxyethyl cellulose electrolyte for use in supercapacitor, Mater Renew Sustain Energy, Volume 4, Page No. 10, 2015.
56. **K. H. Teoh, Chin-Shen Lim, Chiam Wen Liew, S. Ramesh**, Preparation and performance analysis of barium titanate incorporated in corn starch-based polymer electrolytes for electric double layer capacitor application, Journal of Applied Polymer Science, Volume 156 , Page No. 43275, 2016.
57. **M. N. Chai and M. I. N. Isa**, Novel Proton Conducting Solid Bio-polymer Electrolytes Based on Carboxymethyl Cellulose Doped with Oleic Acid and Plasticized with Glycerol, Narure, Volume 6, Page No. 27328, 2016.
58. **N. H. Ahmad and M. I. N. Isa**, Ionic conductivity and electrical properties of xarboxyl cellulose- NH_4Cl solid polymer electrolytes, Journal of Engineering Science and Technology, Volume 11, Page No. 8, 2016.

59. **Shikha Gupta and Pradeep K. Varshney,** Effect of plasticizer concentration on structural and electrical properties of hydroxyethyl cellulose (HEC)-based polymer electrolyt, Ionics, Volume 23, Page No. 1613-1617, 2017.
60. **N. Suganya and V. Jaisankar,** Conducting Polymeric Hydrogel Electrolyte Based on Carboxymethylcellulose and Polyacrylamide Polyaniline for Supercapacitor Applications, International Journal of Nanoscience, Volume 16, Page No. 1760003, 2017.
61. **Anna Railanmaa, Suvi Lehtima¨ki, and Donald Lupo,** Comparison of starch and gelatin hydrogels for non-toxic supercapacitor electrolytes, Applied Physics A, Volume 123, Page No. 459, 2017.
62. **Mohd. Khalid and Ana M. B. Honorato,** Ionically conducting and environmentally safe gum Arabic as a high-performance gel-like electrolyte for solid-state supercapacitors, Journal of Solid State Electrochemistry, Volume 4, Page No. 3585, 2017.
63. **Jagdish Kumar Chauhan, Manindra Kumar, Madhavi Yadav, Tuhina Tiwari and Neelam Srivastava,** Effect of NaClO4 concentration on electrolytic behaviour of corn-starch film for supercapacitor application, Ionics, Volume 4, Page No. 2136, 2017.
64. **N. K. Zainuddin, M. A. Saadiah, A. P. P. Abdul Majeed and A. S. Samsudin,** Characterization on conduction properties of carboxymethyl cellulose/kappa carrageenan blend-based polymer electrolyte system, International Journal of Polymer Analysis and Characterization, Volume 5, Page No. 1446887, 2018.
65. **A.S. Samsudina and M.A. Saadiaha,** Ionic conduction study of enhanced amorphous solid bio-polymer electrolytes based carboxymethyl cellulose doped NH_4Br, Journal of Non- Crystalline Solids, Volume 497, Page No. 19-29, 2018.
66. **C. Nwanya, C. I. Amaechi , A. E. Udounwa R. U. Osuji , M. Maaza and F. I. Ezema** Complex impedance and conductivity of agar-based ion-conducting polymer electrolytes, Applied Physics A, Volume 339, Page No. 8979, 2014.
67. **K. S. Cole, R. Cole**, Dispersion and Absorption in Dielectrics I. Alternating Current Characteristics, Journal of chemical Physics 9 (1941) 341.
68. **A. J. Bard, L.R. Faulkner,** Electrochemical Methods, John Wiley & Sons, New York 1980, Chapter 9.
69. **Barbara H. Stuart,** Infrared Spectroscopy, Fundamentals and applications, John Wiley and Sons Ltd., 2004.

70. **. N. Chai and M. I. N. Isa.,** Carboxyl methylcellulose solid polymer electrolytes: Ionic conductivity and dielectric study, Journal of current Engineering Research, Volume 1, Page No. 23-27.
71. **A. S. A. Khiar, R. Puteh. A . K. Arof**, Conductivity studies of a chitosan-based polymer electrolyte, Physica, Volume 373, Page No. 23-27, 2006.
72. **MelisTufan, Emre Uraz, Caglagul Tosun, and Hasanferdi Gerce**, Synthesis and Characterization of Carboxymethyl Cellulose film from pistachio shells, International Journal of Advance in Science, Engineering and Technology, Volume 4, Page No. 153-155, 2016.
73. **Sudip Mondal, Biswanath Mondal, Apurba Dey, Sudit S. Mukhopadhyay,** Studies on Processing and Characterization of Hydroxyapatite Biomaterials from Different Bio Wastes, Journal of Minerals & Materials Characterization & Engineering, Volume 11, Page No. 55-67, 2012.
74. **Jayapradhi rajendran,** Xanes and ftir Study on Dried and Calcined Bones, 2011.